

INFORMATION TO USERS

This manuscript has been reproduced from the microfilm master. UMI films the text directly from the original or copy submitted. Thus, some thesis and dissertation copies are in typewriter face, while others may be from any type of computer printer.

The quality of this reproduction is dependent upon the quality of the copy submitted. Broken or indistinct print, colored or poor quality illustrations and photographs, print bleedthrough, substandard margins, and improper alignment can adversely affect reproduction.

In the unlikely event that the author did not send UMI a complete manuscript and there are missing pages, these will be noted. Also, if unauthorized copyright material had to be removed, a note will indicate the deletion.

Oversize materials (e.g., maps, drawings, charts) are reproduced by sectioning the original, beginning at the upper left-hand corner and continuing from left to right in equal sections with small overlaps.

Photographs included in the original manuscript have been reproduced xerographically in this copy. Higher quality 6" x 9" black and white photographic prints are available for any photographs or illustrations appearing in this copy for an additional charge. Contact UMI directly to order.

ProQuest Information and Learning
300 North Zeeb Road, Ann Arbor, MI 48106-1346 USA
800-521-0600

UMI[®]

UNIVERSITY OF OKLAHOMA

GRADUATE COLLEGE

OPTICAL OBSERVATIONS OF LIGHTNING BY THE FORTE SATELLITE:
TERRESTRIAL GROUND TRUTH AND IMPLICATIONS FOR THE
INTERPRETATION OF JOVIAN LIGHTNING DATA

A Dissertation

SUBMITTED TO THE GRADUATE FACULTY

in partial fulfillment of the requirements for the

degree of

Doctor of Philosophy

By

CYNTHIA MARIE MACHACEK NOBLE

Norman, Oklahoma

2001

UMI Number: 3028812

UMI[®]

UMI Microform 3028812

Copyright 2002 by Bell & Howell Information and Learning Company.

All rights reserved. This microform edition is protected against
unauthorized copying under Title 17, United States Code.

Bell & Howell Information and Learning Company

300 North Zeeb Road

P.O. Box 1346

Ann Arbor, MI 48106-1346

© Copyright by Cynthia Marie Machacek Noble 2001
All Rights Reserved.

OPTICAL OBSERVATIONS OF LIGHTNING BY THE FORTE SATELLITE:
TERRESTRIAL GROUND TRUTH AND IMPLICATIONS FOR THE
INTERPRETATION OF JOVIAN LIGHTNING DATA

A Dissertation APPROVED FOR THE
SCHOOL OF METEOROLOGY

BY

Joe Wynn

Susan Postawko

William Rust

Donald R. MacGowan

William H. Beasley

ACKNOWLEDGMENTS

I would like to thank my advisors Susan Postawko and William Beasley for their guidance through this dissertation. I would also like to thank Matt Kirkland, Dave Suszcynsky, and Tess Light at Los Alamos National Laboratory for giving me access to the FORTE data and helping me with all my silly IDL questions. Thank you to the School of Meteorology for a computer and a place to sit. Most of all, thank you to my husband Seth and to my Mom and Dad for putting up with the mood swings and for being there to lean on when the going got tough. Thanks to everybody who sent me warm fuzzies along the way. It's been quite a roller coaster ride!

TABLE OF CONTENTS

Abstract.....	vi
1. Introduction.....	1
2. Studies of Lightning Using Spaceborne Platforms.....	8
2a. Terrestrial Satellite Lightning Studies.....	8
2b. Terrestrial "Superbolts".....	12
2c. Terrestrial Lightning Studies Using FORTE.....	12
2d. Jovian Lightning Studies.....	16
3. Motivations and Questions to be Addressed.....	25
4. Instruments.....	27
4a. The FORTE Photodiode Detector (PDD).....	27
4b. The National Lightning Detection Network (NLDN).....	28
4c. The New Mexico Tech. Lightning Mapping Array (LMA).....	30
5. Comparison between PDD and NLDN detected events.....	32
5a. Overview of PDD data.....	32
5b. The PDD/NLDN data set for "Summer" 1998.....	45
5c. Analysis Methods and Results.....	55
5d. Discussion.....	80
6. Comparison between PDD and LMA detected events.....	84
6a. Coincident data on 25 June, 2000 during STEPS.....	84
6b. Analysis Methods and Results.....	89
6c. Discussion.....	111
7. Summary, Conclusions, and Future Work.....	114
Glossary of Acronyms.....	118
References.....	119

ABSTRACT

Lightning and storm electrification have been studied from many different viewpoints and with many different instruments. The myriad of viewpoints and instruments often see the results or effects of different processes within the lightning flash. The challenge becomes to understand how the data from the different instruments and different points of view relate to each other. Optical detection instruments aboard satellites have been used to study lightning on earth and on other planets, most notably Jupiter. Terrestrial satellite data has been promoted as an in indicator of moist convective processes in the atmosphere, which can be used as proxies for convection in such applications as model initialization, convective parameterization, and global climate studies. Jovian lightning data has been used to indicate dynamic processes in Jovian thunderstorms and to infer where and when, and therefore why, such storms occur in the Jovian atmosphere. This study seeks to address how optical satellite lightning data relate to the physical characteristics of the lightning flash which produced the optical signals, and therefore gain some insight on how to better interpret the limited amount of optical lightning data from Jupiter.

To accomplish this aim, data from the National Lightning Detection Network (NLDN) and the New Mexico Tech Lightning Mapping Array (LMA) are used to provide ground-truth for optical lightning data from the Fast on-Orbit Recording of Transient Events (FORTE) Photodiode Detector (PDD). Several conclusions are made based on the analyses presented here. First, PDD events with peak estimated optical power greater than or equal to 10^{11} W (“bright” events) are much more likely to be cloud-to-ground (CG) events than PDD events with smaller peak optical power. Furthermore, CG events associated with a “bright” PDD event are more likely to be positive than for PDD events with smaller peak optical power, and than for climatology. Second, in general, the likelihood that a PDD event will be associated with a CG flash decreases with decreasing peak optical power. Third, if a flash is detected by the PDD, it tends to reach higher above the ground, have a greater horizontal extent, and a longer duration than flashes that are not detected by the PDD. Fourth, it is likely that the lightning processes which are mapped by the LMA may not directly correlate to the lightning processes which produce the optical

signals to which the PDD is the most sensitive. However, the PDD and the NLDN often seem to see aspects of the same return stroke, with the NLDN recording the connection to ground and the PDD recording optical signals that are produced once the return stroke process propagates up into the cloud. Finally, what this study shows is that the actual relationship between optical signals recorded from a satellite-based instrument and the physical lightning channels themselves may not be so simply described as simple scattering through a cloud from a point or line source. In order to better interpret the Jovian lightning data, perhaps more complex scenarios, based on the situations that are seen for terrestrial lightning, need to be considered.

CHAPTER 1

INTRODUCTION

Throughout history, lightning has been a subject of human awe and fascination. We have long searched for a way to explain the how and why behind the flash and thunder of lightning discharges. As our ability to observe and understand the world has advanced from what could be seen with the naked eye and heard with the unaided ear to more sophisticated observation methods, our understanding has progressed far beyond the mythological musings of our ancestors. We now have an understanding of electrical charge generation, breakdown, and discharge inside thunderstorms. However, despite all of the advances in lightning research, especially over the latter part of the twentieth century, many questions remain unanswered.

In the modern day and age, we have come at the problem of understanding lightning from many different angles. From a ground-based point of view, high speed photography, electric field mills, precipitation charge and size measuring instruments, point-discharge sensors, devices which measure changes in the electric field, and other instruments have been used to investigate the structure and velocity of cloud-to-ground (CG) discharges and the electrical environment in and around parent thunderstorms (see *MacGorman and Rust [1998]* for an overview of instrumentation that has been used to investigate the electrical nature of storms). Rockets, balloons and aircraft have been used to carry electric field meters, precipitation particle counters, and other instruments designed to take in-situ measurements of the electrical and microphysical characteristics inside storm-

clouds. High altitude aircraft have been used to sample electric fields and currents above thunderstorms and to investigate electrical discharge phenomena above the storm tops, such as red sprites and blue jets. The spatial and temporal structure of lightning channels have been investigated using acoustical, radar, and Very High Frequency (VHF) radio mapping techniques (*MacGorman and Rust [1998]; Thomas et al. [2000]*). The location of cloud-to-ground (CG) flashes has been determined using Direction Finding (DF) techniques, Time of Arrival (TOA) techniques, or a combination of the two, using arrays of ground-based detection stations (*Cummins et al. [1998]*). Satellites have been used to detect the optical and radio frequency emissions from lightning, and to gain insight into the location and frequency of lightning from a global perspective (*Turman [1977]; Turman and Edgar [1982]; Christian and Latham [1998]; Reeve and Toumi [1999]; Suszcynsky et al. [2000]; Thomas et al. [2000]*). Lightning has even been studied from aboard the space shuttle. Lightning occurring on other planets in our solar system has been investigated using Earth-based telescopes and spacecraft-borne cameras and radio frequency sensors (*Levin et al. [1983]; Hansell et al. [1995]; Hobarra et al. [1997]; Little et al. [1999]*).

Each of these many observation platforms may sample a different aspect of the lightning discharge or the parent storm environment which produced it. Taken alone, no single observation platform can provide the complete physical, temporal, or environmental understanding for a single lightning flash. The challenge is to learn how the different observable pieces fit together. If a complete physical understanding of the lightning discharge process is to be reached, with an eye toward using lightning data to initialize weather forecast models or as a possible predictor for the severity of storms, the relationship between the different observables, the lightning discharge itself, and the characteristics of the parent storms must be considered.

The goal of this study is to work on a small piece of this rather complex puzzle. It has been claimed that satellite observations of lightning can be of great use to the meteorological and climatological communities, and that optical techniques are perhaps the best way to study lightning from a space-based platform (*Christian and Latham [1998]; Christian [1999]; Little et al. [1999]; Reeve and Toumi [1999]; Williams et al. [1999]*). The general question that this study seeks to address is whether physical characteristics of a

lightning flash (such as whether that flash is Intracloud (IC) or CG) can be determined using optical data collected from satellite-based observing systems. This will be conducted with one eye toward Jupiter, so that any insights gained with respect to the terrestrial satellite lightning data can be used to improve the interpretations of the Jovian optical lightning data collected by the Voyager and Galileo missions, and to help provide direction for future Jovian lightning studies.

The question of how the optical signals from lightning may relate to flash or storm characteristics is important for many reasons. Increased lead-time on lightning detection (as from a satellite-borne sensor which may detect the optical emissions from IC flashes in advance of the first CG detected by ground-based systems such as the National Lightning Detection Network (NLDN)) could help reduce the number of lightning-related injuries and deaths which occur per year (*Lopez and Holle [1996]; Lopez and Holle [1997]*). In the western United States, lightning ignites more than 80% of the forest fires per year, and in other areas where lightning-caused fires account for a small percentage of the total number of fires, they often account for over 50% of the total area burned (*Price and Rind [1994a]*). Satellite climatologies for lightning, especially if they can somehow be related to the occurrence of "dry" thunderstorms (*Rorig and Ferguson [1999]*), could help with the allocation and deployment of firefighting resources. Increased detection of lightning over remote areas could also help with fire-prediction efforts, potentially leading to a decrease in property and resources lost. Satellite lightning data, in conjunction with other regional lightning climatologies, could also help provide the information necessary for a more efficient allocation of resources and lightning-protection equipment by power utilities (*Lopez et al. [1997]*) resulting in fewer power outages due to lightning.

From the point of view of weather prediction, satellite observations of lightning could be of great importance. Lightning is an indicator of moist convective processes. Where there is lightning, there are likely deep convective clouds (though the opposite is not always true). There is much room for improvement in the parameterization and/or representation of convective processes in models used for numerical weather prediction. Lightning flash rates, as observed from space, show possible relationships to many storm parameters, such as total ice content (*Christian and Latham [1998]*), updraft strength

(*Schroeder and Baker [1999]*; *Bondiou-Clergerie et al. [1999]*), vertical mass flux (*Schroeder and Baker [1999]*), and convective rainfall (*Tapia et al. [1998]*; *Reuter and Kozak [1999]*). If such relationships do indeed exist and can be quantified, they could be used to produce real-time, global or regional distributions of hard-to-measure atmospheric properties such as latent heating. These distributions can then be assimilated into weather-prediction models to improve on forecasts (*Chang et al. 1999*). Satellite lightning data, used in conjunction with other meteorological data, such as radar or GOES imagery, can be used to track the development, severity, and location of storms and can be a great help in nowcasting situations (*Turman [1978]*; *Roohr and Vonder Haar [1994]*; *Christian and Latham [1998]*; *Tapia et al. [1998]*).

Unlike ground-based detection systems, satellites have the advantage of a much more global point of view. Lightning can be detected over remote or mountainous areas, where radar coverage is problematic. Depending on whether the parent storms are influenced by continental or oceanic air masses, satellite lightning data could be of great use in the prediction of flash floods (*Tapia et al. [1998]*; *Areitio et al. [1999]*; *Petersen et al. [1999]*; *Soula et al. [1999]*) and other potentially hazardous phenomena. Optical satellite lightning data can also be used to identify preferred storm locations and seasonal weather patterns in areas such as the Himalayan mountains (*Boeck et al. [1999]*) which would otherwise be very difficult to study.

Ground-based cloud-to-ground location networks (such as the NLDN) have led to improved lightning and thunderstorm duration climatologies. Previous climatologies were based on "thunderstorm days"—a measurement that relies on the detection of thunder at weather observing stations (*Changnon [1993]*; *Huffines and Orville [1999]*). The improved climatologies can be used to track short and long-term changes in thunderstorm location and intensity, to understand what physical processes control the frequency and occurrence of convective storms, and to assess risk related to thunderstorms (*Changnon [1993]*; *Zajac et al. [1999]*). Optical flash data from satellites could improve further on the NLDN climatologies of thunderstorm occurrence and duration, as satellite detection is not biased toward continental regions, can detect cloud flashes as well as ground flashes (*Turman [1978]*; *Christian [1999]*), and presumably will remove some of the locational

biases for lightning flash density that exist with systems like the NLDN (*Huffines and Orville [1999]*). These much improved climatologies for such things as lightning flash-rate and location could allow for more accurate monitoring of long and short-term variations in lightning activity across the globe (*Turman [1978]*). These global variations can be correlated with other climate-change indicators, such as wet-bulb land and sea surface temperatures (*Beasley [1995]; Reeve and Toumi [1999]*). Short and long term variations in the seasonal and geographical distribution of lightning are thus possible indicators of how weather patterns and related hazards, such as fires ignited by CG lightning, may change as a result of global warming (*Beasley [1995]; Price and Rind [1994b]; Reeve and Toumi [1999]*). Lightning also plays a key role in the natural formation of Nitrous Oxides (NO_x), which are in turn important for atmospheric ozone. Therefore, satellite climatologies of lightning could also show how changes in weather patterns due to global warming may have an affect on atmospheric composition (*Beasley [1995]; Sanger et al. [1999]*).

Though it may seem esoteric in comparison to the study of terrestrial lightning, there are good reasons to study lightning on Jupiter. On Jupiter, lightning is thought to be an indicator of moist convective processes (*Ingersoll et al. [2000]; Little et al. [1999]*). The detection of lightning (and its frequency and location) can provide clues to understanding the meteorology, atmospheric dynamics, and cloud microphysics in Jovian storms (*Levin et al. [1983]; Rinnert [1985]; Little et al. [1999]; Ingersoll et al. [2000]; Gierasch et al. [2000]*). The presence of lightning on Jupiter and its probable relation to the presence of water clouds and moist convection, could be an important link in determining the planet's total water budget. This, in turn, is important for theories regarding how such giant planets form (*Little et al. [1999]*), and in the end could have implications for theories regarding the formation of the solar system itself. On Jupiter, as on Earth, the chemical processes that take place within lightning channels can be important in the production of certain trace gasses, and can help explain the presence and concentrations of some atmospheric constituents (*Levin et al. [1983]; Rinnert [1985]; Little et al. [1999]*). Lastly, the study of lightning on Jupiter is important because it can be related to our understanding of the physical processes behind storm electrification and

lightning discharges here at home. These processes are by no means completely understood; the atmosphere of a planet like Jupiter, which is in some ways similar to and in some ways very different from that of Earth, provides a ready-made laboratory in which to test theories of cloud electrification and lightning. In the end, this could lead to a better understanding of the physical and dynamical processes occurring in the atmospheres of both planets, and also to a better understanding of lightning and cloud electrification in general.

With all of this in mind, this study seeks to take a comparative-planetology approach to the study of lightning on both Earth and Jupiter. As most of the Jovian lightning data is spacecraft-based and optical in nature, this study is primarily interested in how the optical data from lightning, as seen from above the storms using a satellite-based observation platform, can or cannot be related to flash-type, flash polarity, and various other lightning flash characteristics. The focus will be Earth-based, using optical lightning data from the Fast on-Orbit Recording of Transient Events (FORTE) satellite. Of particular interest are optical signals with estimated optical source power greater than 10^{11} W (signals that were termed "superbolts" by *Turman* [1977]), since analysis of Jovian lightning data indicates that many of the lightning flashes detected at Jupiter had optical power characteristics in this range (*Borucki et al.* [1982]; *Ingersoll et al.* [1998]; *Little et al.* [1999]).

This dissertation is organized in the following manner. Chapter two provides background information on terrestrial satellite lightning studies and the work that has been done to study lightning on Jupiter from spacecraft-borne instruments. Chapter three gives the motivations behind this study, and states the specific questions to be addressed. Chapter four describes the three different types of instruments that are used in this study, namely the Photodiode Detector (PDD) aboard the FORTE satellite, the National Lightning Detection Network (NLDN), and the Lightning Mapping Array (LMA) from the New Mexico School of Mines and Technology. Chapter five discusses how data from the NLDN were used as ground truth for the PDD in order to investigate the possible relationship between estimated source power of satellite events and lightning flash-type and polarity. Chapter six discusses a case study from June 25, 2000 when the PDD, the LMA, and the NLDN all made simultaneous observations of the same storm, and investigates the

possible relationships between detection of lightning by the PDD and the physical dimensions of the lightning flash. Chapter six also discusses how observations by the three different observing systems relate to each other. Chapter seven gives a summary and conclusions, and discusses what the next steps might be for future work.

CHAPTER 2

STUDIES OF LIGHTNING USING SPACEBORNE PLATFORMS

2a. TERRESTRIAL SATELLITE LIGHTNING STUDIES

Terrestrial satellite studies of lightning began in the 1970's. Satellite-borne instruments provided a much wider vantage point than that available from the ground or even from aircraft, and expanded the state of knowledge regarding how lightning is distributed over the globe. Though terrestrial satellite data was and is in some ways much more plentiful than the amount of data that has been collected at Jupiter, it is also somewhat limited by the nature of the instruments and missions flown.

The first terrestrial satellite lightning studies used optical sensors on Orbiting Solar Observatory satellites, but due to sunlight or moonlight reflections these sensors could only detect lightning during nighttime conditions with a new moon (*Turman [1979]*). The orbit of the Vela satellite allowed the observation over the whole earth during night and day, but the detection threshold of the optical sensor was such that only the brightest flashes could be recorded (*Turman [1977]*). The Defense Meteorological Satellite Program (DMSP) missions collected data over the whole earth, but only at local midnight with the "SSL" sensor (*Turman [1978]*), and along a ground-track footprint at dawn and dusk with the PiggyBack Experiment (PBE) (*Turman and Edgar [1982]*). The SSL was able to detect a

wider range of lightning flashes than the Vela optical instruments, but operational constraints and "conflicting operational priorities" were such that only a small amount of data was collected. The PBE collected approximately 30,000 lightning "triggers" but the dawn/dusk nature of the observations prevented an evaluation of the optical lightning characteristics over the entire diurnal cycle.

More recently, missions to study lightning from space have been flown by both NASA and Los Alamos National Laboratory. NASA's Optical Transient Detector (OTD) could detect lightning during both nighttime and daytime light conditions, but due to the nature of its orbit this instrument sampled the earth on a 55 day cycle, and could not be used to investigate meteorological phenomena with periodicities shorter than 55 days (*Christian and Latham [1998]; Christian [1999]*). NASA's current Lightning Imaging Sensor (LIS), is a part of the Tropical Rainfall Measurement Mission (TRMM). The LIS improves on the 50% detection efficiency of the OTD, but as a part of the TRMM mission, is focused on the tropics and can sample lightning activity only between 35° N latitude and 35° S latitude (*Christian [1999]; Christian et al. [1999b]*). Los Alamos National Laboratory's current lightning measurement mission is aboard the Fast On-Orbit Recording of Transient Events (FORTE) satellite. FORTE carries both optical and radio frequency (RF) lightning detection sensors, and was designed to observe lightning over the entire diurnal cycle. However, the increased background brightness of the sunlit Earth is such that the FORTE optical sensors operate at much reduced sensitivity during the day (*Suszcynsky et al. [2000]; Kirkland et al. [1998]; Suszcynsky et al. [1999]*).

The terrestrial satellite studies of the 1970's and early 1980's enabled the generation of more reliable global lightning distribution maps in terms of space and time than those that could be made with ground-based observations. Optical studies also allowed for a characterization of optical power distributions for lightning flashes that could be detected from space, and an estimation of global flash rates.

Observation of over 7,000 flashes from 1,000 storm complexes made with the Orbiting Solar Observatory (OSO) satellites produced good nocturnal lightning maps; from which it was possible to conclude that the bulk of lightning activity is located over land (*Turman [1979]*). Worldwide lightning occurrence data was improved further by the results from the DMSP PBE sensor. This sensor observed lightning over the globe at

local dawn and local dusk, and was able to observe optical lightning signals with far more sensitivity than the Vela or the OSO missions (*Turman [1979]*). Global lightning distributions from the PBE showed several interesting characteristics. The PBE data seemed to confirm the idea that lightning occurred preferentially over land masses, although interestingly, they found that a greater fraction of global lightning activity occurred over the ocean at dawn (37%) compared to the amount of global lightning activity which occurred over the oceans at dusk (15%) (*Turman and Edgar [1982]*). It was also seen that the latitude of peak lightning activity moves to the north and south seasonally with the sun's position. The dawn/dusk observations by the PBE also showed that the latitudinal "bands" of greatest lightning activity marched northward and southward with the seasons. The areas of greatest lightning activity were in good agreement with lightning-intensive areas identified by other observational methods (*Turman [1979]*).

Data from the Vela and DMSP SSL sensor were of use for categorizing the optical power distributions for lightning detected by a space-borne platform. Observations by the Vela satellite were such that only very bright flashes (with optical source power greater than about 3×10^{12} W) (*Turman [1977]*; *Turman [1979]*). These bright flashes were termed "superbolts" by Turman in 1977, and will be discussed in detail in the next section. The DMSP SSL sensor observed lightning storms during 10 of its 15 operational orbits and recorded approximately 10,000 lightning flashes from 24 storm complexes, along with corresponding visible and infrared cloud imagery (*Turman [1978]*). Frequency of occurrence for peak lightning power was obtained in the range of 10^8 – 10^{10} W. The median source power was on the order of 10^9 W, and approximately 2% of all recorded flashes had a source power greater than 10^{10} W. The global flash rate from the SSL data was determined to be approximately 2 flashes per km^2 per year (*Turman [1978]*). The PBE data were used to determine a global flash rate of 40–120 flashes per second, with a seasonal variation of about 10% (*Turman and Edgar [1982]*).

After the DMSP studies, the subject of measuring lightning from space was not revisited until NASA launched the OTD in 1995, and NASA and Los Alamos National Laboratory launched the LIS aboard the TRMM satellite, and the FORTE satellite in 1997.

respectively. Lightning climatologies from the OTD and LIS added support for the strong continental bias of terrestrial lightning (*Kawasaki and Yoshihashi [1999]*). Analysis of the OTD data also showed that radiance of lightning optical signals tended to be greater over the oceans, smaller when lightning activity is high, and greater in the northern hemisphere winter than summer (*Christian and Latham [1998]*). LIS and OTD global lightning maps revealed more information regarding differences in oceanic and continental lightning. Though lightning is less frequent over the oceans, it seems that the size of the optical flashes in the LIS images (a similar concept to the "spot" sizes discussed above for the Voyager and Galileo images of Jovian lightning) tended to be greater for oceanic lightning, and that the radiance of oceanic flashes tends to be higher than the radiance of continental flashes (*Boccippio et al. [1998]*). Global flash rates determined from the OTD are ~40 flashes per second, which is considerably lower than the commonly cited historical reference of 100 flashes per second (*Boccippio et al. [1998]*). Collection and analysis of LIS data is ongoing.

The instrumentation aboard Los Alamos National Laboratory and Sandia National Laboratory's FORTE satellite includes two sensors to detect the optical emissions from lightning. A CCD array called the Lightning Location System (LLS) provides a geolocation of detected lightning events, and a Photodiode Detector (PDD) provides optical power-time curves for detected lightning events. The satellite also carries a system of three broadband radio receivers to detect RF emissions from lightning. Analysis of more than 600,000 optical triggers from the first 18 months of operation for the FORTE satellite agrees favorably with the geographic and seasonal results found in earlier satellite studies. The FORTE data also allows for the characterization of the peak optical source power distribution of the detected lightning. In general agreement with the results from the DMSP missions, it was found that the median peak optical power of the lightning optical signature is $\sim 1 \times 10^9$ W (*Kirkland et al. [1998]*; *Kirkland [1999]*, *Kirkland et al. [2001]*). It was also confirmed that flashes with energies greater than 10^{11} W (Turman's "superbolts") could be observed by FORTE. Kirkland's results regarding superbolts and a summary of the work that has been done to take advantage of the FORTE's dual-phenomenology (optical and RF) approach to understand the optical data better are discussed in Section 2b

and Section 2c respectively.

2b. TERRESTRIAL “SUPERBOLTS”

In the analysis of lightning data from the Vela satellites, *Turman [1977]* noticed a class of lightning signals with peak optical source powers more than 100 times greater than that of average lightning signals. These "bright" flashes, with peak optical source powers of $\sim 10^{11}$ W or greater, have been observed in subsequent satellite studies (*Turman [1978]*; *Rhodes et al. [1998]*; *Kirkland et al. [1998]*; *Kirkland [1999]*; *Kirkland et al. [2001]*), and represent the top 1-2% of all observable flashes. In the Vela data, "superbolts" were detected worldwide with most the most frequent occurrence over the North Pacific Ocean. Based on the geographic and seasonal distribution of superbolts, *Turman [1977]* postulated that these bright optical signatures may be associated with intense, positive CG events in winter thunderstorms, and with severe thunderstorm activity in the warmer seasons. However, *Turman* lacked the data necessary to examine the question in detail.

Kirkland [1999] revisited the superbolt question using data from the FORTE Photodiode detector, which could record the power-time histories for the optical lightning flash. *Kirkland* analyzed approximately 18 months of PDD data, with about 600,000 lightning triggers. He found that "superbolts" are globally ubiquitous, occurring in regions of the globe where lightning activity is expected, and that they seem to be associated with both negative and positive CG events. *Kirkland* postulated that such "superbolts" simply represent the upper tail of the source power distribution for normal lightning.

2c. TERRESTRIAL LIGHTNING STUDIES USING FORTE

Because the FORTE satellite carries both radio-frequency and optical instruments aboard a single platform, it has an advantage of being able to compare how the different types of instruments observe the same lightning event. Such comparisons are important when one considers the question of how the different emissions from lightning, as seen

from space, may relate to the physical characteristics of the lightning itself. This dual-phenomenology approach is also important if one is to consider how the physical processes responsible for either the optical or radio-frequency signals may differ. This in turn will make it possible to glean greater physical significance from comparisons between the two types of data sets. The focus of the summary presented in this section will be on the data from the FORTE PDD, how FORTE's dual phenomenology approach has been used to characterize the optical signals, and how the unique, multiple instrument character of the FORTE mission has been used to further the understanding of how scattering of light through clouds may affect the optical signals seen by a satellite-borne sensor.

Kirkland et al. [2001] present an overview of the FORTE Photodiode Detector (PDD), and a summary of its data. Their overview considered approximately 687,000 PDD events classified as lightning emissions, which were collected between the launch of the FORTE satellite in 1997 and mid-December 2000. The median peak power for PDD events was found to be $\sim 1 \times 10^{10}$ W, consistent with the results of *Turman (1978)*. This is to be expected, since the instrument flown on the DMSP satellite was very similar to the FORTE PDD. The median optical energy for PDD events was found to be ~ 450 kJ, which agrees well with previous ground-based and aircraft-based measurements. *Kirkland et al.* made estimates of the "effective pulse width" for the PDD power-time pulse. This quantity was calculated by integrating the observed PDD signal over the length of the data-window to obtain the energy of the PDD event, and then dividing this energy by the peak irradiance observed during that time. The median effective pulse width was found to be ~ 590 μ s, and in general the effective pulse width varied inversely with peak optical power. The fact that this relationship could result from varying amounts of cloud-induced extinction and signal broadening due to scattering of light by cloud particles was used to infer that the signals detected by the PDD typically originate from the in-cloud portion of a lightning discharge. *Kirkland et al.* also inferred that the brightness of the PDD event may be due to the amount of intervening cloud between the lightning channel and the spacecraft.

Suszcynsky et al. [2000] examined time-correlated PDD and very-high-frequency (VHF) data from FORTE with two main goals in mind. First, they sought to demonstrate that a dual-phenomenology approach could be used to identify lightning types (CG vs IC)

from space. Second, Suszcynsky et al. sought to use the correlated optical and RF data to study basic lightning emission processes, the effect of clouds on the propagation of transient optical signals, and the general global phenomenology of lightning. They examined PDD and VHF events which occurred between September 5, 1997 and April 15, 1998. During this time, the VHF receivers and the PDD were operated autonomously, and the coincidence rate was therefore affected by the triggering and sensitivity biases of the different instruments. It was found that VHF-optical pairs could be characterized as being associated with either CG or IC events based on the optical and VHF waveforms, but that these characterizations could be made based mostly on the characteristics of the associated VHF spectrograms. For a typical IC flash, the FORTE VHF data was generally characterized by impulsive, broadband bursts and the optical data was often highly structured. For CG flashes, the VHF portion of the optical-VHF pair could be associated with either the stepped leader, the attachment process, or the actual return stroke (for the case of an initial return stroke detection) or with the dart leader processes (for the case of a subsequent return stroke). For both initial and subsequent return stroke cases, the optical portion of the optical-VHF pair was determined to be produced by the in-cloud portion of the discharge. The optical signals lagged behind the arrival of the associated VHF signals by a mean value of $243 \mu\text{s}$. This time-difference was determined to be due to the time for the lightning discharge to propagate from the attachment point to an in-cloud region (with a mean value of $105 \mu\text{s}$) and an additional time-delay due to the scattering of light through the clouds. This scattering delay was determined to be $\sim 138 \mu\text{s}$ (representing an additional 41 km path length) for light from CG events, a result that is consistent with previous studies which modeled the propagation of light through clouds (*Thomason and Krider [1982]*). One unexplained feature of the PDD/VHF pair data set compiled by Suszcynsky et al. is the near absence of IC events. Because IC flashes occur more commonly than CG flashes, the lack of IC events in the PDD/VHF pair data would imply that FORTE preferentially detects CG events. Yet, when the optical or VHF data sets are considered individually, detection seems to be preferential to IC events. Whether the preference for CG events among the VHF/optical pairs is due to some physical cause, the different triggering biases of the VHF receivers and the PDD, or some combination of the two remains to be investigated.

Light et al. (2001b) have expanded further upon the work of Suszcynsky et al.

(2000) by examining 222 PDD/VHF pairs with longer (6-8 ms) record times. These data were collected during January 2000, with the PDD and radio-frequency receivers slaved to the FORTE LLS (meaning that PDD and VHF records were recorded whenever a lightning event was detected by the LLS). The advantage of using the PDD and VHF instruments in slave mode was that a location was then available for every PDD/VHF pair, and the triggering was due to the detection biases of only one instrument. The advantage of the longer PDD and VHF record times was that each record contained multiple VHF and optical impulses. Light et al. characterized the lightning type of each event pair using the VHF signatures (according to the discrimination techniques outlined by *Suszcynsky et al.* [2000]). They found that the rate of PDD/VHF coincidence depended on the type of the lightning discharge. Nearly 100% of VHF signals from negative return strokes appeared to have a clearly associated optical pulse. Only 50% of VHF signatures from impulsive IC events had an associated optical counterpart, and IC lightning events often showed complicated, nearly continuous VHF and optical emissions which did not clearly correlate with each other. The intensities of the VHF and optical pulses did not show a well-defined relationship for any lightning type. Many of the VHF records contained pulse pairs which were due to the radiated pulse and its reflection from the ground. In conjunction with the locations from the LLS data and the position of the satellite, these pulse pairs were then used to estimate the heights of several IC events. The height distribution ranged from 6-13 km, with the number of events decreasing sharply at higher altitudes.

Suszcynsky et al. [2001] examined optical lightning events that were simultaneously observed by the FORTE PDD and the FORTE LLS. When used together, the high temporal resolution of the PDD data and the high spatial resolution of the LLS give a detailed picture of the temporal and spatial characteristics of terrestrial lightning as seen from space. The coordinated data were also used to investigate how the PDD waveforms and LLS pixel characteristics may relate to intensity of the lightning event and subsequent scattering of the optical emissions. When the LLS pixel multiplicity was compared to PDD detected event intensity and PDD optical pulse widths, the results strongly suggested that, in general, LLS pixel multiplicity is closely related to the detected intensity of the optical lightning event and its horizontal extent with respect to source-satellite line of sight. On average, lightning events with higher detected optical energy

densities seemed to illuminate more cloud area than lightning events with relatively “weak” detected energy densities, resulting in a greater number of LLS pixels that were activated.

Expanding on the work of *Thomason and Krider [1982]*, *Light et al. (2001a)* used a Monte Carlo approach to model the transport of light through clouds, with the specific goal of addressing the effect of scattering on the detection and characteristics of optical waveforms collected by satellites. This modeling study differed from previous cloud-scattering model studies in that it considered both finite and infinite cloud geometries and used simulated emission sources with arbitrary spatial and temporal properties. The model was designed so that direct comparisons between model results and the optical power-time history waveforms collected by the FORTE PDD could be made. It was found that the position of the lightning event within the cloud, relative to the position of the observer can result in more than an order of magnitude variation in observed peak optical intensity of the event. It was also found that the combination of cloud shape and viewing angle could have as great an effect on observed lightning intensity as the cloud optical depth. This modeling study supported the conclusion of *Kirkland et al. [1998]*: events with larger than average peak brightness and small effective pulse widths show little evidence of having been broadened due to scattering, and that this is probably due to a relatively unobstructed line of sight between the lightning event and the satellite. The study also examined the subset of PDD events with very wide pulse widths (> 1 ms wide), and found that these events were likely due to “temporally extended” IC flashes.

2d. JOVIAN LIGHTNING STUDIES

Though the existence of lightning was theorized to explain the abundance of certain trace gasses in the Jovian atmosphere, lightning on Jupiter was not observed directly until the Voyager 1 spacecraft visited the planet in 1979. Night-side photographic observations revealed extensive clusters of optical flashes attributed to lightning (*Cook et al. [1979]*; *Borucki et al. [1982]*). In addition to its camera, Voyager 1 also carried a plasma-wave instrument that measured low frequency plasma waves and radio emissions in the magnetosphere of Jupiter. During the spacecraft's closest approach to the planet.

dispersive radio-frequency signals identified as "whistlers" were detected in several groups (Gurnett *et al.* [1979]). On Earth, such RF signals from lightning (known as "whistlers" because of the sound they make when observed on audio frequency equipment) have been observed and characterized. These signals can travel long distances along planetary magnetic field lines and, because of their well known dispersion characteristics, can be distinguished from other signals even in a noisy environment. The source regions for such whistlers can be determined by tracing the magnetic lines from the observation point back to the ionosphere (Levin *et al.* [1983]; Kurth *et al.* [1985]). Jovian whistlers, once identified as such, provided validation of the interpretation that the bright spots seen on the Voyager images were in fact from lightning (Gurnett *et al.* [1979]; Levin *et al.* [1983]; Kurth *et al.* [1985]; Borucki and Williams [1986]). Based on the optical and RF data from Voyager 1, a number of conclusions were drawn regarding the energetics, flash rates, geographic locations, and atmospheric depth of Jovian lightning.

Borucki *et al.* [1983] found that the optical energy radiated per flash was similar to terrestrial "superbolts", and that the total radiated energy per flash was 1.7×10^{12} J. This value was determined based only on those flashes that were of great enough optical power to be above the detection threshold of the camera. Whistler evidence indicates that the majority of Jovian flashes may have been too dim to be seen by the camera; hence, it was thought that the 1.7×10^{12} J value was much larger than the average total energy per flash that would be determined if all flashes could be taken into account (Borucki *et al.* [1982]; Levin *et al.* [1983]). Based on the optical data and an estimate of optical efficiency of 1.5×10^{-3} , and under the assumption that the energy distribution for Jovian and Terrestrial flashes are the same, Borucki *et al.* were able to determine an energy dissipation rate of 0.4×10^{-3} W/m². This is similar to the terrestrial value, for which estimates are between 0.2×10^{-3} and 0.7×10^{-3} W/m² (Borucki *et al.* [1982]). More recent interpretation of the whistler data from Voyager 1, which focused on the determination of whistler wave amplitudes and a reexamination of the propagation characteristics of Jovian whistlers, estimated the mean radiated power per flash in the RF range (0-20 kHz) to be 4.5×10^6 W (Hobara *et al.* [1995]). Further refinements in ray tracing and amplitude determination,

assuming that all whistler-producing events occurred at a pressure of 1 bar (sea level pressure on Earth), produced radiated power per flash in the range 10^2 - 10^5 W. The terrestrial value over the same bandwidth, 10^4 W, lies in this range.

The Voyager 1 optical data implied a flash rate of 4 flashes per km^2 per year, again assuming that the "superbolt-like" Jovian flashes detected by the camera were at the upper tail of the energy distribution, and that the energy distributions for Terrestrial and Jovian lightning were the same (*Borucki et al.* [1982]). Whistler evidence implied a flash rate as high as 40 flashes per km^2 per year (*Borucki et al.* [1983]; *Levin et al.* [1983]). This range of 4-40 flashes per km^2 per year was somewhat higher than the terrestrial value of 2-7 flashes per km^2 per year (*Borucki et al.* [1982], *Levin et al.* [1983]). However, *Kurth et al.* [1985] pointed out that the upper bound estimate of ~ 40 flashes per km^2 per year was based on the assumption of ducted whistlers (which travel parallel to the magnetic field lines). In the non-ducted case, whistler propagation could be at angles as large as 19° with respect to the field line, meaning that the area for source locations from which whistlers could travel to the spacecraft could be much larger, and the corresponding estimates of lightning flash rates would decrease (*Kurth et al.* [1985]). Other difficulties in estimating lightning flash rates from whistler data, such as estimates of the fraction of lightning that occurred in the source area without producing whistlers and estimates of the fraction of whistlers that were too weak to be detected, also make this whistler-derived upper bound on flash rate uncertain to within an order of magnitude (*Levin et al.* [1983]).

Geographic locations for both the optical and RF lightning data from Voyager 1 have been determined. The optical lightning flashes were observed from 30° to 55° north latitudes, with concentrations of flashes at 30° , 45° , 50° , and 54° latitude (*Levin et al.* [1983]), and at a geographic longitude of about 25° - 50° (*Kurth et al.* [1985]). The optical lightning data seemed to show a preference for the northern hemisphere, and seemed to show a preference for latitudes which correspond with westerly jets (*Levin et al.* [1983]). With just the Voyager 1 data, it was impossible to determine if this geographic distribution of optical flashes from lightning represented the true geographic distribution of Jovian

lightning or whether the distribution was more a reflection of observation strategy and camera sensitivity (*Levin et al. [1983]*). The Voyager 1 data were also limited by camera pointing-angle uncertainty, a lack of visible reference points in the images, and a complicated slewing of the camera during exposure that created an uncertainty in lightning location of about 3° in latitude and 2° in longitude (*Borucki and Magalhaes [1992]*). Whistlers were observed in both hemispheres at a latitude of about 66° or higher, and over a range of longitudes (*Kurth et al. [1985]*; *Hobara et al. [1997]*). As was noted above, the location of the whistler source area could be off by as much as 19° , so considerable uncertainty remains in the determination of lightning locations via the whistler method. When the locations of the optical lightning flashes and the whistler source locations were compared, it was found that the two did not coincide (*Kurth et al. [1985]*). However, this was no cause to doubt the identification of either the bright spots on the night-side photographs or the whistler source regions as lightning, since it was likely that the optical and RF observation methods were simply observing different lightning sources (*Kurth et al. [1985]*). In fact, *Kurth et al.* reported that it would have been impossible to detect whistlers which corresponded to the optical flash observations because no wide band RF data was recorded at the longitude and radial distance from Jupiter necessary for such a measurement. *Borucki et al. [1982]* also pointed out that it was likely that the majority of the lightning events detected by RF data were not seen by the Voyager camera because the flashes were either too dim or too deep in the clouds for the amount of light that reached the camera to be above the detection threshold.

Based on the Voyager 1 data, and the apparent coincidence between the optical lightning locations and the latitudes of westward-moving jets in the Jovian atmosphere, *Cook et al. [1979]* suggested that lightning occurred in water clouds, and was associated with moist convective motions driven by latent heat release (similar to terrestrial convective thunderstorms). *Cook et al.* based their determination on the idea that if the lightning were occurring in the upper ammonia clouds of Jupiter, that it would have been much more easily detected by the Voyager camera. *Borucki and Williams [1986]* explored this idea further by comparing flash spot sizes on the Voyager images with intensity distributions calculated using various assumptions regarding the altitude of the flash and a Monte Carlo

model to describe the scattering through clouds, aerosols and other Jovian atmospheric constituents. Because the Voyager 1 images are all multiple exposures, most of the bigger lightning "spots" represented a composite of multiple flashes. To get around this problem, Borucki and Williams used data from small, non-overlapping spots which were assumed to be from single flashes. The best agreement between modeled spot sizes and measured spot sizes was found for lightning activity occurring in a lower cloud centered at a depth of 5 bars. This corresponds to temperatures near 0° C and is consistent with the depth of water clouds predicted by models of the Jovian atmosphere . Calculated spot sizes for lightning occurring in the upper ammonia clouds were much smaller than observed spot sizes, which also implied that the lightning sources for the Voyager images occurred at a much deeper level. This investigation supported the theory that on Jupiter, as on Earth, lightning discharges are a possible indicator of moist convective processes.

Hobara et al. [1997] used the whistler data to make some characterizations of Jovian flash type. By examining peak frequency in the RF frequency spectra for flashes of various intensity, Hobara et al. concluded that RF intensive lightning, with a peak frequency less than 1 kHz, had similar characteristics to upward current strokes on Earth. They also proposed that many other events may have frequency spectra characteristics similar to terrestrial CG return strokes. It should be noted, however, that these comparisons were based on only a few events and are by no means conclusive.

The Voyager 1 data confirmed the existence of Jovian lightning. It also seemed to imply that the energetics, power distributions, and flash rates for Jovian lightning are similar to terrestrial values. In addition, Voyager 1 data implied that the processes behind terrestrial and Jovian lightning may be similar, with charge generated by convective motions in water clouds, and that these storms had preferred latitude locations. It should be stressed that these conclusions are based on an extremely limited set of data. The Voyager images represent approximately 380 seconds of observation time (*Borucki and Magalhaes [1992]*). The whistler data is made up of 90 whistler events, culled from 141 forty-eight second wide-band frames (*Kurth et al. [1985]*). Though the interpretation of these data seemed convincing, a larger data set is clearly needed before any of the results can be considered to be conclusive.

The optical lightning data from Voyager 2 expanded the data set somewhat. Three

96 second exposures from the wide angle camera on Voyager 2, originally obtained to study the Jovian ring, showed bright spots on the night side of the planet that could be attributed to lightning (*Borucki and Magalhaes [1992]*). The Voyager 2 images were taken with a narrow band violet filter, which reduced the camera response by a factor of 7.2 relative to the clear filter used in the Voyager 1 images. Therefore, the Voyager 2 images are dimmer and show only the brightest areas of lightning activity, but they are improved over the Voyager 1 images in that they have a uniform sensitivity over a much larger area of the the planet's night side. Also, in each of the three Voyager 2 images, the illuminated limb of Jupiter is identifiable. The presence of the well-defined planetary limb in these images allowed for accurate determination of the latitudes and longitudes for the lightning events, whereas for the Voyager 1 images there was much more uncertainty in the location of lightning events, due to the lack of a visible reference point. Approximately 12 separate storms, occurring more or less simultaneously, have been identified in the Voyager 2 images.

The observed energies for the Voyager 2 images were much greater than the observed energies for the Voyager 1 images. This was to be expected, because of the greater distance of the spacecraft from the planet, and the increased detection threshold of the Voyager 2 camera compared to that of Voyager 1. Individual flashes could not be distinguished in the Voyager 2 images, so flash rates and energetics for single flashes could not be determined. However, Borucki and Magalhaes made estimates of the average energy dissipation rate of lightning based on the optical energy represented in each image, the area covered by each image, and the exposure time. They determined the average energy dissipation rate from lightning to be approximately 50% greater than the estimate based on the Voyager 1 images. This result was surprising, since the Voyager 1 images included flashes that would have been too dim to be detected in the Voyager 2 images; possible explanations for the difference in energy dissipation rates included a difference between the laboratory-derived spectrum for Jovian lightning and the actual Jovian lightning spectrum, or variations in lightning activity with time (as the Voyager 2 images were taken 128 days after the Voyager 1 images).

Of the 12 storms imaged by Voyager 2, most were located in a narrow latitude band at $\sim 49^\circ$ North latitude. One storm occurred at $\sim 60^\circ$ North Latitude, and two storms

occurred at near 14° N latitude. No lightning was observed in the southern hemisphere, though a relatively large portion of this hemisphere was covered by the Voyager 2 images. However, much of the southern area covered was between 0° and about 30° S latitude, and if lightning is expected at high latitudes in the Jovian atmosphere, southern hemisphere lightning would not necessarily have been detected by these images. Based on the geographic locations of the Voyager 2 lightning data, Borucki and Magalhaes inferred that Jupiter's internal heat source was the most likely driving factor behind Jovian convection (rather than the absorption of sunlight, as on Earth), and that the predicted redistribution of this internal heat toward the poles may explain the fact that lightning seems to occur preferentially at higher latitudes. The lightning activity that occurred near 14° N latitude was restricted to a special "disturbed" region of the Jovian atmosphere. It was theorized that the storms in the "disturbed" region may be due to lifting motion caused by westerly flow over a "hill" in the potential temperature surface at the 5 to 10 bar level. Borucki and Magalhaes also made attempts to correlate centers of lightning activity to cloud features at the same locations in the dayside Voyager 2 images. No unusual cloud features were found to be associated with the bright band of lightning activity at 49° N latitude. Because convective activity in the lower water cloud would not necessarily produce observable variations in the ammonia cloud deck above, this finding was consistent with the theory that lightning is generated in Jovian water clouds.

Yair et al. [1995a; 1995b] used an axisymmetric cloud model to investigate the dynamics and microphysical processes involved in Jovian moist convection, and to investigate the generation and separation of charge in Jovian thunderclouds. *Yair et al.* [1995a] found that microphysical processes in the Jovian clouds were very efficient, producing large precipitation particles on relatively short time scales. Their model showed that Jovian thunderclouds could have a vertical depth as large as 40 to 50 km, and could reach above the 2 bar pressure level. Modeled Jovian thunderclouds were very dense cumulus clouds, with updraft speeds of 50 m sec⁻¹ in the development stage and a mixed phase region composed primarily of ice particles. *Yair et al.* found that high enough concentrations of graupel and hail should exist in the mixed region for cloud electrification to be possible. When electrification was added to the axisymmetric cloud model (*Yair et*

al. [1995b]), it was found that non-inductive graupel-ice charging mechanisms could produce electric fields large enough to exceed breakdown values quite rapidly. Lightning flashes were assumed to neutralize a 20 km channel, and calculated flash rates suggested that the Voyager 1 images may have captured multiple superimposed flashes, instead of single flashes, because of the long exposure time. Energies for simulated Jovian lightning flashes were found to be on the order of 10^9 to 10^{10} J in the optical range, which is in agreement with energy estimates based on the Voyager 1 and Voyager 2 images.

Unlike the Voyager missions to Jupiter, which captured evidence of lightning mostly by serendipity, the Galileo mission to Jupiter contained observation strategies and instrumentation designed to investigate Jovian lightning directly. The Galileo probe, which descended into the Jovian atmosphere in 1995, carried a lightning and radio emission detector (LRD). The LRD detected a lightning-like radio source at a distance of about 15,000 km from the detector, but otherwise did not detect much in the way of signals from lightning (*Yair et al.* [1998]; *Little et al.* [1999]). Most of the lighting data from the Galileo mission were optical in nature. The Galileo orbiter carried a Solid State Imager (SSI) which had a better response at some optical wavelengths than the Voyager cameras, and also was able to image the the night side of Jupiter from above the terminator. The ability to obtain images when half of the planet below the spacecraft was sunlit and half was in darkness allowed for storm locations on the dayside of the planet to be investigated much closer in time to the observation of the night-side lightning flashes. Because Galileo was also an orbiter, it was able to image Jovian lightning with a much larger number of frames over a longer period of time and was able to survey more of the planet, and some of Galileo's images have better spatial resolution than the Voyager images. Galileo collected optical lightning data during two orbits in 1997 (*Little et al.* [1999]; *Ingersoll et al.* [1998]).

Lightning storms were found at a variety of latitude bands, with particularly intense regions at $\sim 50^\circ$ North and South. Storms were found in both the northern and southern hemispheres, though the northern hemisphere was found to have more lightning activity overall. The bands of lightning activity were found to correspond to areas of cyclonic shear near the centers of westward jets (which supported the geographic distribution

implied by the Voyager data) (*Little et al.* [1999]). In certain Galileo images, the camera "scanned" westward while the shutter was open, so that individual flashes from one storm could be separated in the frame. These flashes were distributed along a horizontal line in the frame, and allowed for estimates of single-flash energies. The recorded optical energies were once again similar to terrestrial "superbolt" values (*Ingersoll et al.* [1998]), though the largest single-flash energy recorded by Galileo was 2.5 times greater than the largest energies seen by Voyager 1, smaller than the energies of most storm "spots" seen by Voyager 2, and about 3 times greater than terrestrial superbolt values (*Little et al.* [1999]). The shape of the "spots" on the Galileo images was used to estimate the depth of the Jovian lightning activity, under the assumption that the appearance of these spots was the result of scattering from a point source below the cloud tops. It was found that lightning should be occurring at depths within or below the Jovian water clouds, possibly as deep as 8 bars in some regions (*Little et al.* [1999]).

Attempts were also made to associate areas of lightning activity seen in the Galileo images with visible cloud features. These correlations were made possible by the observations of the lightning center locations during both sunlight and nighttime conditions, closely separated in time, and by night-side images of lightning against clouds illuminated by light from Jupiter's moon Io (*Little et al.* [1999]; *Gierasch et al.* [2000]). It was found that lightning centers closely corresponded with bright white cloud features—which have lifetimes on the order of days, and are optically thicker and perhaps as much as 15 km higher than their surroundings (*Little et al.* [1999]; *Ingersoll et al.* [2000]). It was also found that the lightning most likely occurred in water clouds with tops about 50 km below those of the bright white clusters, with a base of the water cloud at about 6 bars (*Ingersoll et al.* [2000]). *Gierasch et al.* [2000] theorized that these Jovian thunderstorms may be similar to terrestrial Mesoscale Convective Complexes. The Galileo images provided further evidence that microphysical processes in convective water clouds are responsible for Jovian lightning, that Jovian moist-convection is driven by the planet's poorly-understood internal heat source instead of sunlight, and that moist convection may be the energy source responsible for forcing larger scale eddy motions in the Jovian atmosphere (*Ingersoll et al.* [2000]).

CHAPTER 3

MOTIVATIONS AND QUESTIONS TO BE ADDRESSED

Optical lightning signatures on Jupiter are similar in brightness to terrestrial superbolts, or perhaps even greater in terms of brightness, energetics, and size. But what does this mean? Does it mean that on both planets these bright flashes are simply at the upper tail of the lightning optical power distribution, or can such optical signatures be related to flash-type, polarity, or height at which the lightning is occurring within the clouds? This is the primary question that this study seeks to address: what, besides the presence of lightning in some form, can be determined from the optical signature of a single flash, or even numerous flashes?

Terrestrial satellite studies have scratched the surface of this question. Unlike the limited data on the planet Jupiter, on Earth flashes have been recorded by the millions. Earth also has the advantage over Jupiter in that we have the ability to observe lightning flashes and their parent storms from above, below, and even in the middle, providing "ground truth", or in some cases "cloud truth", for optical and RF signatures which the satellites see from space. Yet, even with all these observational advantages, many questions remain.

Many studies have investigated the relationship of satellite-detected lightning to such storm characteristics as convective rainfall rates, ice content, updraft strength, vertical mass flux, relationship to difficult-to-measure storm parameters such as latent heating for

use in model initiation, development of storm severity, short and long-term variations in preferred storm location, and even global change. But most current studies, due to the nature of the instruments flown, have concentrated primarily on relating satellite-derived lightning flash rates or flash densities to storm parameters such as those listed above. Little has been done to investigate whether the optical power characteristics of satellite-detected lightning flashes can be related to storm parameters or lightning phenomenology.

This study seeks to advance the satellite study of lightning by investigating the relationship between the characteristics of lightning flashes as seen from space and the characteristics of the lightning discharges themselves. If information can be mined from the power of the recorded optical flash with regards to flash-type (CG vs IC) and discharge location within the clouds, and if this in turn might be related to storm dynamics, the results could be useful in terms of hazard prevention, the tracking and classification of convective storms across the globe, and possibly even the investigation of global climate change. Additionally, it will add to the general level of understanding of storm electrification and the mechanisms of lightning discharge. Finally, terrestrial information can be applied to the interpretation of the relatively limited data on Jovian lightning and could improve inferences regarding the dynamics and microphysics of Jovian storms, the composition of the Jovian atmosphere, and possibly even the formation of the solar system in which we live.

The specific questions to be addressed here are as follows:

- 1) Are “bright” optical events (with estimated source power $> 10^{11}$ Watts, what Turman (1977) called “superbolts”) associated with positive cloud-to-ground flashes?
- 2) Is the estimated source power of a PDD event related to flash-type?
- 3) Why does the PDD detect some flashes but not others? Is this related to the physical dimensions of the discharge?
- 4) Do the PDD and the National Lightning Detection Network see different parts of the lightning discharge, and how does what one instrument sees relate to what the other sees?

CHAPTER 4

INSTRUMENTS

This chapter describes the instruments that are used in this study. Section 4a summarizes the characteristics of the FORTE Photodiode Detector, which is the optical satellite-borne instrument that provided the data being investigated here. Section 4b gives relevant details regarding the National Lightning Detection Network, data from which are used to investigate the flash-type and polarity characteristics of time-correlated PDD events in Chapter 5. Section 4c describes the 3D Lightning Mapping Array operated by the New Mexico School of Mines and Tehcnology, which is used in Chapter 6 to investigate how the physical characteristics of the lightning channels may or may not affect whether a flash is detected by the PDD.

4a. THE FORTE PHOTODIODE DETECTOR (PDD)

The Fast on-Orbit Recording of Transient Events (FORTE) satellite was launched on August 29, 1997. It was designed to address technology issues associated with treaty verification and the monitoring of nuclear tests from space, and is operated jointly by Los Alamos National Laboratory and Sandia National Laboratory. Part of the purpose of the experiment was to understand the nature and variability of transient optical signals that occur naturally, such as those due to lightning. To accomplish this goal, FORTE carries VHF broadband receivers and an Optical Lightning System (OLS) consisting of a CCD

array for imaging and location of optical events (called the Lightning Location System (LLS)) and a Photodiode Detector (PDD) to record the power-time histories of optical transients. FORTE is in a nearly circular, 70° inclination orbit. FORTE orbits at about 825 km altitude and has an orbital period of about 100 minutes.

The FORTE PDD is described in detail by *Kirkland et al.* [2001]. The PDD is a broadband (0.4-1.1 μm) silicon photodiode detector that collects waveforms of amplitude versus time for transient optical signals. The PDD has an 80° field of view which, at an 825 km altitude orbit, translates into a viewing footprint of about 1200 km diameter on the Earth's surface, centered on the sub-satellite point. In its typical configuration, a recorded PDD event is 1.92 ms long, with 15 μs time resolution.

When operating in the internal trigger mode, a PDD event is triggered when the signal exceeds a noise-riding threshold for at least five consecutive samples. (The number of consecutive samples which must exceed the triggering threshold is variable and can be set anywhere from one to thirty-one, but in the PDD's typical configuration this number is set to five.) This protocol eliminates false triggers due to energetic particles. The PDD can also be operated in one of two slave modes. When slaved to the VHF receivers, a PDD trigger is forced whenever a VHF signal is received. When slaved to the LLS, a PDD trigger is forced whenever the CCD array records a pixel event. There is a minimum intertrigger delay of about 4.4ms which results in a ~2.5 ms minimum dead time between successive records. The trigger times for PDD records are GPS (Global Positioning System) time-stamped to a 1 μs precision.

The PDD provides 12 bit sampling with a piece-wise linear dynamic range that covers four orders of magnitude. The sensitivity of the instrument is better than 10^{-5} W/m^2 . Several background compensation modes allow the instrument to detect lightning at night and during the day (with decreased sensitivity).

4b. THE NATIONAL LIGHTNING DETECTION NETWORK (NLDN)

The National Lightning Detection Network (NLDN) began in the late 1980's when

several different networks of lightning location systems were merged together to provide lightning information on a national scale. Data from the merged and upgraded system is managed and distributed commercially by Global Atmospheric Incorporated. The system employs a combination of Time Of Arrival (TOA) and Magnetic Direction Finding (MDF) to locate lightning. A description of these techniques can be found in MacGorman and Rust (1998). A complete description of the NLDN after its 1995 upgrade can be found in *Cummins et al.* [1998]; this information is summarized below.

The upgraded NLDN consists of 106 ground stations. Of these, 59 are original TOA sensors (LPATS-III sensors), and 47 are newer IMPACT sensors (which are a combined technology sensors which use both MDF and TOA techniques at the same sensor, for improved accuracy in lightning location). The stations are located so that each area of the country is covered by both the TOA and IMPACT sensors. The sensitivity and waveform criteria were adjusted on both the TOA and IMPACT sensors so that both sensor types detect CG flashes with similar sensitivity and flash-type discrimination in the upgraded NLDN system.

Data from a subset of the 106 stations are used to compute an optimum lightning location for each flash using a least-squares method to minimize the location error. With the IMPACT sensors, the process determines not only stroke location but also includes an additional term in the error function that includes precise timing information. This improved location algorithm overcomes many of the problems that arise by using either TOA or MDF information alone to locate the flash.

The location accuracy is described as the maximum dimension of a confidence region around the stroke location. For the upgraded NLDN system, the median location accuracy is 500 m. The detection efficiency for flashes with peak current ≥ 5 kA ranges from 80% to 90%, depending on the region. Subsequent strokes in a flash can be detected with approximately 50% detection efficiency. This estimate is based on the assumption that subsequent strokes have peak currents about half as large as first stroke peak currents. Lightning flashes with peak currents < 5 kA can be detected by the NLDN, but their detection efficiency is unknown.

After the 1995 upgrade, the increase in sensitivity and the different waveform criteria have made it such that the NLDN may misidentify a certain number of events with

small positive peak currents (between +5 and +15 kA). These events are classified by the system as positive CG events, but it is likely that a significant fraction of them result from relatively large, long duration in-cloud events. For this reason, Cummins et al. (1998) recommend that the subset of small positive NLDN events be regarded as IC events, unless they can be verified as CG events by some other means.

4c. THE NEW MEXICO TECH LIGHTNING MAPPING ARRAY

The Lightning Mapping Array (LMA), developed by the New Mexico Institute of Mines and Technology, is described in detail by *Rison et al. [1999]* and *Krehbiel et al. [2000a]*. The system is based on the Lightning Detection And Ranging (LDAR) system that was developed for use at the NASA Kennedy Space Center. The LMA measures the time-of-arrival from impulsive VHF radiation at six or more stations and uses the difference in arrival times to locate the source of the radiation pulse.

Each station detects a peak intensity of VHF radiation in the 6 MHz bandwidth of an unused television channel (e.g. channel 3, centered at 63 MHz). The time and magnitude of the peak radiation received during a 100 μ s window is recorded whenever the VHF signal exceeds a noise threshold. The system takes advantage of GPS timing to record the peak signal time with 50 ns accuracy. Events that are strong enough to be recorded by six or more stations can be located in three spatial dimensions and time. The time-of-arrival technique employed by the LMA allows for the sorting of simultaneous activity either from a given lightning discharge or from multiple discharges in different locations. This is important in large storm systems where lightning activity is widespread and nearly continuous. Location errors are typically 100 m over the network. The errors increase with distance from the network, especially in the determination of the height of the radiation sources, such that the mapping of lightning activity becomes two dimensional at long ranges.

Mazur et al. [1997] discusses the nature of radiation mapped with the LDAR system, on which the LMA is based. They point out that continuously propagating positive leaders do not emit sufficiently strong VHF radiation to be detected well by this kind of

system. Radiation sources from slow negative breakdown processes at the tips of propagating negative leaders do emit strongly enough to be well detected.

CHAPTER 5

COMPARISON BETWEEN PDD AND NLDN DETECTED EVENTS

In this chapter, data from the FORTE Photodiode Detector (PDD) and coincident events from the National Lightning Detection Network (NLDN) are used to investigate two questions. First, are “bright” PDD events (with estimated source power $> 10^{11}$ W, what *Turman* [1977] called “superbolts”) associated with positive cloud-to-ground flashes? Second, is the optical power of a PDD event related to flash-type (CG vs IC)?

The chapter is organized as follows. In order to provide an orientation to the PDD data, section 5a discusses a survey of two years of PDD data. Section 5b describes the time-correlated PDD and NLDN data that are used to investigate the two questions stated above. The PDD data and NLDN data are compared in Section 5c, and Section 5d discusses the results.

5a. OVERVIEW OF PDD DATA

In order to familiarize the reader with data from the FORTE PDD, this section examines some characteristics of the PDD data which were collected over a two year period. Annual and seasonal distributions of PDD trigger locations across the globe are presented. The method used to estimate the peak optical power at the source for PDD

events is described. These peak optical power estimates are then used to examine the seasonal and global distributions of “bright” PDD events.

From December 1, 1997 through November 30, 1999, the FORTE PDD detected more than one million optical events that were classified as having been caused by lightning. (See *Kirkland et al.* [2001] for a description of the techniques that were used to discriminate between triggers caused by noise, energetic particles, and lightning in the PDD data.) Approximately 400,000 of these events were recorded in “1998” (December 1997–November 1998) and approximately 650,000 were recorded in “1999” (December 1998–November 1999). More than 90% of the PDD lightning events recorded during this two year period were triggered internally by signals which exceeded the PDD detection threshold. Approximately 9% of the events were slaved off of the Lightning Location System, and approximately 0.5% of the events were slaved off of the FORTE VHF receivers. No attempt has been made to distinguish between events recorded using the different trigger modes. As the overall objective of this study is to examine the nature of optical satellite lightning data, the fact that less than one percent of the PDD data was forced by the VHF receivers should not have a significant affect on analysis. It should also be noted that the greater number of lightning triggers in 1999 is due to an increased sensitivity of the spacecraft instrumentation and refined data-logging techniques, rather than an actual, physical increase in the amount of lightning occurring over the globe.

When the PDD is triggered, it has no way to determine the exact location of the source. The source could be anywhere within the 1200 km diameter footprint of the PDD field of view. For the purpose of investigating where the PDD detects lightning events across the globe, the source locations are approximated by the latitude/longitude locations of the sub-satellite point. Admittedly, this includes considerable error in the source locations, but it is still useful for survey purposes. The sub-satellite point locations for PDD triggers are plotted for 1998 and 1999 in Figures 1 (a) and (b), respectively. These annual global maps of PDD trigger locations show features in general agreement with previous studies (e.g. *Turman and Edgar* [1982]; *Boccippio and Christian* [1998]), and add support to the previous conclusion that lightning occurs most frequently over land masses.

In order to investigate what seasonal patterns might exist in the locations of PDD

Subsatellite Locations of PDD Lightning Events, Dec. 1997 – Nov. 1998

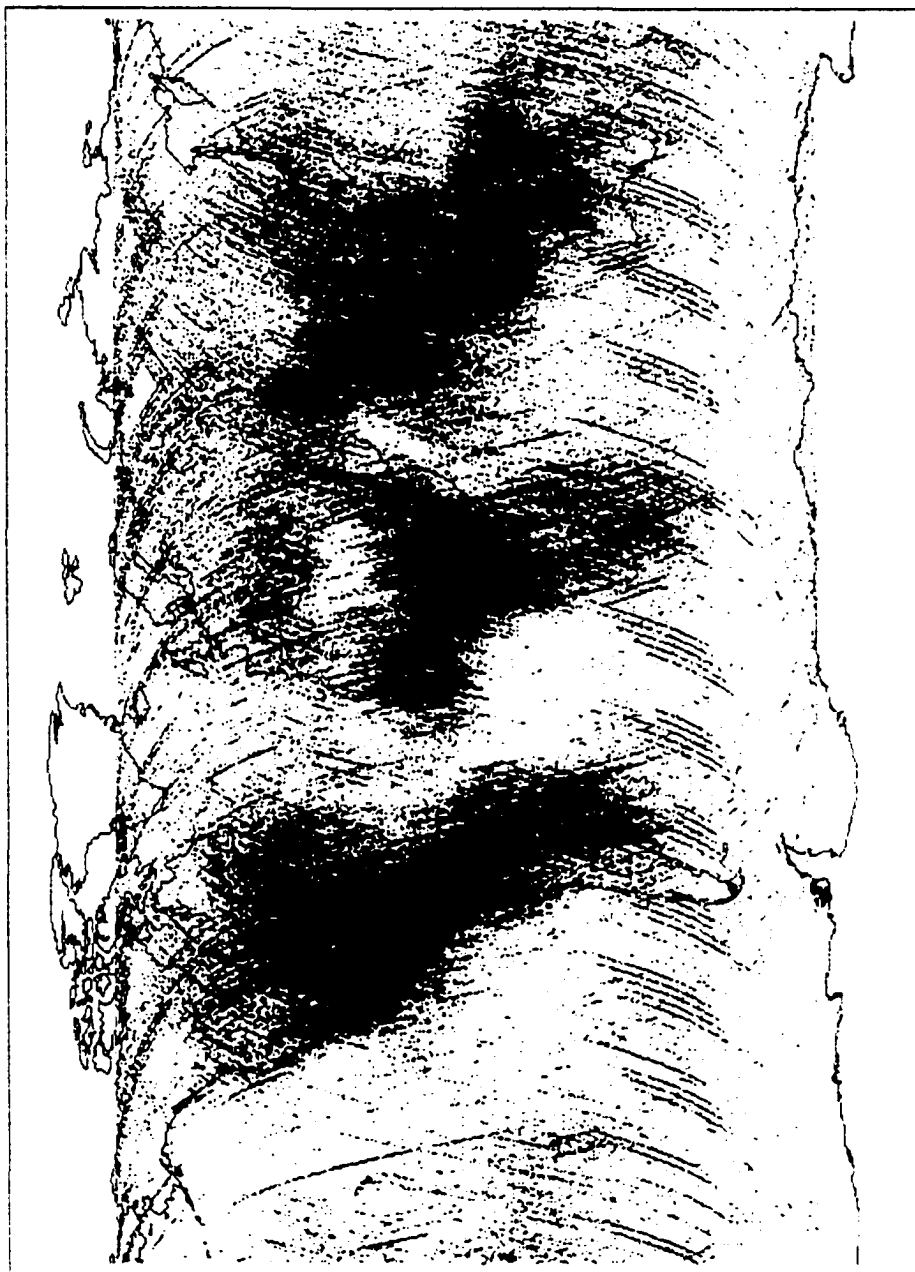


Figure 1(a):

Each dot represents the subsatellite location (Lat/Lon) for ~400,000 PDD lightning events during "1998". The subsatellite location is the lat/lon location of the point directly below the satellite.

Subsatellite Locations of PDD Lightning Events: Dec. 1998 - Nov. 1999

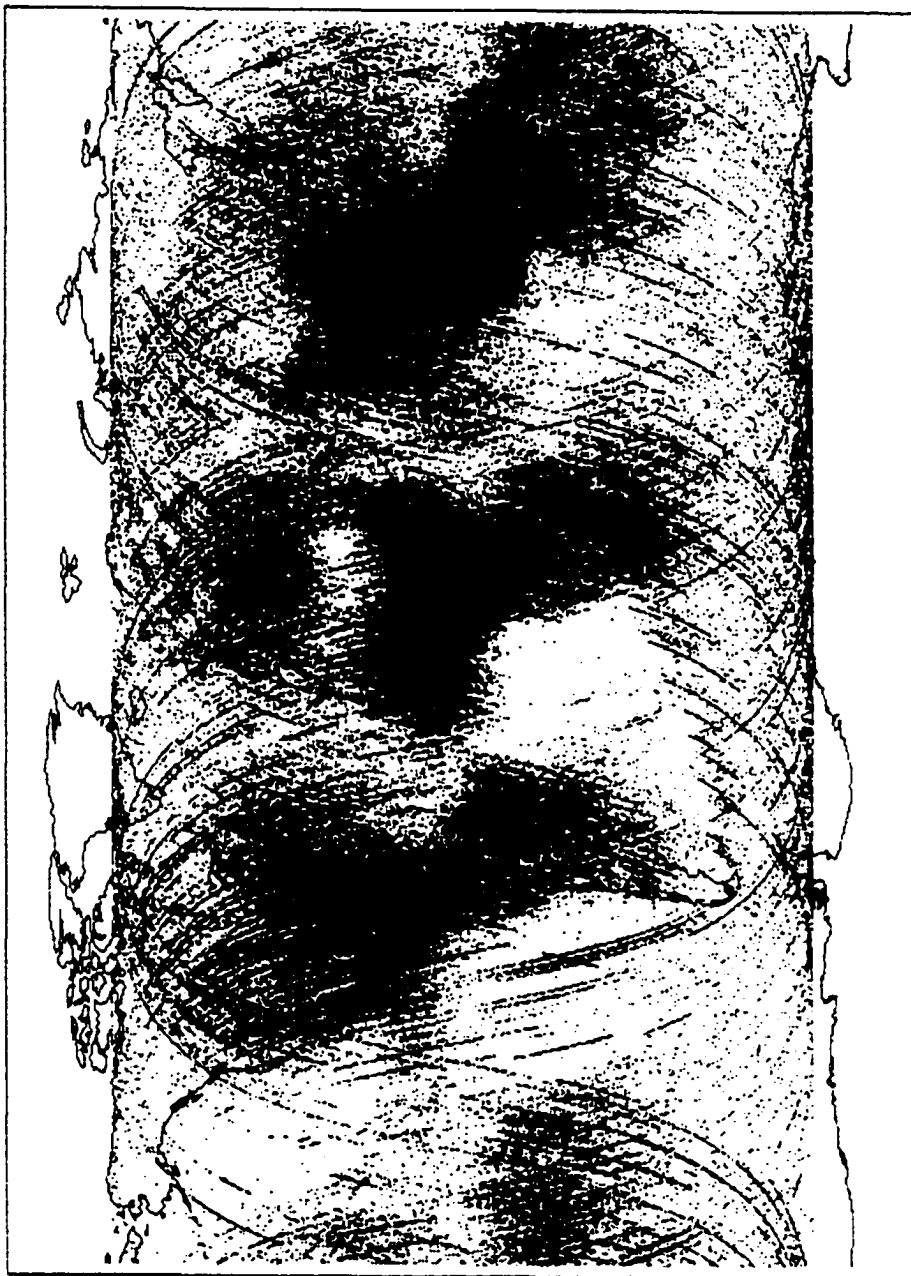


Figure 1(b):
Each dot represents the subsatellite location (Lat/Lon) for ~650,000 PDD lightning events during "1999".

lightning events, the seasons are defined according to three-month groupings. "Winter" is defined as December, January, and February. "Spring" is defined as March, April, and May. "Summer" is defined as June, July, and August. And "Autumn" is defined as September, October and November. These seasonal time periods were chosen so that the resulting distributions of PDD event locations would roughly correspond to the dawn/dusk seasonal distributions of DMSP data produced by *Turman and Edgar* [1982]. The seasonal plots for PDD lightning-trigger locations in 1998 are presented in Figures 2 (a)–(d). Figures 3 (a)–(d) shows the seasonal plots for PDD lightning-trigger locations in 1999.

PDD lightning events tend to occur mostly south of the equator during the Winter. There is a transitional period in Spring, during which the greatest activity is still in the southern hemisphere, but closer to the equator, and activity in the northern hemisphere increases. For Summer, the activity occurs mainly north of the equator. This is followed by another transitional period in Autumn, where lightning is occurring in both hemispheres. The seasonal migration of active areas, such that greatest activity occurs mostly in warm season conditions, agrees well with the movement of lightning "bands" found in *Turman and Edgar's* DMSP studies. It is interesting to note that for certain areas, such as off the tip of Southeast Asia and Indonesia, lightning-triggered PDD events seem to occur year round. Another interesting feature is the apparent lack of lightning triggers over the South Atlantic Ocean. This hole in PDD lightning activity over the south Atlantic has been dubbed the "South Atlantic Anomaly" by the FORTE science team. Whether it is caused by some meteorological phenomenon or whether it is caused by some quirk in the spacecraft instrumentation (or a combination of the two) remains to be investigated.

The peak optical power at the source for PDD events is estimated using several assumptions. First, because the exact location of the source event within the PDD field of view is unknown, the event is assumed to be located directly below the satellite (at the sub-satellite point location). Second, the optical signal at the spacecraft is assumed to be the result of isotropic radiation from a point source. Third, scattering due to cloud particles is not taken into account. The peak optical power at the source for PDD events is then calculated from the peak irradiance detected at the satellite, using a simple $4\pi r^2$ relationship, where r is the altitude of the satellite ($r = 825$ km). The assumption of a point source is

Subsatellite Locations of PDD Lightning Events: Dec. 1997, Jan. 1998, Feb. 1998



Figure 2 (a): PDD lightning events during “Winter” 1998
Each dot represents the subsatellite location (Lat/Lon) for PDD lightning events for December 1997 through February 1998.

Subsatellite Locations of PDD Lightning Events: Mar. 1998, Apr. 1998, May 1998



Figure 2 (b): PDD lightning events during “Spring” 1998
Each dot represents the subsatellite location (Lat/Lon) for PDD lightning events for March 1998 through May 1998.

Subsatellite Locations of PDD Lightning Events: Jun. 1998, Jul. 1998, Aug. 1998

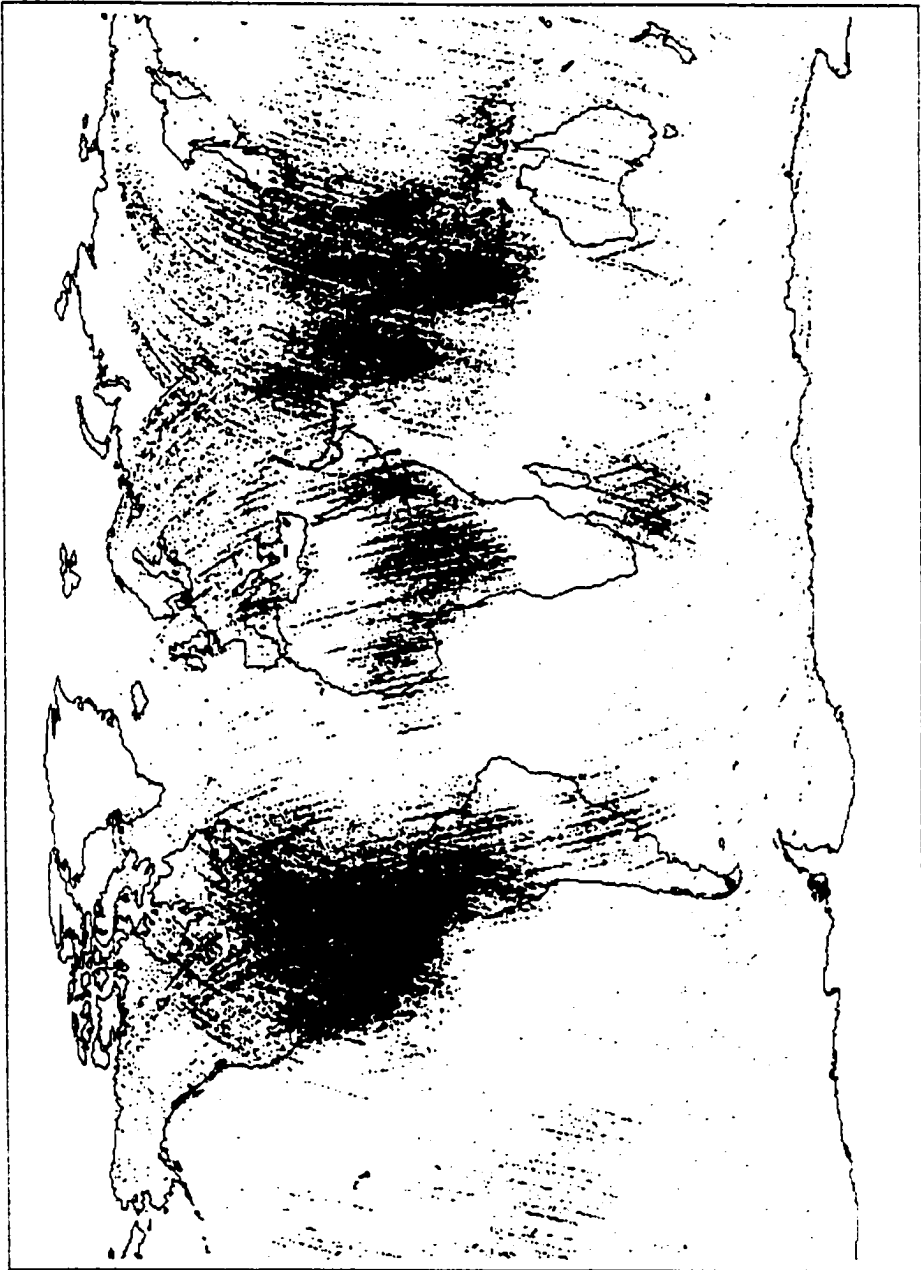


Figure 2 (c): PDD lightning events during “Summer” 1998
Each dot represents the subsatellite location (Lat/Lon) of PDD lightning events for June 1998 through August 1998.

Subsatellite Locations of PDD Lightning Events: Sep. 1998, Oct. 1998, Nov. 1998



Figure 2 (d): PDD lightning events during “Autumn” 1998
Each dot represents the subsatellite location (Lat/Lon) for PDD lightning events for September 1998 through November 1998.

Subsatellite Locations of PDD Lightning Events: Dec. 1998, Jan. 1999, Feb. 1999



Figure 3 (a): PDD lightning events during “Winter” 1999
Each dot represents the subsatellite location (Lat/Lon) for PDD lightning events for December 1998 through February 1999.

Subsatellite Locations for PDD Lightning Events: Mar. 1999, Apr. 1999, May 1999



Figure 3 (b): PDD lightning events during “Spring” 1999
Each dot represents the subsatellite location (Lat/Lon) for PDD lightning events for March 1999 through May 1999.

Subsatellite Locations for PDD Lightning Events: Jun. 1999, Jul. 1999, Aug. 1999



Figure 3 (c): PDD lightning events during “Summer” 1999
Each dot represents the subsatellite location (Lat/Lon) for PDD lightning events for June 1999 through August 1999.

Subsatellite Locations of PDD Lightning Events: Sep. 1999, Oct. 1999, Nov. 1999

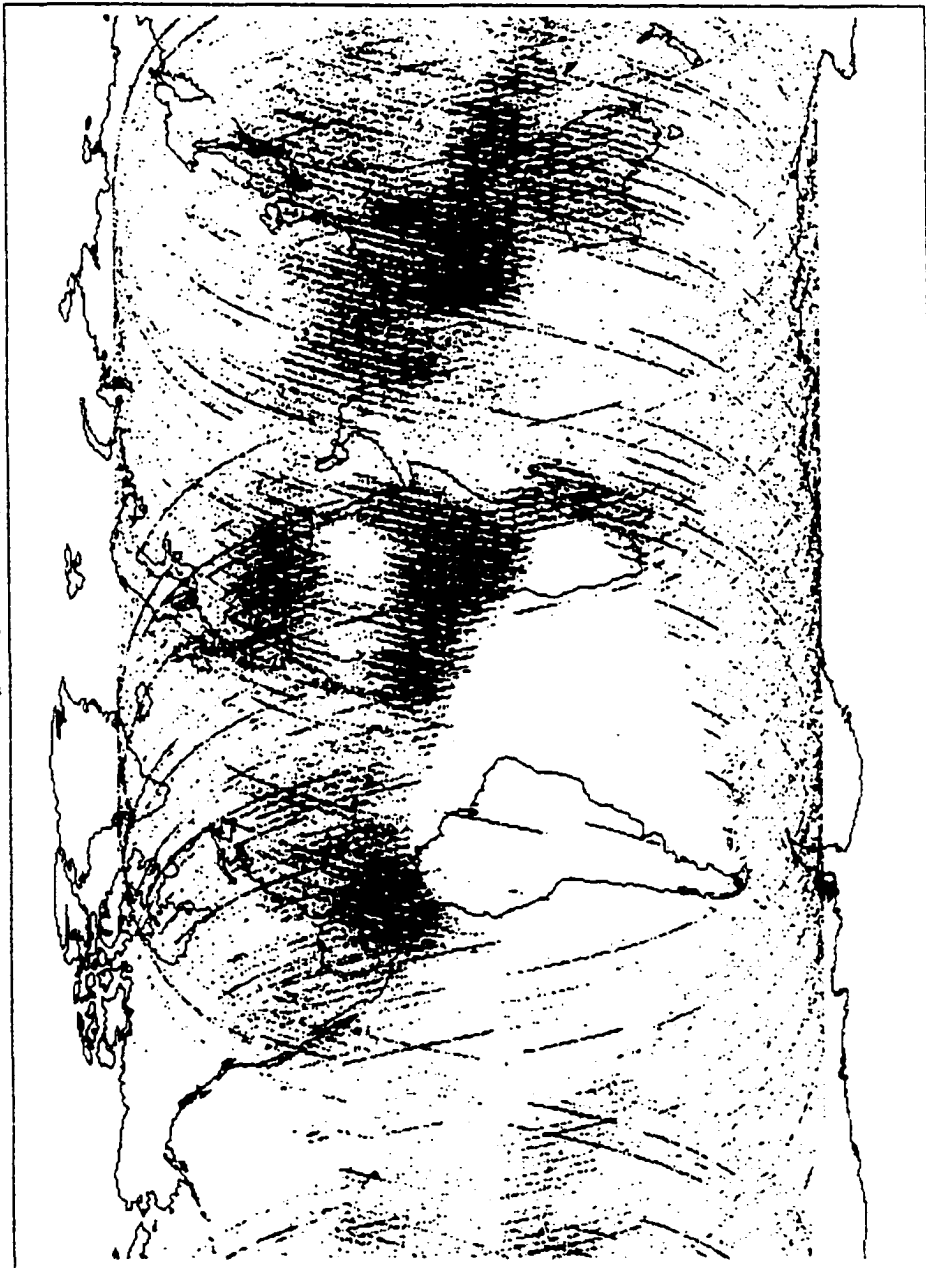


Figure 3 (d): PDD lightning events during “Winter” 1998
Each dot represents the subsatellite location (Lat/Lon) for PDD lightning events for September 1999 through November 1999.

perhaps not the best assumption to simulate a real lightning event, but it is used here because it can be done simply and because it is the same technique used by Turman [1977, 1978] and so allows comparisons with his results. The estimates represent a lower-bound on the actual optical power of PDD event sources. For the two years of data considered here, the median value for peak optical source power is $\sim 1 \times 10^9$ W. This is in agreement with Turman's studies and FORTE studies which considered a smaller sample size of PDD events (Kirkland *et al.* [2001]).

The estimates of peak source power for PDD lightning-triggers allow for an examination of the global and seasonal distribution of "bright" events (with estimated peak optical source power greater than 1×10^{11} W). These bright events make up approximately 0.4% of the total population of PDD lightning-triggers. Seasonal distributions for bright PDD lightning-triggers are plotted in Figures 4 (a)–(d) and Figures 5 (a)–(d). The sub-satellite locations of bright events are plotted as plus-signs (+). The sub-satellite locations for all PDD lightning-triggers during each time period are also plotted on the maps as light gray dots, so that the seasonal patterns in the locations of bright events can be compared to the seasonal patterns for the full population of PDD lightning-triggers. One can see a clustering of bright PDD events off the coast of Japan during northern hemisphere "winter". This is in good agreement with the findings of Turman [1977]. It is easy to see that the bright events tend to occur in areas where lightning-triggers are otherwise prevalent. However, there is some apparent clustering of bright PDD events within these areas of high seasonal activity. Whether there is a meteorological or physical reason for this clustering remains to be explored.

5b. THE PDD/NLDN DATA SET FOR "SUMMER" 1998

This study does not have access to the raw PDD data. Instead, data from the FORTE PDD is available through a database prepared by M.W. Kirkland and T.E. Light and made available through Los Alamos National Laboratory. In this database, the PDD data are categorized according to trigger class (lightning, noise, or energetic particles)

Subsatellite Locations of "Bright" PDD Lightning Events: Dec. 1997, Jan. 1998, Feb. 1998

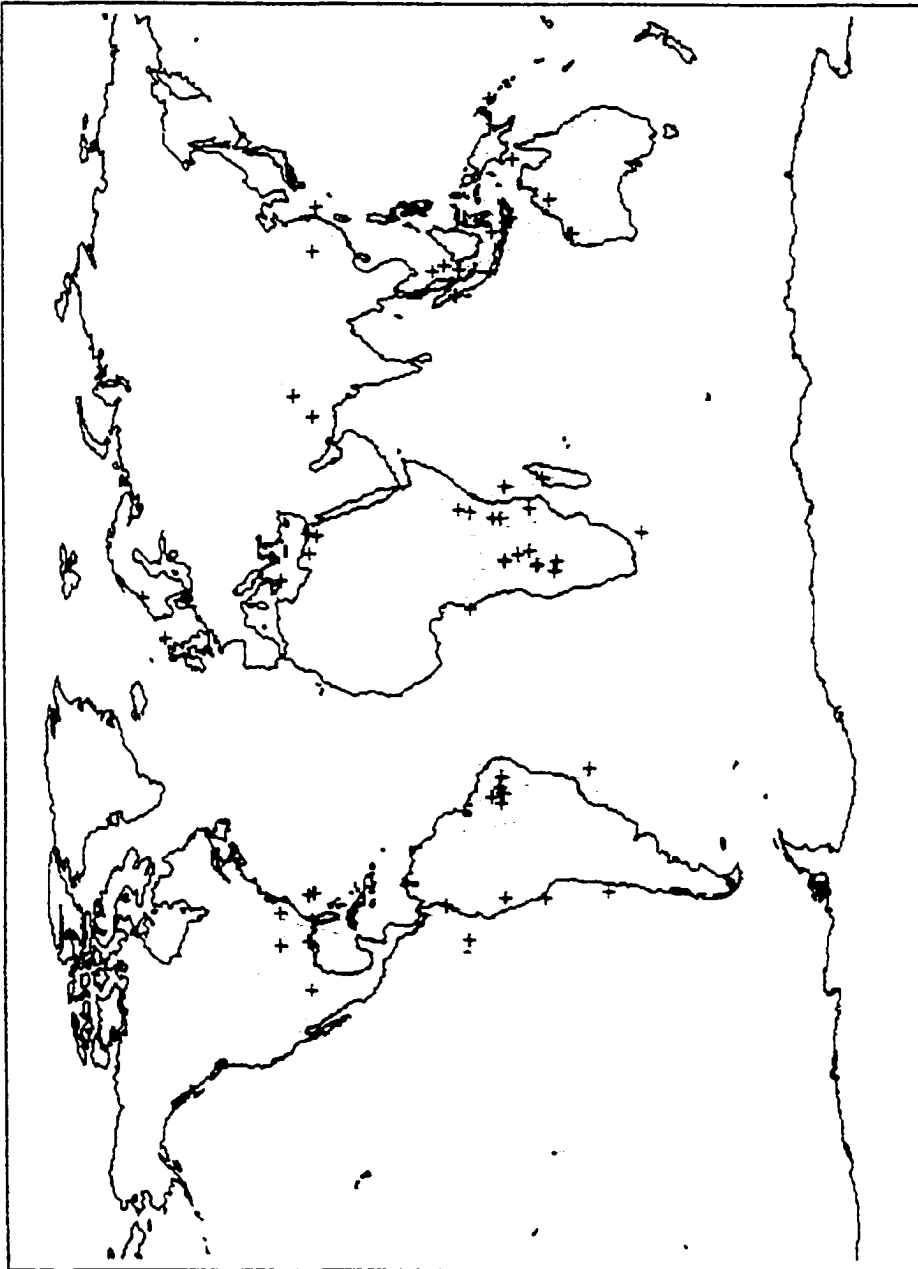


Figure 4 (a): "Bright" PDD lightning events for Winter 1998

Plus signs (+) indicate subsatellite locations of PDD events with estimated peak optical source power $\geq 1 \times 10^{11}$ W. Light gray dots indicate the subsatellite locations for all PDD lightning-triggers (December 1997 through February 1998).

Subsatellite Locations of "Bright" PDD Lightning Events: Mar. 1998, Apr. 1998, May 1998

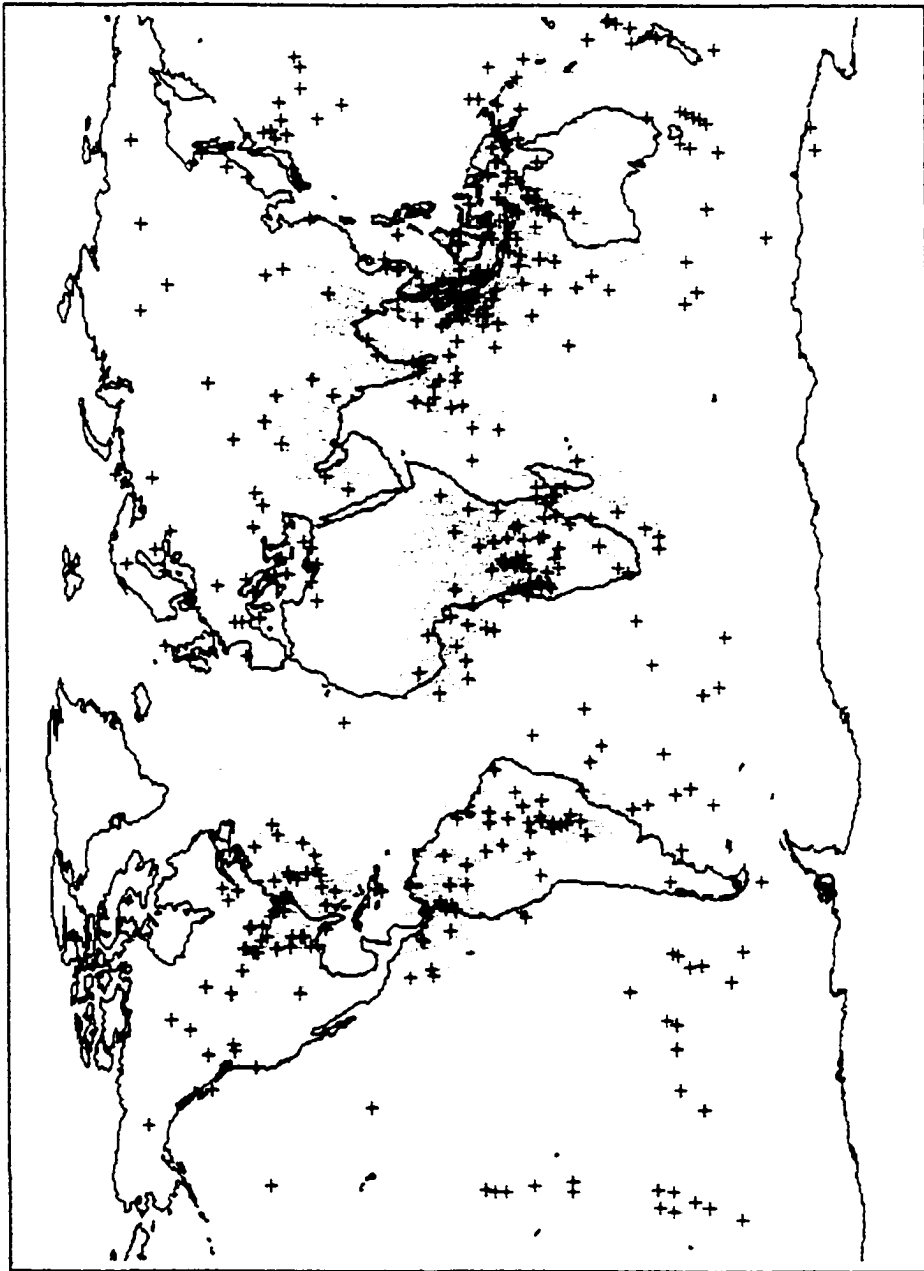


Figure 4 (b): "Bright" PDD lightning events for Spring 1998

Plus signs (+) indicate subsatellite locations of PDD events with estimated peak optical source power $\geq 1 \times 10^{11}$ W. Light gray dots indicate the subsatellite locations for all PDD lightning-triggers (March 1998 through May 1998).

Subsatellite Locations of "Bright" PDD Lightning Events: Jun. 1998, Jul. 1998, Aug. 1998

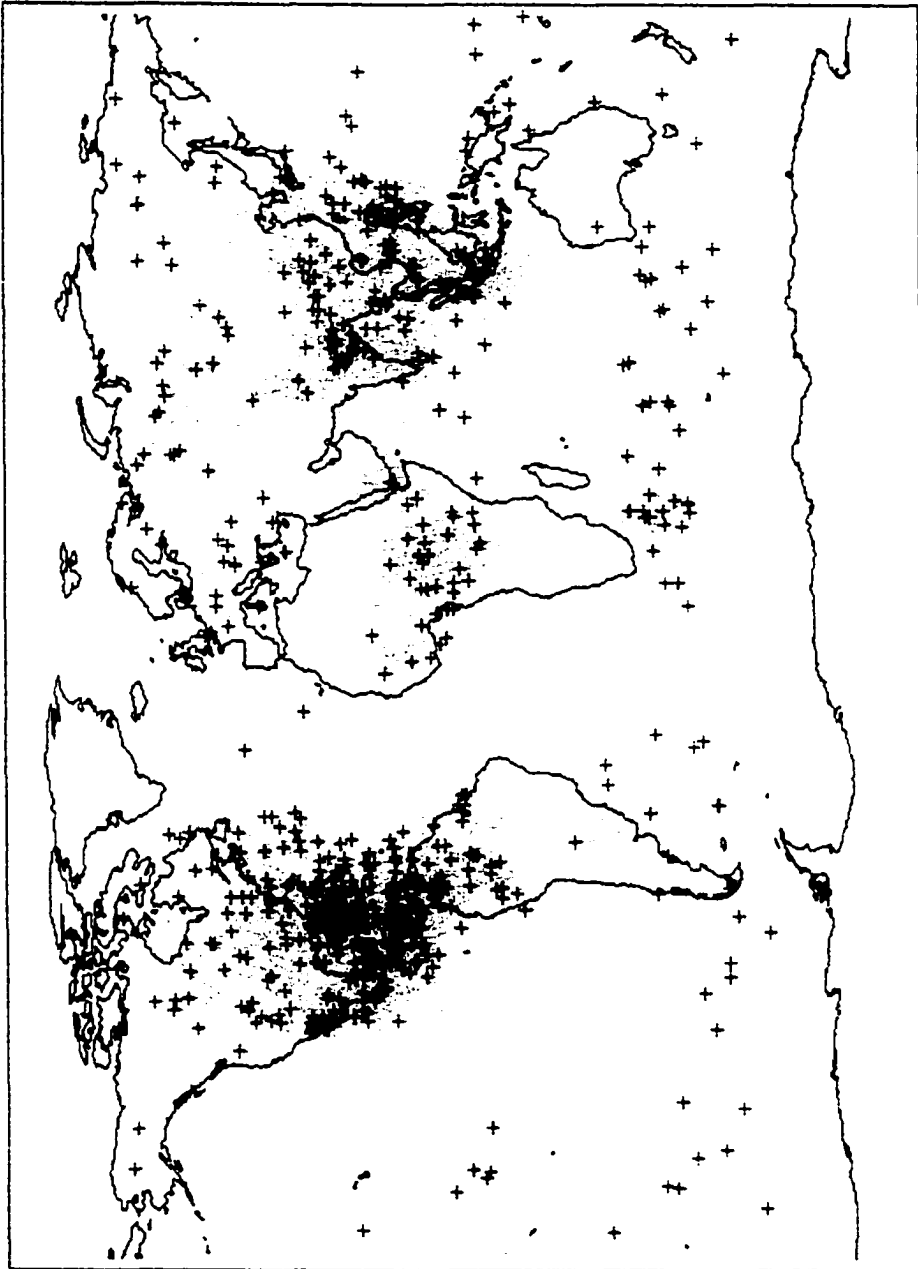


Figure 4 (c): "Bright" PDD lightning events for Summer 1998
Plus signs (+) indicate subsatellite locations of PDD events with estimated peak optical source power $\geq 1 \times 10^{11}$ W. Light gray dots indicate the subsatellite locations for all PDD lightning-triggers (June 1998 through August 1998).

Subsatellite Locations of "Bright" PDD Lightning Events: Sep. 1998, Oct. 1998, Nov. 1998



Figure 4 (d): "Bright" PDD lightning events for Autumn 1998
Plus signs (+) indicate subsatellite locations of PDD events with estimated peak optical source power $\geq 1 \times 10^{11}$ Watts. Light gray dots indicate the subsatellite locations for all PDD lightning-triggers (September 1998 through February 1998).

Figure 5 (a)

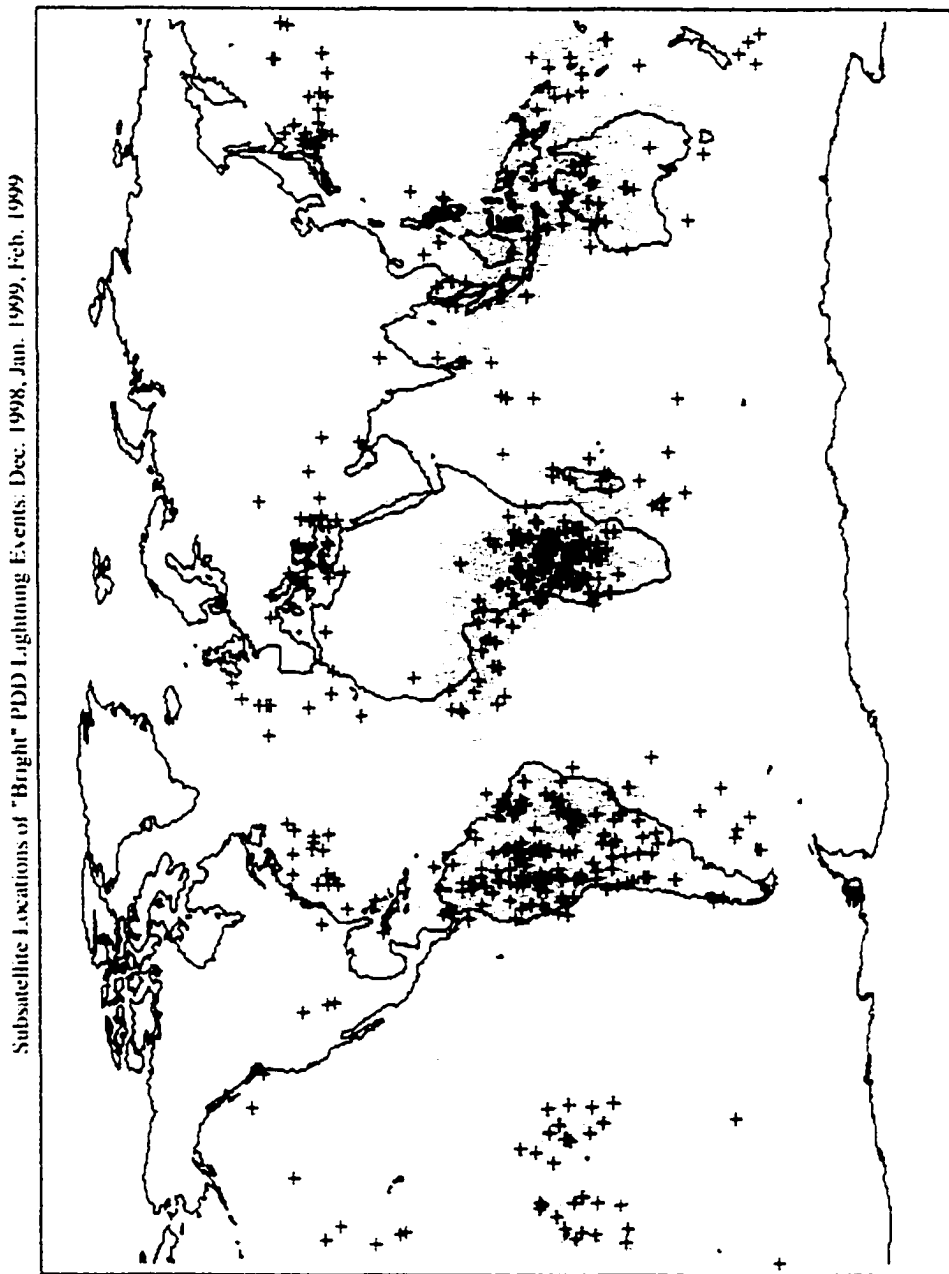


Figure 5 (a): "Bright" PDD lightning events for Winter 1999
Plus signs (+) indicate subsatellite locations of PDD events with estimated peak optical source power $\geq 1 \times 10^{11}$ Watts. Light gray dots indicate the subsatellite locations for all PDD lightning-triggers (December 1998 through February 1999).

Subsatellite Locations of "Bright" PDD Lightning Events: Mar. 1999, Apr. 1999, May 1999

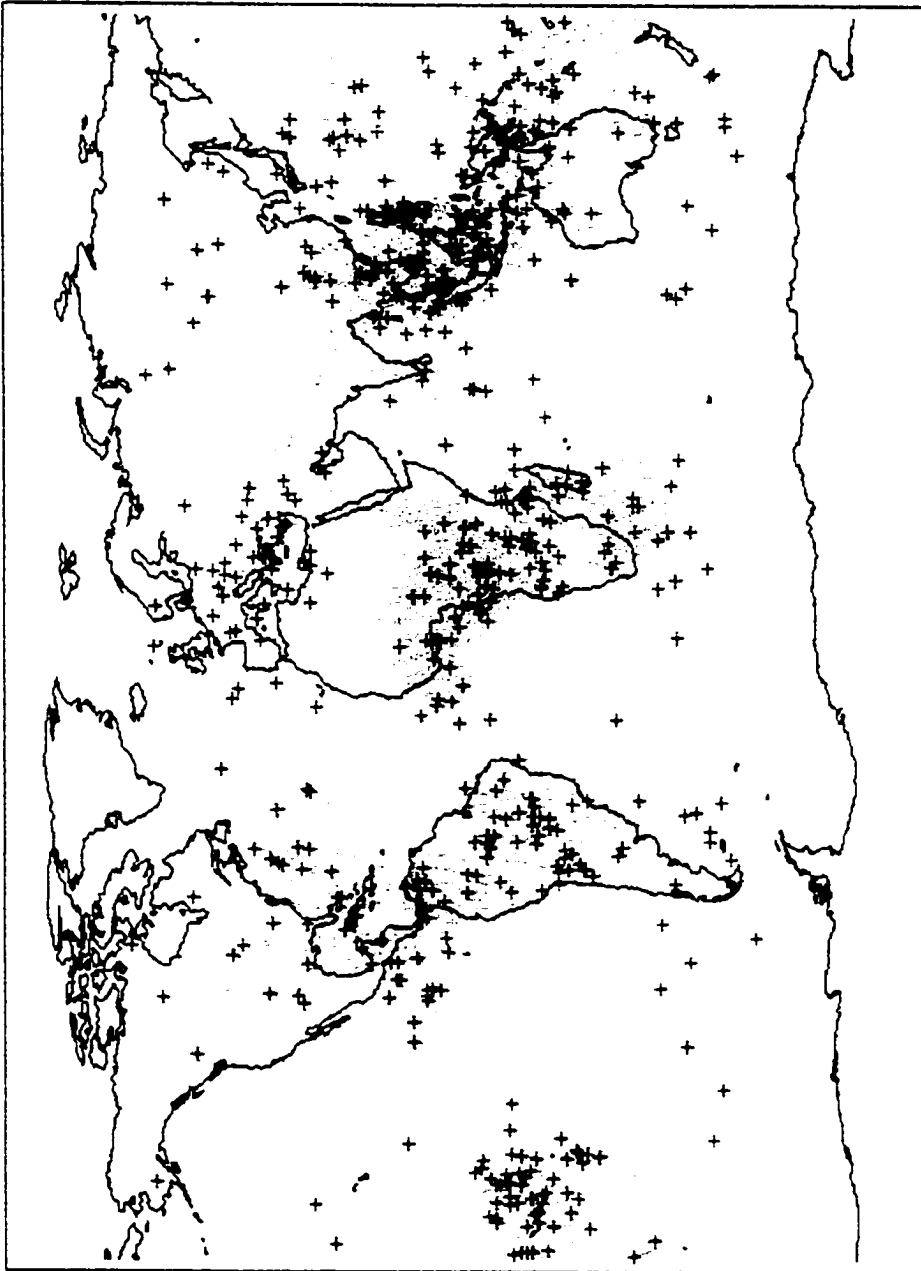


Figure 5 (b): "Bright" PDD lightning events for Spring 1999
Plus signs (+) indicate subsatellite locations of PDD events with estimated peak optical source power $\geq 1 \times 10^{11}$ Watts. Light gray dots indicate the subsatellite locations for all PDD lightning-triggers (March 1999 through May 1999).

Subsatellite Locations for "Bright" PDD Lightning Events: Jun. 1999, Jul. 1999, Aug. 1999

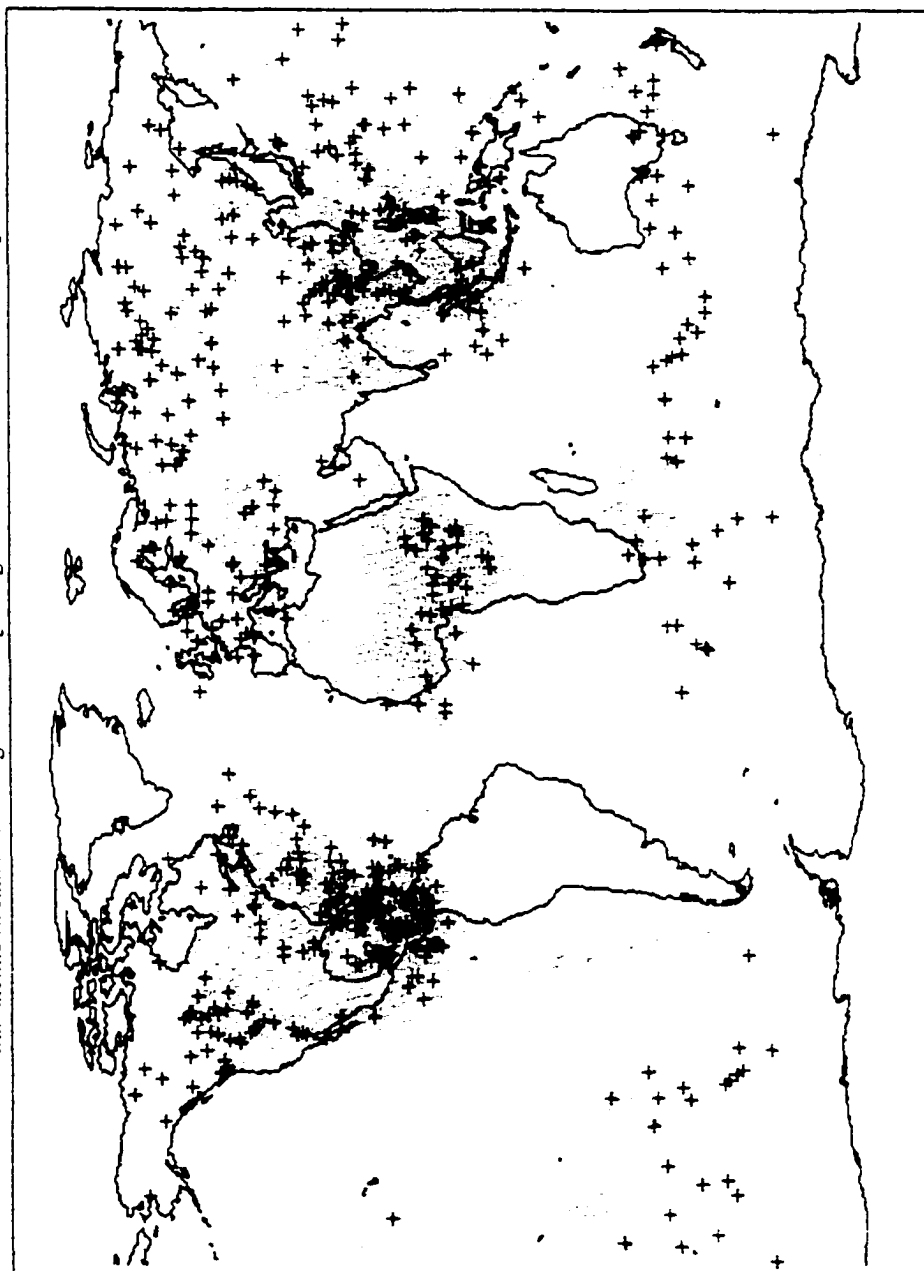


Figure 5 (c): "Bright" PDD lightning events for Summer 1999
Plus signs (+) indicate subsatellite locations of PDD events with estimated peak optical source power $\geq 1 \times 10^{11}$ Watts. Light gray dots indicate the subsatellite locations for all PDD lightning-triggers (June 1999 through August 1999).

Subsatellite Locations of "Bright" PDD Lightning Events: Sep. 1999, Oct. 1999, Nov. 1999

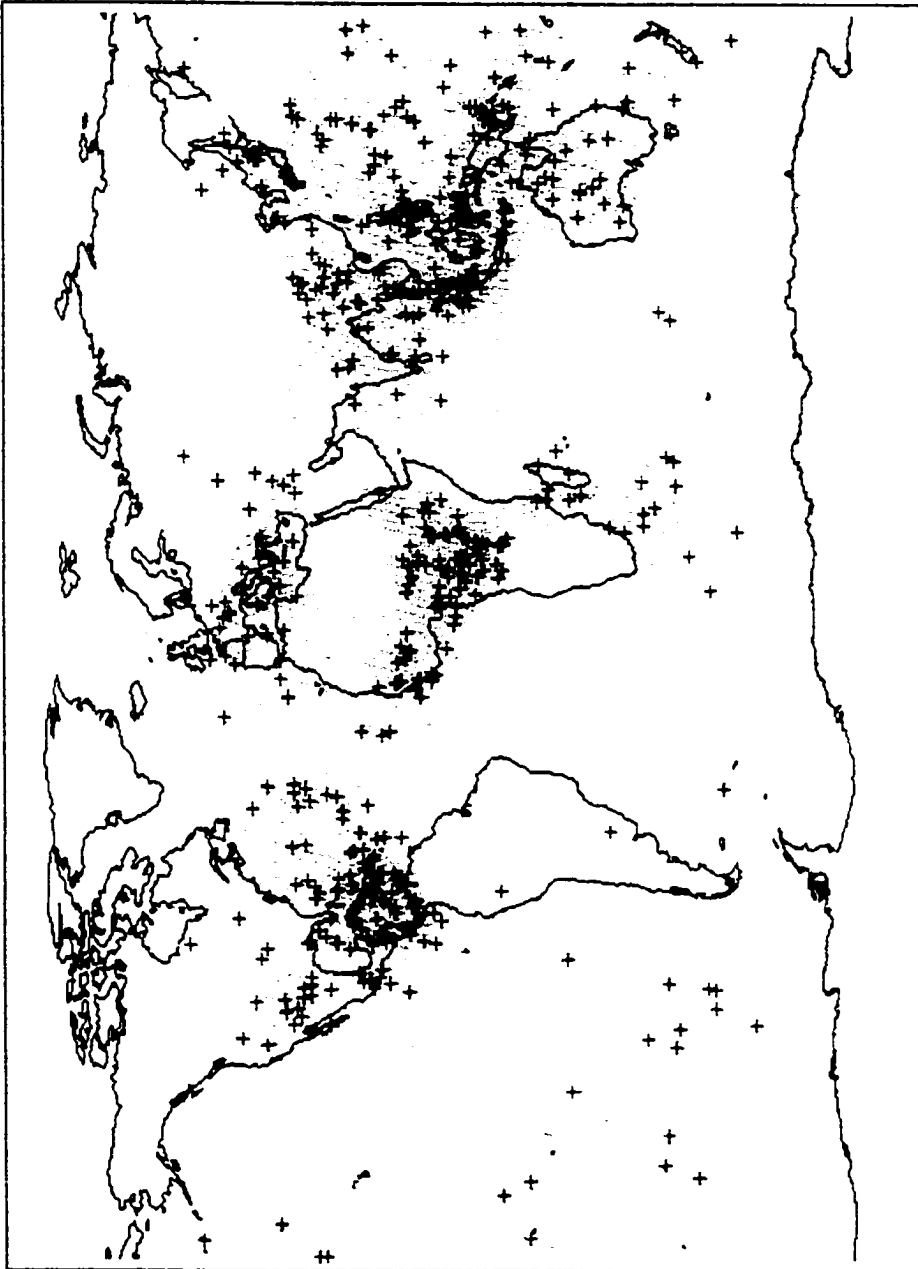


Figure 5 (d): "Bright" PDD lightning events for Winter 1999
Plus signs (+) indicate subsatellite locations of PDD events with estimated peak optical source power $\geq 1 \times 10^{11}$ Watts. Light gray dots indicate the subsatellite locations for all PDD lightning-triggers (September 1999 through November 1999).

trigger mode (internal PDD, slaved to the LLS or slaved to the VHF). Information about the PDD event, including trigger time, maximum irradiance, integrated energy, and whether or not there is a coincident FORTE LLS or FORTE VHF event is available.

To compare NLDN data to data from the FORTE satellite, Los Alamos National Laboratory obtained a specific, custom data set from Global Atmospheric Inc. *Kirkland et al.* [2001] summarizes the unique points of this NLDN data set. These data were processed using “relaxed criteria” in order to maximize the detection probability of IC and distant CG events (to provide some measure of ground truth over the ocean). These data were provided in a stroke-level format with microsecond timing precision. Specifically, no maximum limit on the range between the event and the sensors was applied, and the reprocessing accommodated ionospherically propagated signals. The resultant event data included “unverified” event locations from CG discharges occurring thousands of kilometers outside of the NLDN network. No polarity was assigned to these very distant events, and locations for these events have a much greater error than the location error for events located within the NLDN network. The “relaxed criterion” data also included very energetic IC events which occurred within or near the NLDN network.

For April through September 1998, information on whether there are time-correlated NLDN events is available in the PDD database. These time correlations were made by M.W. Kirkland when he prepared the database, using the “relaxed criterion” NLDN data set described above. The distance between an NLDN event location and the FORTE satellite and a time-offset for the optical signal to travel that distance were calculated. This time-offset was then subtracted from the PDD event time, to correct for “time of flight” from the point of origin to the satellite. The NLDN event times and the corrected PDD event times were then compared. If an NLDN event location was in the PDD field of view and that NLDN event was found to occur within 30 ms of the corrected PDD time, then the correlation was recorded in the PDD database. However, due to a quirk in the way the database was written, these correlations are only available east of -100.0° Longitude. NLDN event information that is available through the PDD data base includes position, time, polarity, and flash-type. No information on flash multiplicity was included.

5c. ANALYSIS METHODS AND RESULTS

In theory, the time-correlated PDD/NLDN events should represent the subset of lightning flashes containing CG flashes that were seen by both systems. That is, flashes containing connections to ground that were detected in some manner by the PDD and that occurred within the detection range of the NLDN should also have been seen by the NLDN. This assumption works best over the continental United States (within and just outside the NLDN network), where the NLDN detects CG flashes with 80-90% efficiency. The assumption is less valid for distant CG events that occur out over the oceans, where such events are detected by the NLDN with a greatly reduced efficiency and greater error in determining the locations.

For the PDD/NLDN data set presented in the PDD database, the subset of PDD events which have a flash-level correlation to a CG event reported in the relaxed criterion NLDN data is known. In order to estimate what percentage of the total population of PDD events were associated with CG events, the total number of PDD events recorded over the geographic area covered by the NLDN data was determined. Because a PDD lightning event can be located anywhere within the PDD field of view, the maximum and minimum latitudes and longitudes for the sub-satellite points of PDD events which had associated NLDN events were used to define limits on the geographic area for which PDD events would be considered. The total population of PDD events that occurred over the correlation-region were chosen to be all PDD events with sub-satellite locations in a latitude-longitude box with a northern bound at 63.3° north latitude, a southern bound at 0.0° north latitude, a western bound at -110.0° longitude, and an eastern bound at -27.5° longitude. Of the ~243,000 PDD lightning triggers which occurred globally during the April-September 1998 time period, ~76,000 were in the "NLDN correlation region" and ~9,000 of these were correlated with an NLDN event. For the remainder of this discussion, the subset of PDD events which occurred in the correlation region will be referred to as East Continental US PDD events.

The peak power at the source for all PDD events occurring in the April-September period of 1998 were estimated using the same procedure described in Section 5a. Monthly distributions of the frequency of occurrence for these peak power values were then plotted

for the total global population of PDD events, for the East Continental US subset, and for the subset of PDD events which had a time-correlated NLDN event (PDD/NLDN events). The results are presented in Figures 6 (a)–(f) (Total Global PDD events), Figures 7 (a)–(f) (East Continental US events), and Figures 8 (a)–(f) (PDD/NLDN events). Similarities and differences in Figures 6, 7, and 8 are discussed in section 5d.

In order to investigate the possible relationship between PDD peak source power and flash-type or flash-polarity, the Global, East Continental US, and PDD/NLDN data were divided according to the following four power ranges:

- 1) $10^{11} \text{ W} \leq \text{pwr}$ ("bright" events)
- 2) $10^{10} \text{ W} \leq \text{pwr} < 10^{11} \text{ W}$
- 3) $10^9 \text{ W} \leq \text{pwr} < 10^{10} \text{ W}$
- 4) $10^8 \text{ W} \leq \text{pwr} < 10^9 \text{ W}$

The results are detailed in Table 1. The "Tot PDD" column gives the total number of PDD events that were detected worldwide for the given month. The "Num ECONT" in Table 1(b) and the "Num w/ NLDN" in Table 1(c) give the total number of PDD events in the East Continental US region and the number of PDD/NLDN events, respectively. The next four columns give the number of events that were found in each of the four power ranges defined above. For both the total Global PDD data and the East Continental US data, the majority of PDD events fell into the third and fourth power ranges defined above. It is interesting to note that for the PDD/NLDN events, the majority of events fall in the second and third power bins. This suggests that something related to the discharge processes in ground flashes may produce more optical power when seen from above. One speculation is that processes in a CG discharge might cause the lightning channels to reach higher in storm, but exactly why many CG flashes appear more optically powerful when seen from above remains to be explained.

Totals for percentage of PDD East Continental events that had associated NLDN events were also sorted according to month and according to power range. These results are presented in Table 2 and Table 3. These tables include information on flash-type included in the relaxed criteria NLDN data. "#NLDN AMBIG" values are numbers of events for which the relaxed criteria data did not have information on flash type.

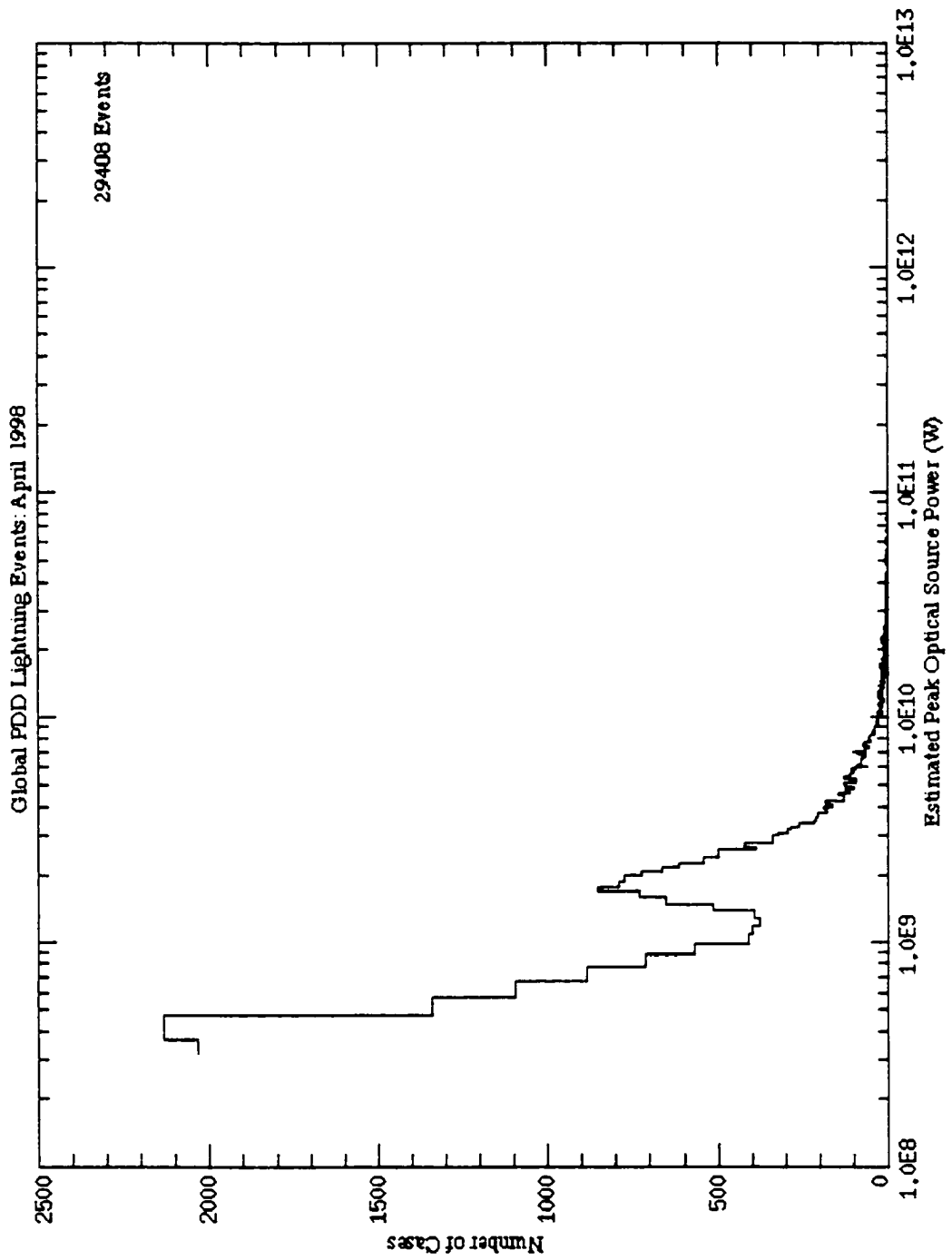


Figure 6 (a): Distribution of Estimated Peak Optical Power for Global PDD Lightning Events — April 1998

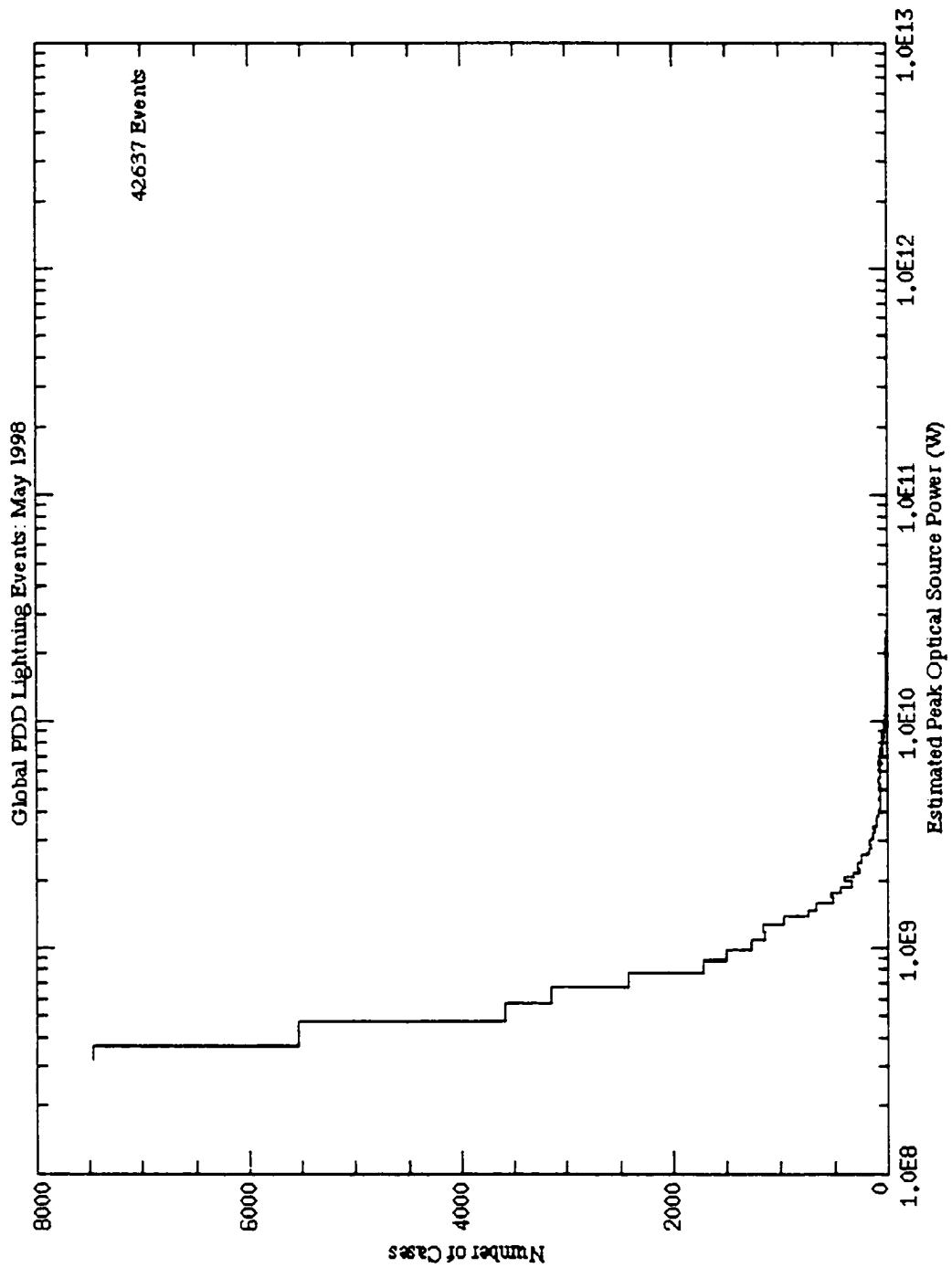


Figure 6 (b): Distribution of Estimated Peak Optical Power for Global PDD Lightning Events — May 1998

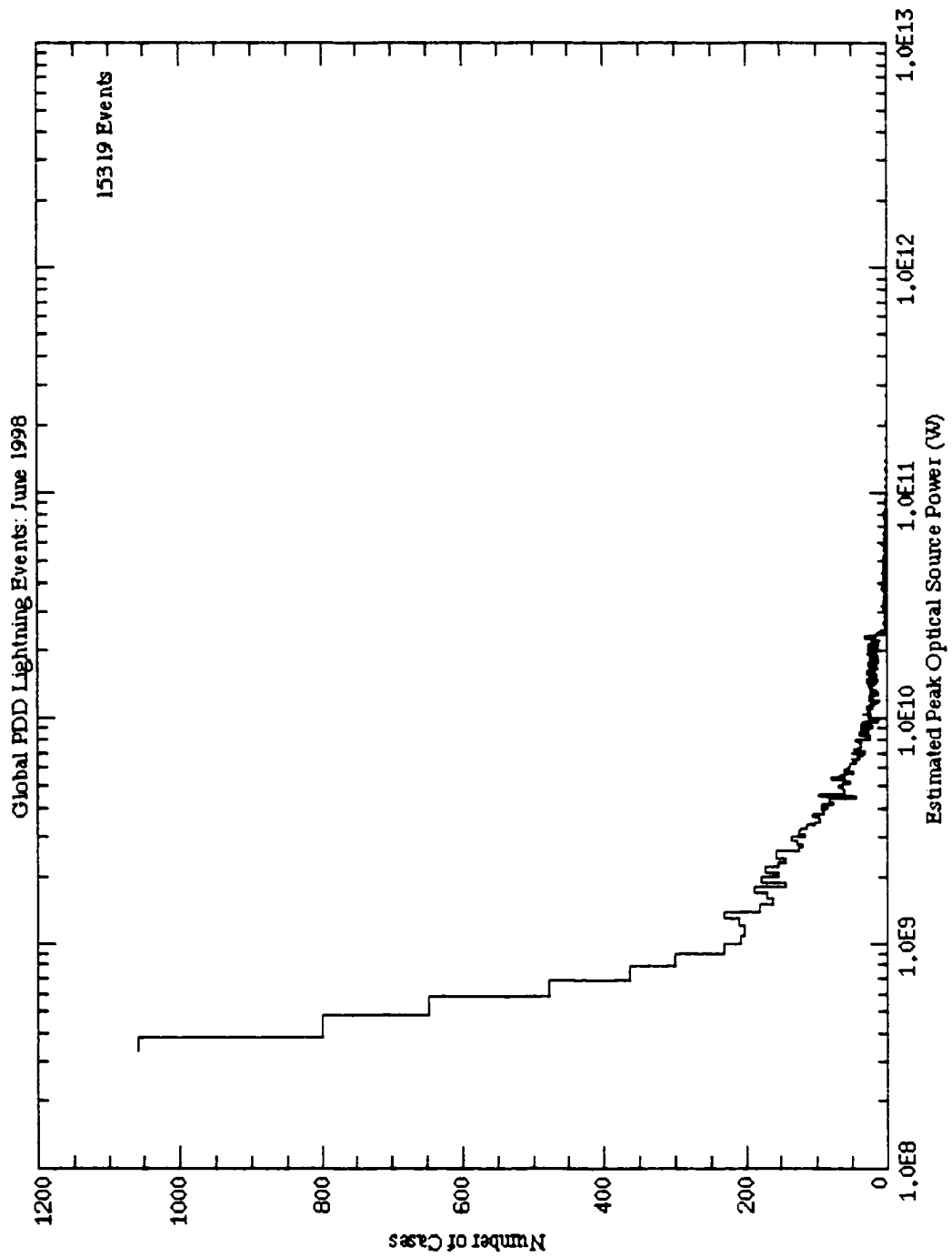


Figure 6 (c): Distribution of Estimated Peak Optical Power for Global PDD Lightning Events — June 1998

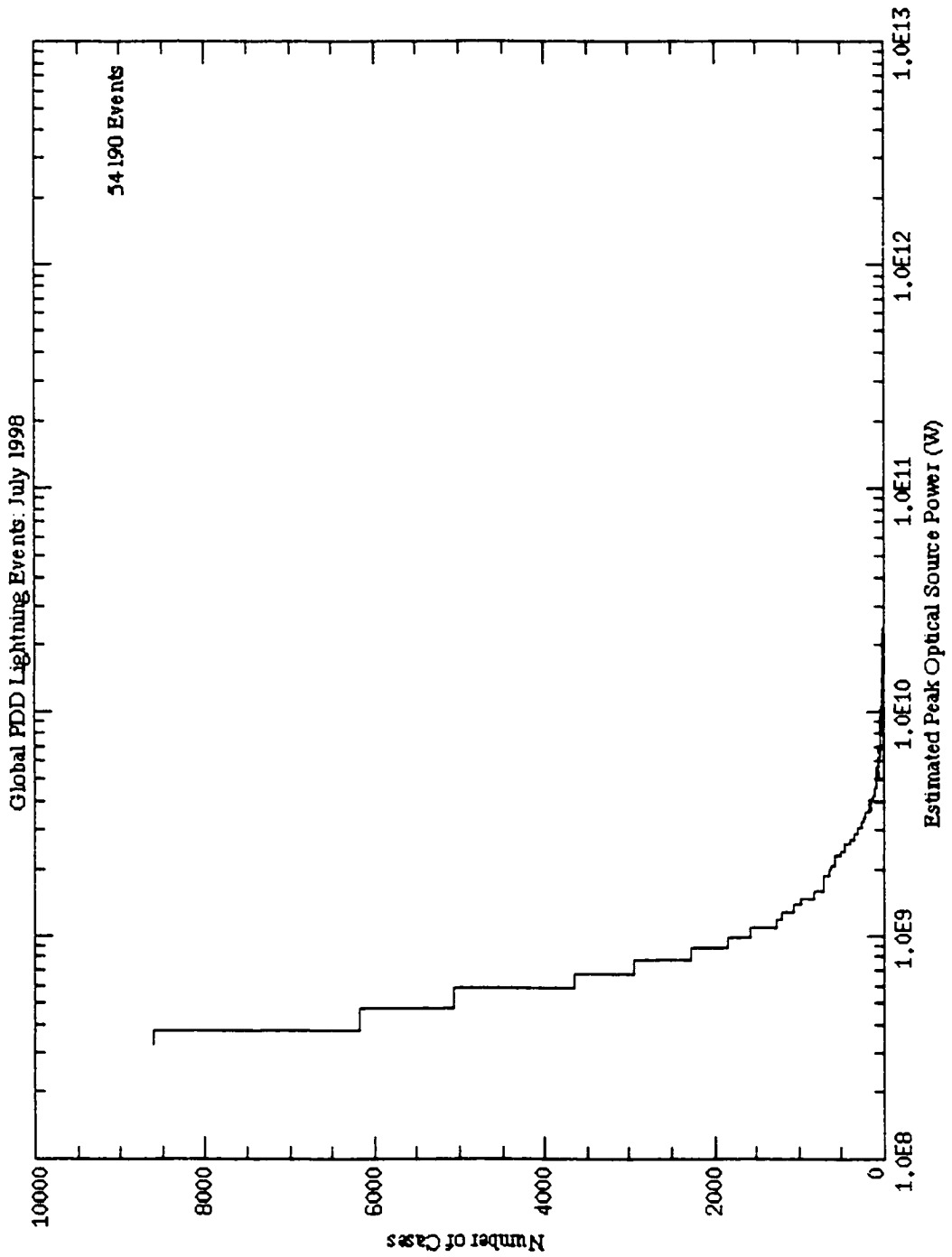


Figure 6 (d): Distribution of Estimated Peak Optical Power for Global PDD Lightning Events — July 1998

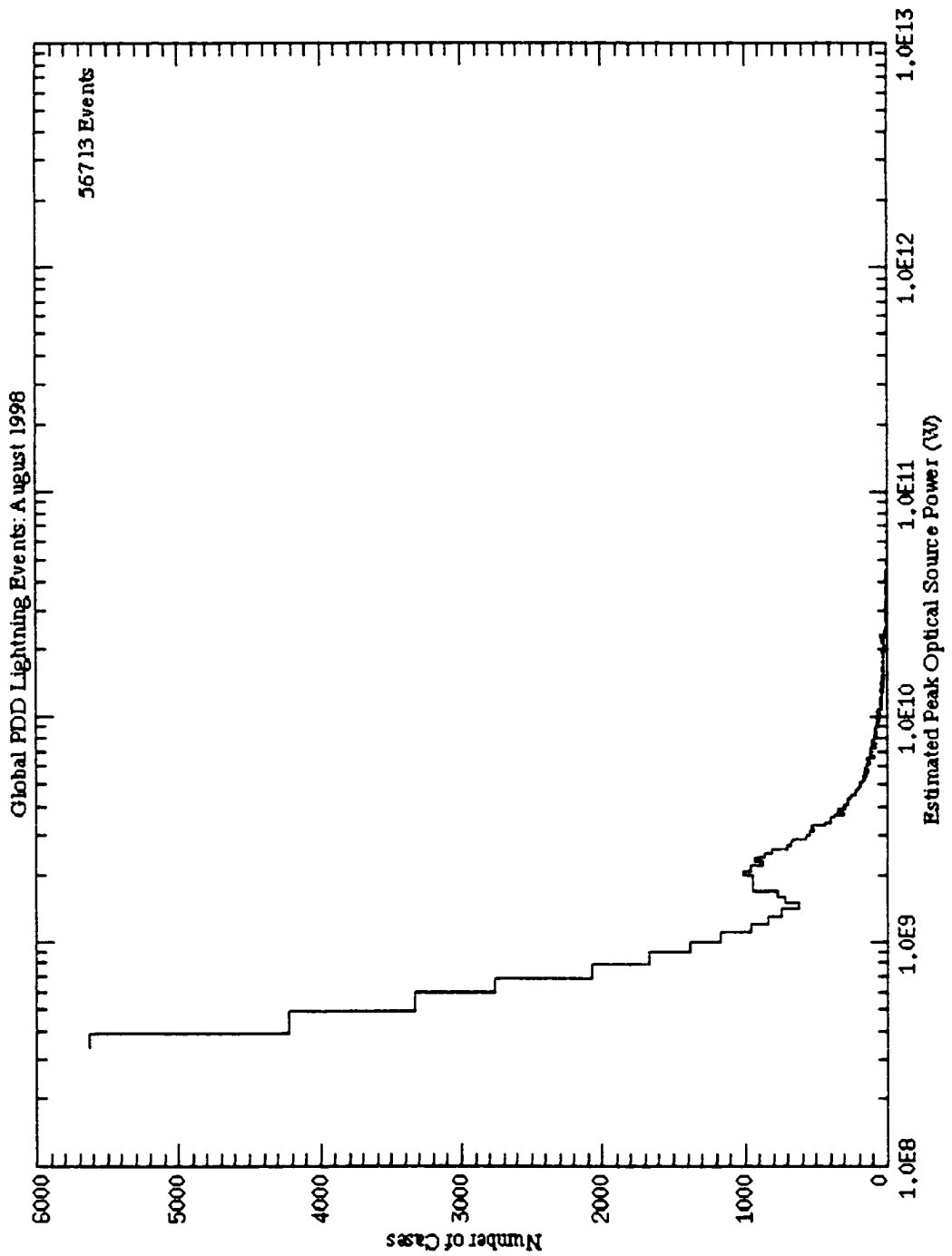


Figure 6 (e): Distribution of Estimated Peak Optical Power for Global PDD Lightning Events — August 1998

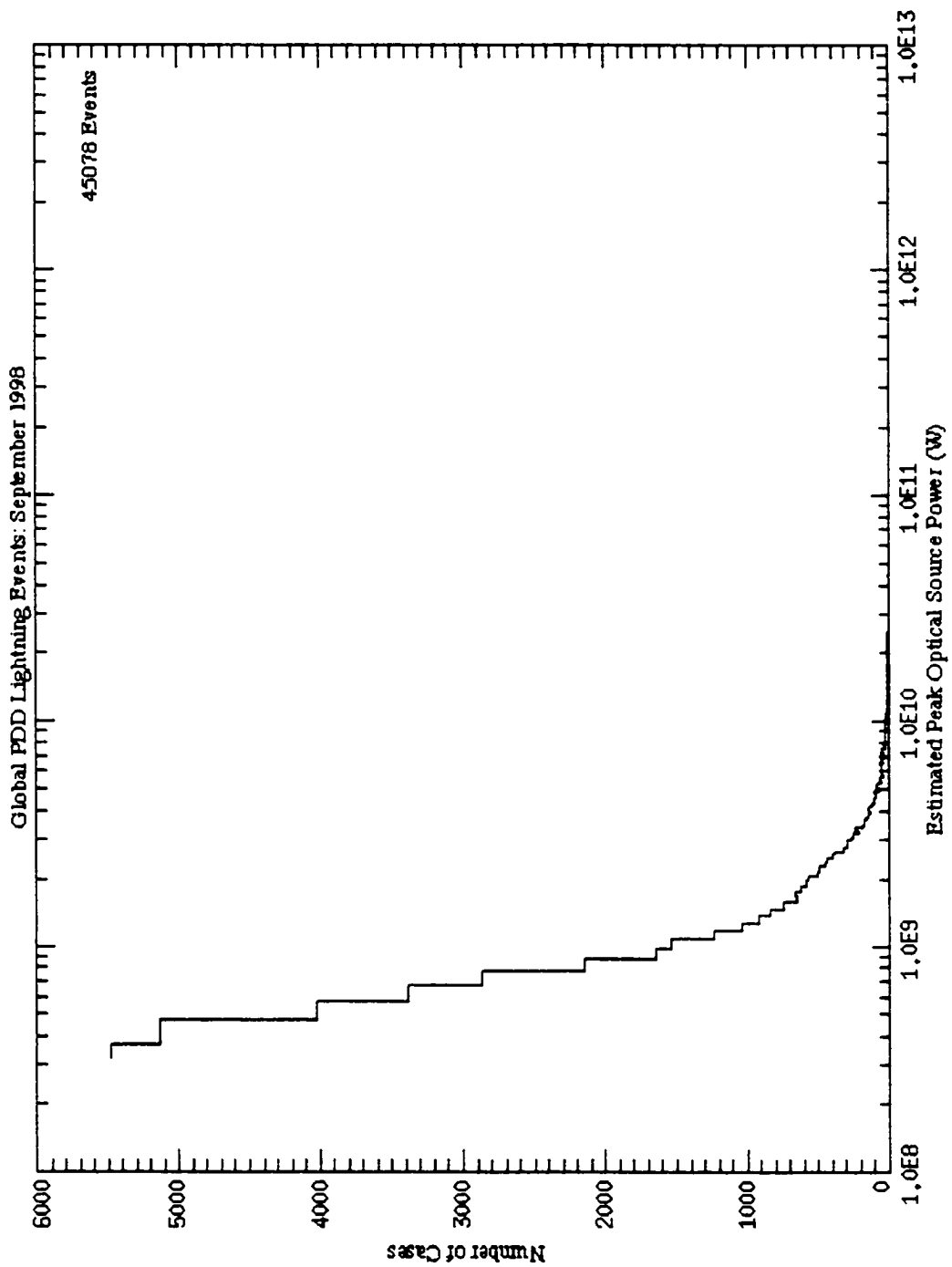


Figure 6 (f): Distribution of Estimated Peak Optical Power for Global PDD Lightning Events — September 1998

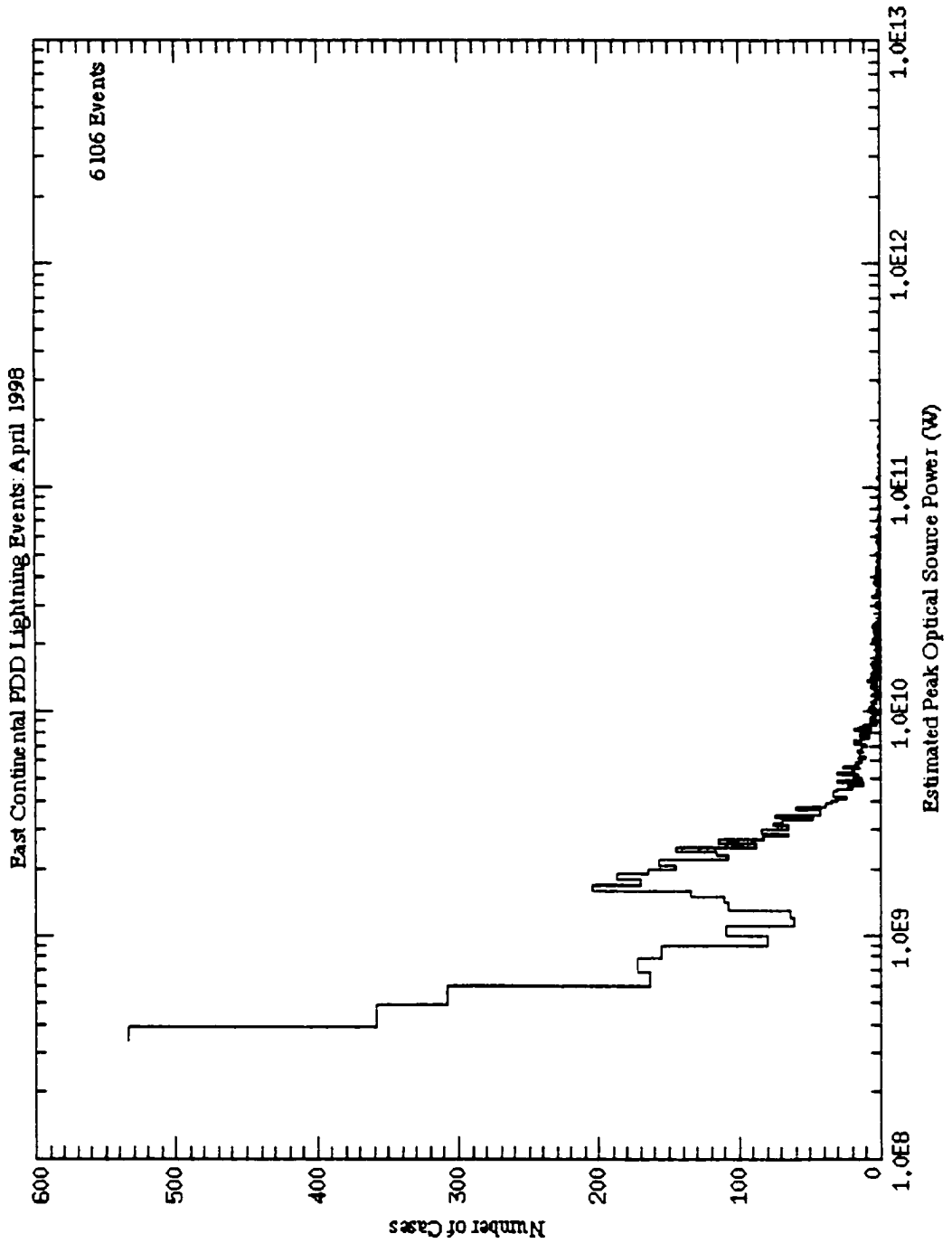


Figure 7 (a): Distribution of Estimated Peak Optical Power for East Continental US PDD Lightning Events — April 1998

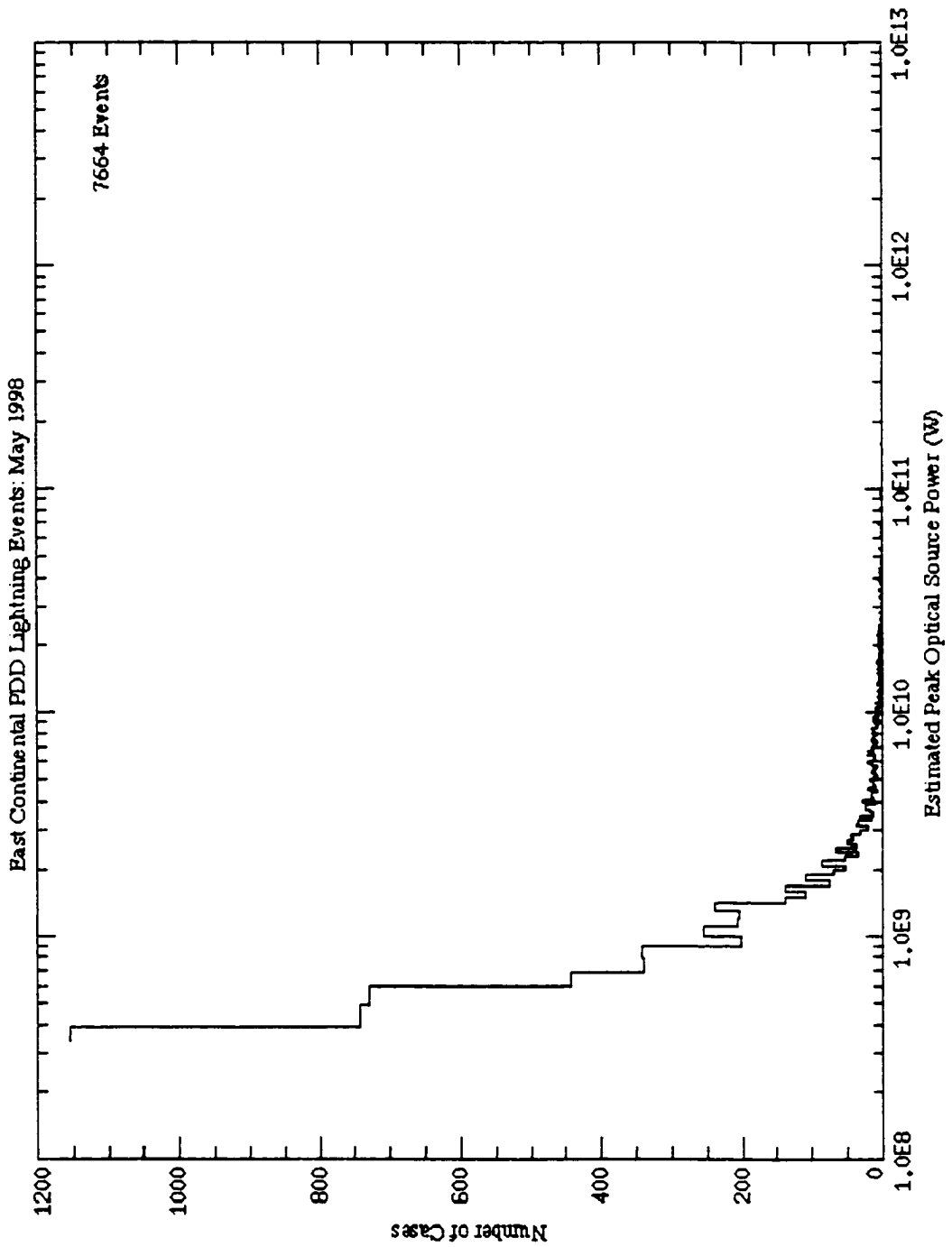


Figure 7 (b): Distribution of Estimated Peak Optical Power for East Continental US PDD Lightning Events — May 1998

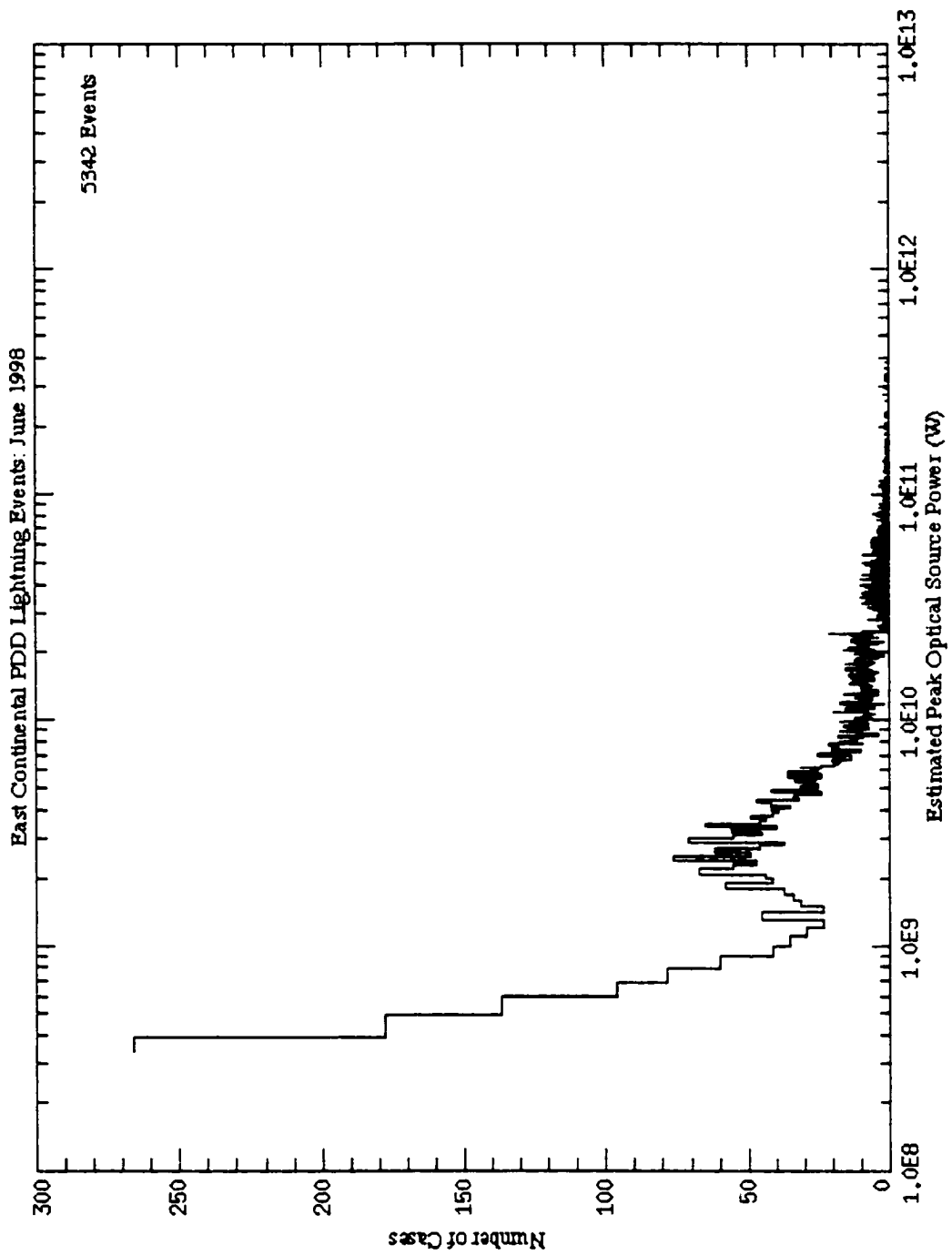
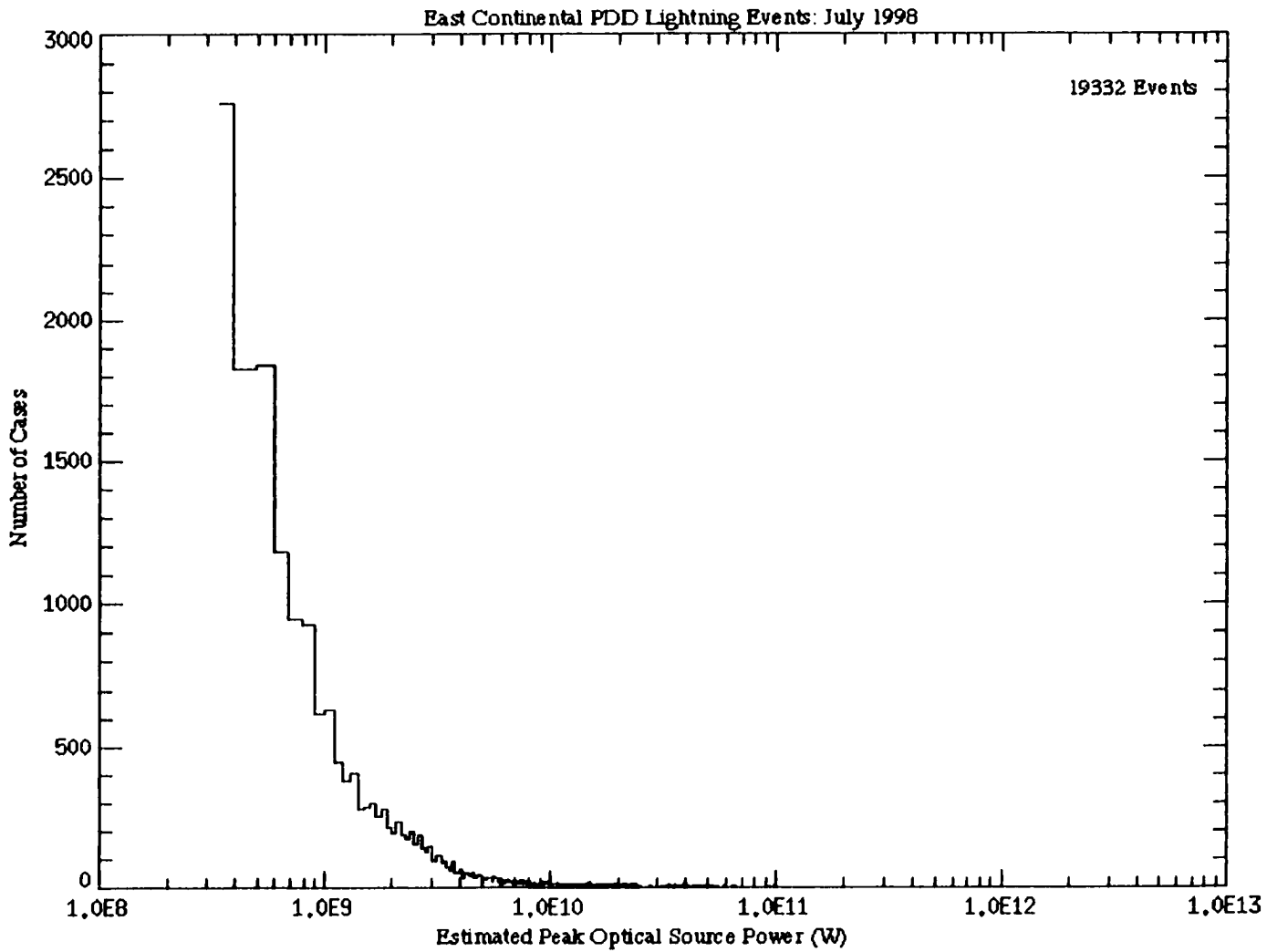


Figure 7 (c): Distribution of Estimated Peak Optical Power for East Continental US PDD Lightning Events — June 1998

Figure 7 (d): Distribution of Estimated Peak Optical Power for East Continental US PDD Lightning Events — July 1998



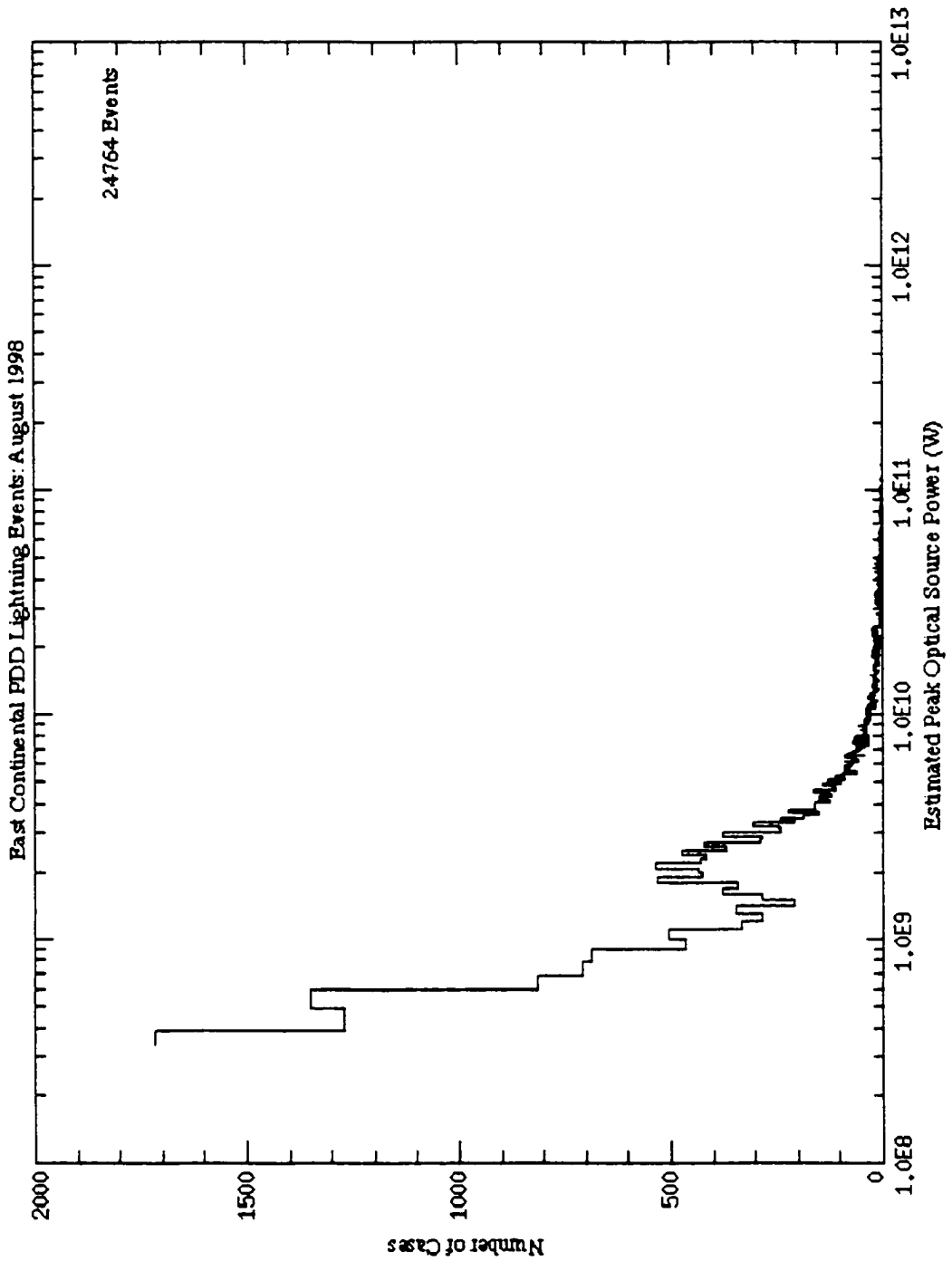


Figure 7 (e): Distribution of Estimated Peak Optical Power for East Continental US PDD Lightning Events — August 1998

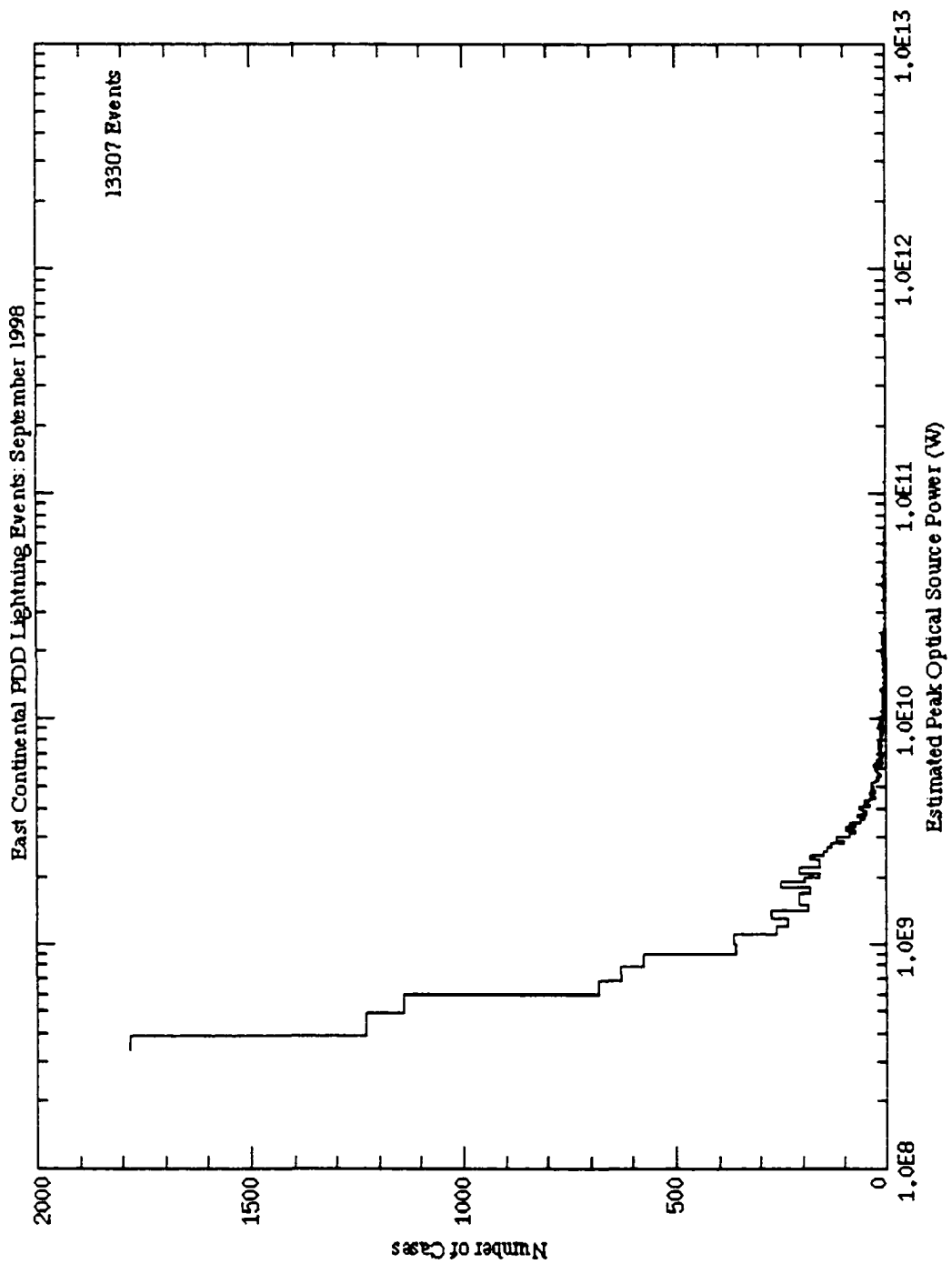


Figure 7 (f): Distribution of Estimated Peak Optical Power for East Continental US PDD Lightning Events — September 1998

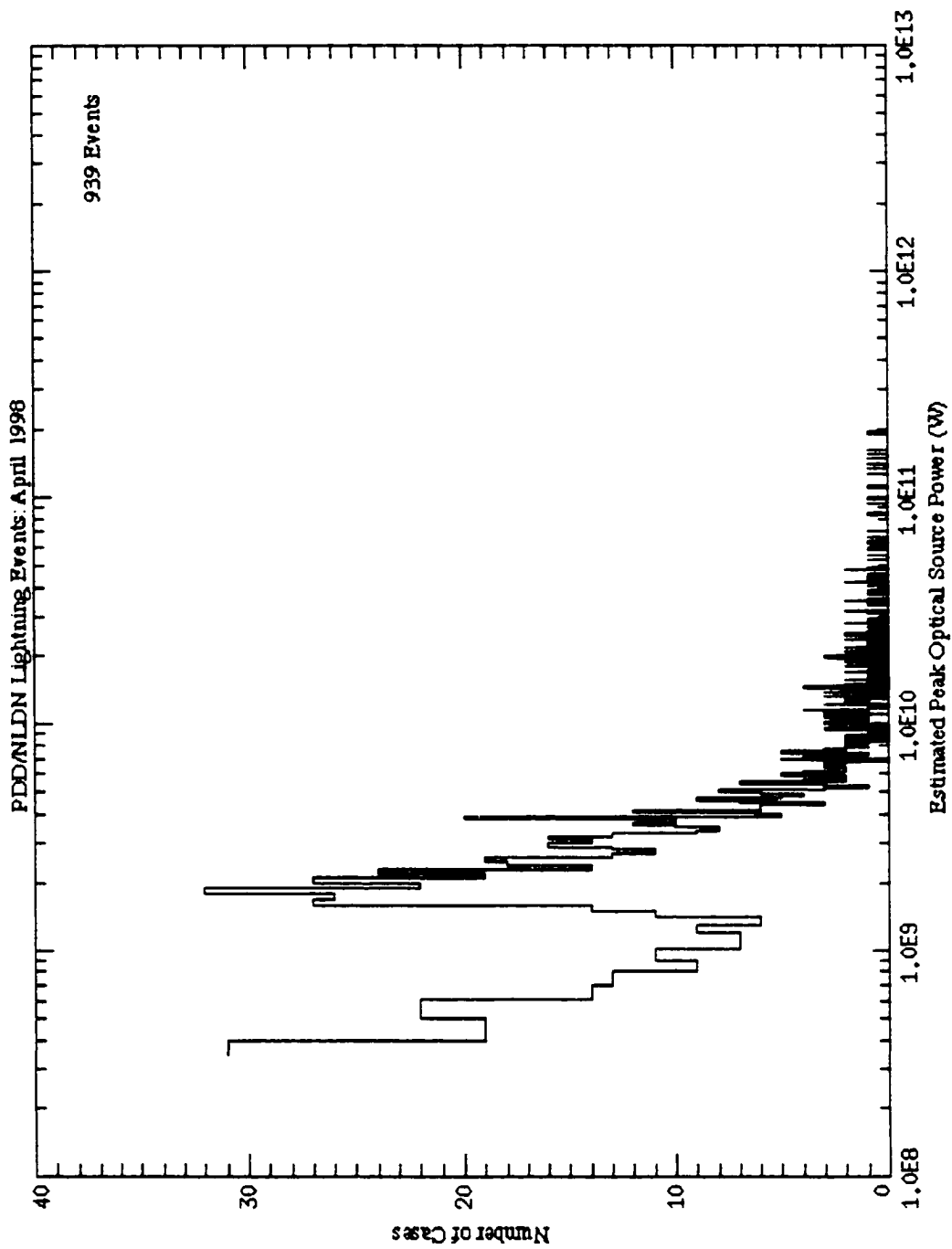


Figure 8 (a): Distribution of Estimated Peak Optical Power for PDD/NLDN Lightning Events — April 1998

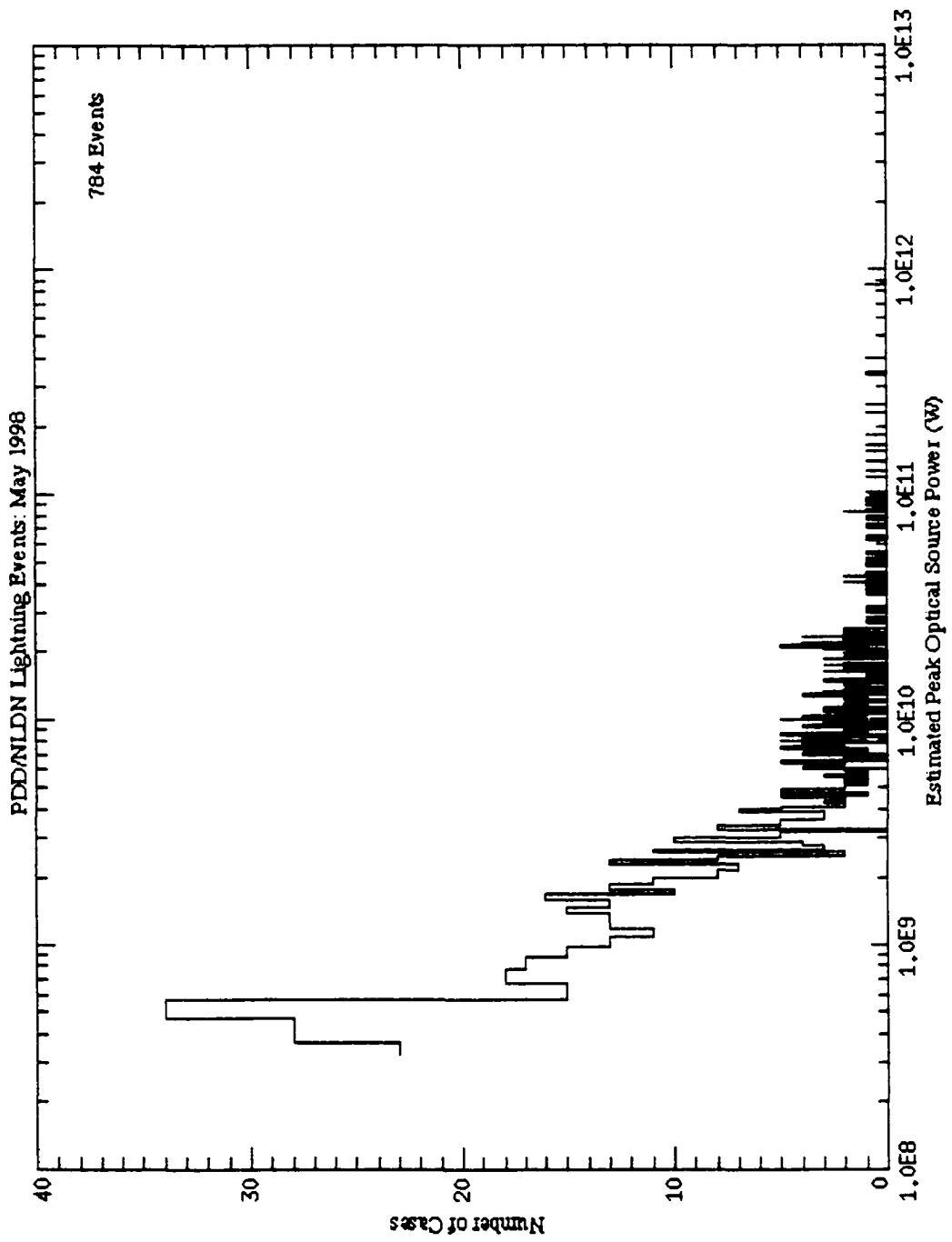


Figure 8 (b): Distribution of Estimated Peak Optical Power for PDD/NLDN Lightning Events — May 1998

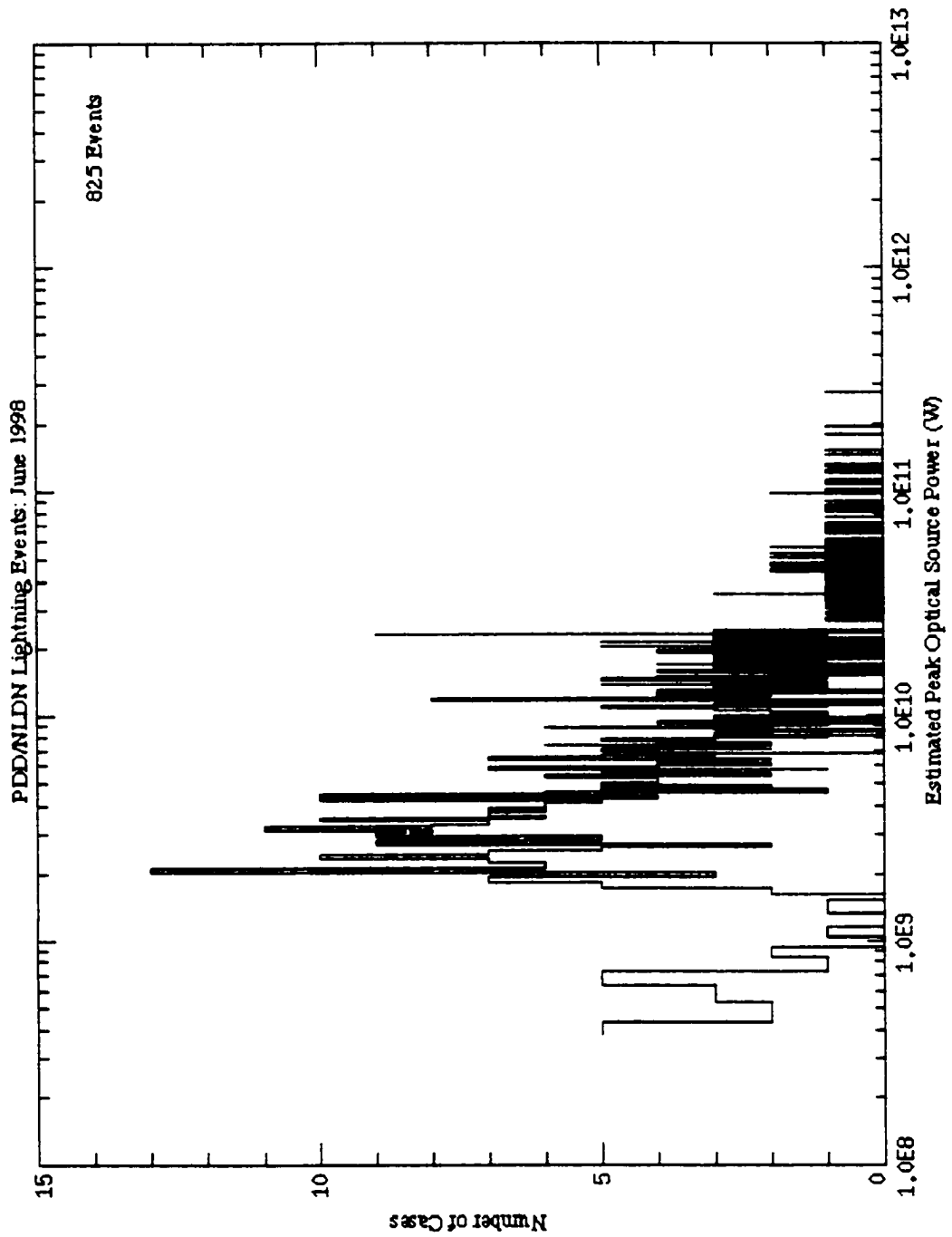


Figure 8 (c): Distribution of Estimated Peak Optical Power for PDD/NLDN Lightning Events — June 1998

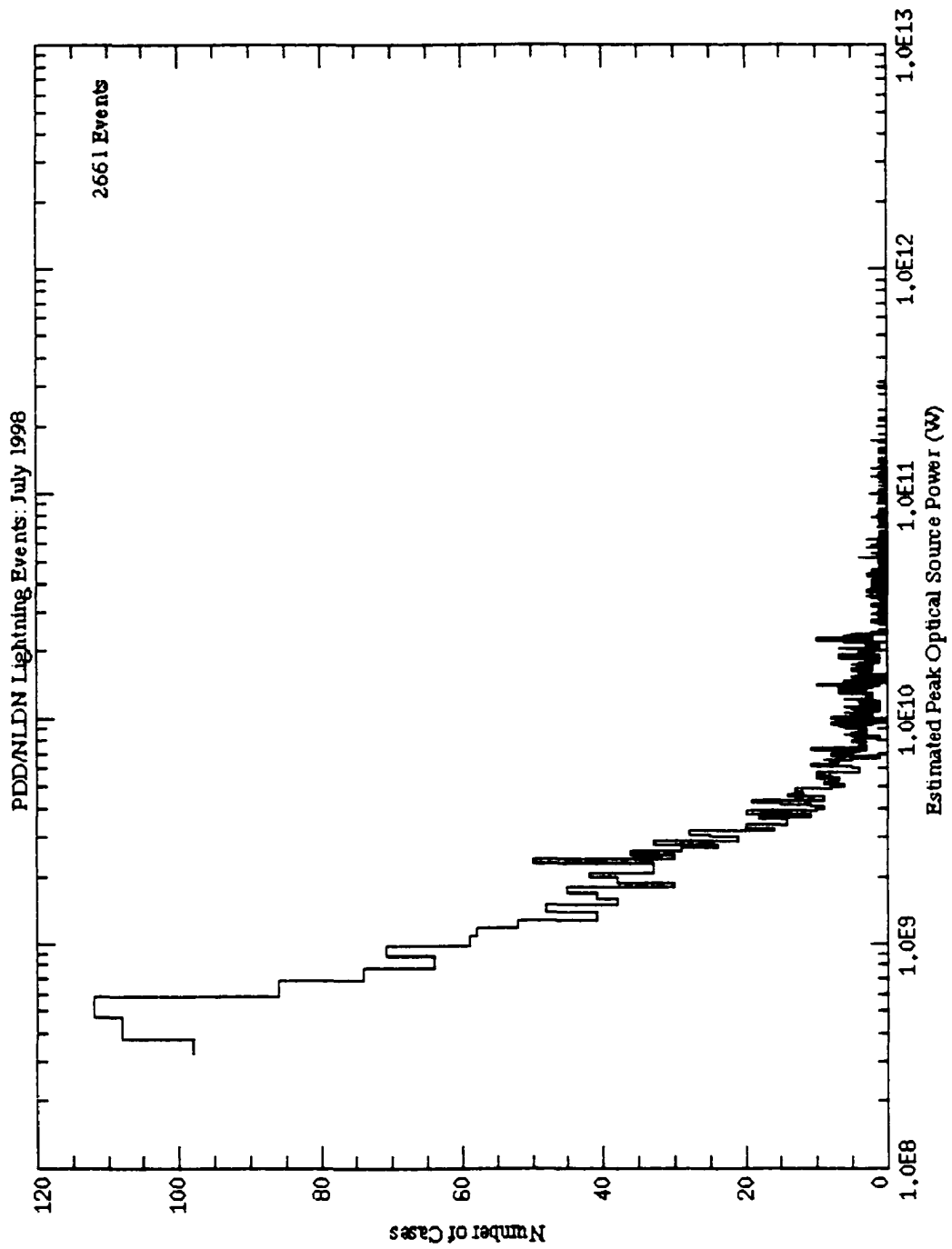


Figure 8 (d): Distribution of Estimated Peak Optical Power for PDD/NLDN Lightning Events — July 1998

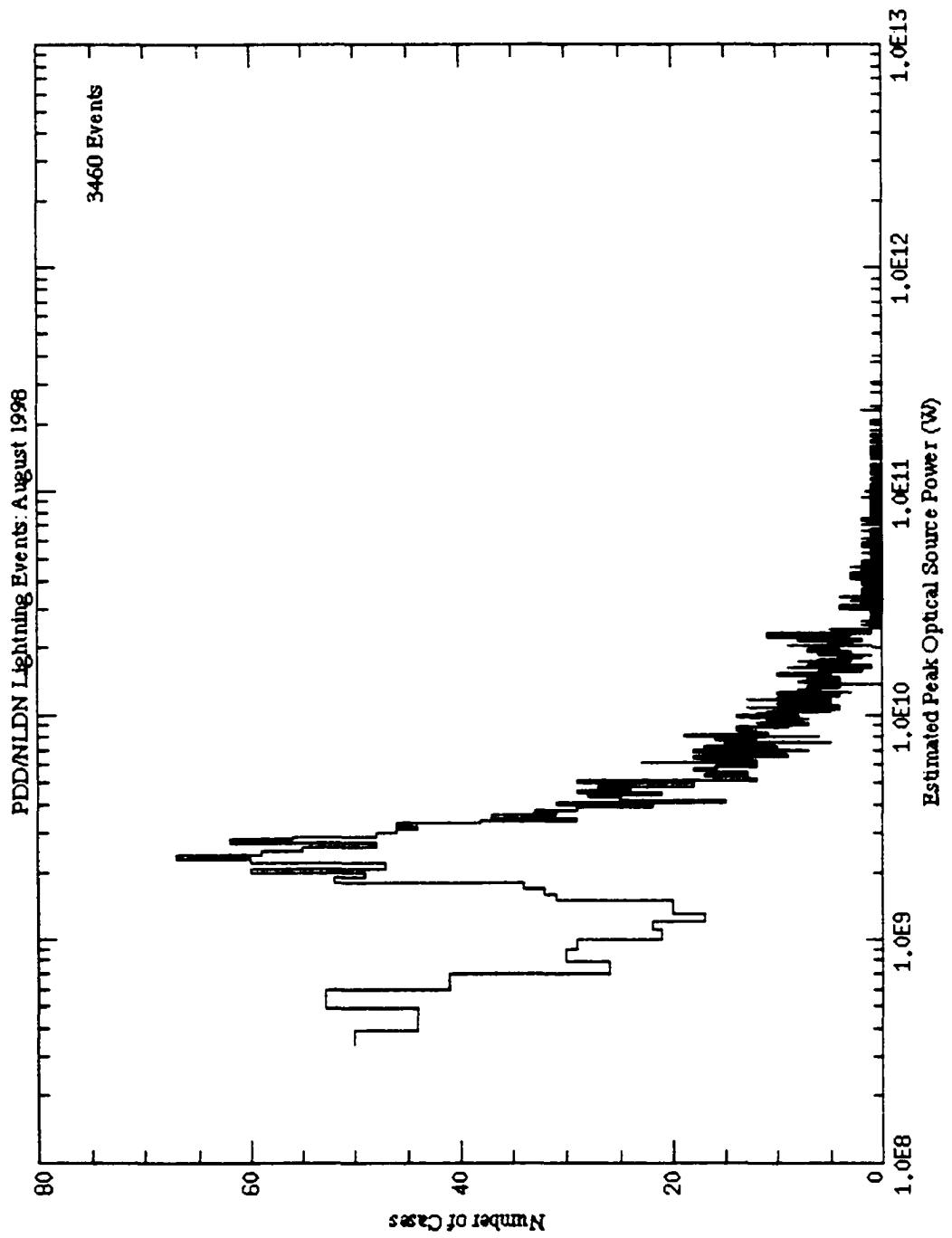


Figure 8 (e): Distribution of Estimated Peak Optical Power for PDD/NLDN Lightning Events — August 1998

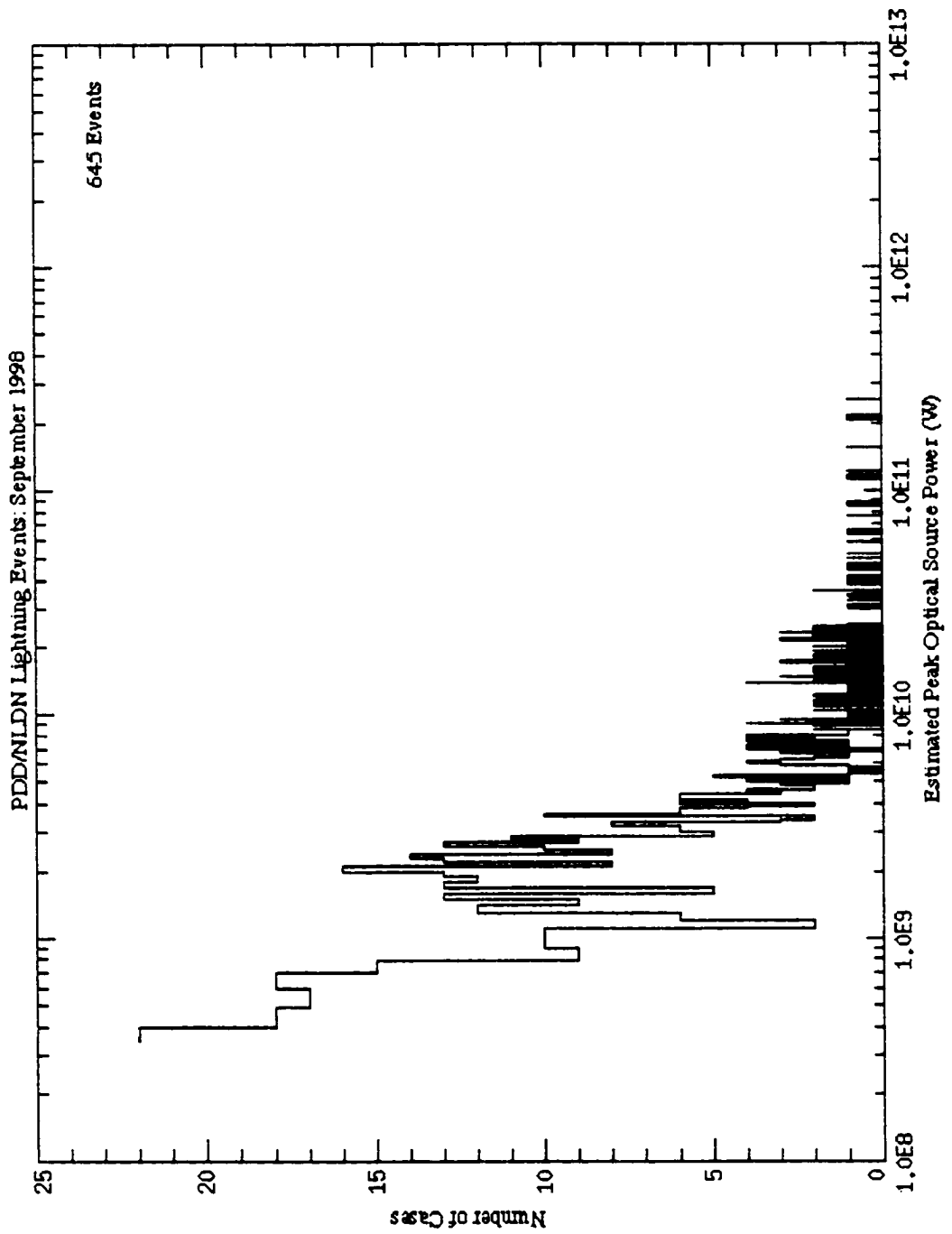


Figure 8 (f): Distribution of Estimated Peak Optical Power for PDD/NLDN Lightning Events — September 1998

TABLE 1: Number of PDD Events According to Estimated Peak Optical Power Ranges

1 (a) Total Global PDD events:

Month	tot PDD	$\geq 10^{11}$	$< 10^{11}$ $\geq 10^{10}$	$< 10^{10}$ $\geq 10^9$	$< 10^9$ $\geq 10^8$
APR	29408	138	2682	18002	8586
MAY	42637	101	2159	16123	24254
JUN	15319	201	4130	7188	3800
JUL	54190	161	3539	20935	29555
AUG	56713	282	6925	28907	20599
SEP	45078	113	2178	18147	24640

1 (b) "East Continental USA" PDD EVENTS:

Month	tot PDD	Num ECONT	$\geq 10^{11}$	$< 10^{11}$ $\geq 10^{10}$	$< 10^{10}$ $\geq 10^9$	$< 10^9$ $\geq 10^8$
APR	29408	6106	24	523	3827	1732
MAY	42637	7664	25	661	3123	3855
JUN	15319	5342	84	1718	2641	837
JUL	54190	19332	82	1721	7742	9787
AUG	56713	24764	142	3652	14204	6766
SEP	45078	13307	56	1101	5933	6217

1 (c) PDD/NLDN Events:

Month	tot PDD	Num w/ NLDN	$\geq 10^{11}$	$< 10^{11}$ $\geq 10^{10}$	$< 10^{10}$ $\geq 10^9$	$< 10^9$ $\geq 10^8$
APR	29408	939	12	185	626	116
MAY	42637	784	15	242	388	139
JUN	15319	825	20	418	369	18
JUL	54190	2661	44	667	1381	569
AUG	56713	3460	50	1080	2070	260
SEP	45078	645	9	147	383	106

Table 2: Breakdown of PDD/NLDN Correlated Events by Power Range for April – September 1998

Table 2 (a) April 1998:

power range (W)	Num ECONT	Num w/ NLDN	% ECONT w/ NLDN	#NLDN CG	#NLDN IC	#NLDN AMBIG
$\geq 10^{11}$	24	12	50.0%	12	0	0
$< 10^{11}$						
$\geq 10^{10}$	523	185	35.4%	184	0	1
$< 10^{10}$						
$\geq 10^9$	3827	626	16.4%	620	4	2
$< 10^9$						
$\geq 10^8$	1732	116	6.5%	111	1	4

Table 2 (b) May 1998:

power range (W)	Num ECONT	Num w/ NLDN	% ECONT w/ NLDN	#NLDN CG	#NLDN IC	#NLDN AMBIG
$\geq 10^{11}$	25	15	60.0%	15	0	0
$< 10^{11}$						
$\geq 10^{10}$	661	242	36.6%	241	1	0
$< 10^{10}$						
$\geq 10^9$	3123	388	12.4%	380	7	1
$< 10^9$						
$\geq 10^8$	3855	139	3.6%	138	1	0

Table 2 (c) June 1998:

power range (W)	Num ECONT	Num w/ NLDN	% ECONT w/ NLDN	#NLDN CG	#NLDN IC	#NLDN AMBIG
$\geq 10^{11}$	84	20	23.8%	15	0	0
$< 10^{11}$						
$\geq 10^{10}$	1718	418	24.3%	241	1	0
$< 10^{10}$						
$\geq 10^9$	2641	369	14.0%	380	7	1
$< 10^9$						
$\geq 10^8$	837	18	2.2%	138	1	0

Table 2 (d) July 1998:

power range (W)	Num ECONT	Num w/ NLDN	% ECONT w/ NLDN	#NLDN CG	#NLDN IC	#NLDN AMBIG
$\geq 10^{11}$	82	44	53.7%	44	0	0
$< 10^{11}$						
$\geq 10^{10}$	1721	667	38.8%	667	0	0
$< 10^{10}$						
$\geq 10^9$	7742	1381	17.8%	1377	4	0
$< 10^9$						
$\geq 10^8$	9787	569	5.8%	561	8	0

Table 2 (e) August 1998:

power range (W)	Num ECONT	Num w/ NLDN	% ECONT w/ NLDN	#NLDN CG	#NLDN IC	#NLDN AMBIG
$\geq 10^{11}$	142	50	35.2%	50	0	0
$< 10^{11}$ $\geq 10^{10}$	3652	1080	29.6%	1078	0	2
$< 10^{10}$ $\geq 10^9$	14204	2070	14.6%	2066	3	1
$< 10^9$ $\geq 10^8$	6766	260	3.8%	259	0	1

Table 2 (f) September 1998:

power range (W)	Num ECONT	Num w/ NLDN	% ECONT w/ NLDN	#NLDN CG	#NLDN IC	#NLDN AMBIG
$\geq 10^{11}$	56	9	16.7%	9	0	0
$< 10^{11}$ $\geq 10^{10}$	1101	147	13.4%	146	0	1
$< 10^{10}$ $\geq 10^9$	5933	383	6.5%	382	1	0
$< 10^9$ $\geq 10^8$	6217	106	1.7%	105	1	0

Table 3: Breakdown of PDD/NLDN Correlated Events by Month for Power Ranges 1-4

3(a) POWER RANGE 1: $10^{11} \text{ W} \leq \text{pwr}$

Month	Num ECONT	Num w/ NLDN	% ECONT w/ NLDN	#NLDN CG	#NLDN IC	#NLDN AMBIG
April	24	12	50.0%	12	0	0
May	25	15	60.0%	15	0	0
June	84	20	23.8%	20	0	0
July	82	44	53.7%	44	0	0
August	142	50	35.2%	50	0	0
September	56	9	16.7%	9	0	0

3(b) POWER RANGE 2: $10^{10} \text{ W} \leq \text{pwr} < 10^{11} \text{ W}$

Month	Num ECONT	Num w/ NLDN	% ECONT w/ NLDN	#NLDN CG	#NLDN IC	#NLDN AMBIG
April	523	185	35.4%	184	0	1
May	661	242	36.6%	241	1	0
June	1718	418	24.3%	241	1	0
July	1721	667	38.8%	667	0	0
August	3652	1080	29.6%	1078	0	2
September	1101	147	13.4%	146	0	1

3(c) POWER RANGE 2: $10^9 \text{ W} \leq \text{pwr} < 10^{10} \text{ W}$

Month	Num ECONT	Num w/ NLDN	% ECONT w/ NLDN	#NLDN CG	#NLDN IC	#NLDN AMBIG
April	3827	626	16.4%	620	4	2
May	3123	388	12.4%	380	7	1
June	2641	369	14.0%	361	7	1
July	7742	1381	17.8%	1377	4	0
August	14204	2070	14.6%	2066	3	1
September	5933	383	6.5%	382	1	0

3(d) POWER RANGE 2: $10^8 \text{ W} \leq \text{pwr} < 10^9 \text{ W}$

Month	Num ECONT	Num w/ NLDN	% ECONT w/ NLDN	#NLDN CG	#NLDN IC	#NLDN AMBIG
April	1732	116	6.5%	111	1	4
May	3855	139	3.6%	138	1	0
June	837	18	2.2%	17	1	0
July	9787	569	5.8%	561	8	0
August	6766	260	3.8%	259	0	1
September	6217	106	1.7%	105	1	0

In order to investigate whether the occurrence of “bright” events, or peak optical power of PDD events in general, is related to flash polarity, polarity information was compiled for each of the four power ranges given above. The results of the polarity analysis are presented in Table 4. The “Num ECONT” column gives the number of PDD events in the East Continental US region for a given month or power range. The “Num w/ NLDN” column gives the number of PDD/NLDN events. The “% ECONT w/ NLDN” column gives the percentage of East Continental Events that had NLDN correlations. The remaining columns give the number of each flash type and each polarity and give what percent of the PDD/NLDN events were made up of each type. The “AMB CG” column represents the subset of PDD/NLDN events that occurred far outside of the NLDN network, for which no peak current or polarity information is available. In addition, the subset of PDD/NLDN events with NLDN peak currents less than +15 kA were classified in the polarity analysis as IC events, as recommended by *Cummins et al.* [1998].

5d. DISCUSSION

Before the results compiled in Section 5c can be used to investigate the question of whether “bright” events are produced by +CG flashes or whether information on flash type or polarity can be gleaned from the estimated peak optical power of lightning-triggered events measured by an instrument such as the FORTE PDD in a global sense, one must first consider whether the East Continental US subset of PDD events shows any regional bias. A comparison of the distributions of peak optical power for the total Global PDD events shown in Figures 6 (a)–(f) and the distributions of peak optical power for the East Continental US events shown in Figures 7 (a)–(f) sheds some light on the issue. For most of the months considered, the distribution of peak source powers for the East Continental US follows the same pattern as the distribution of peak source powers for all PDD events. Hence, the East Continental US population of events can be considered representative of the global distribution (at least in terms of overall PDD event power characteristics) for these months. However, for June, the East Continental US events show a small second peak in the frequency of occurrence of events having peak optical power of $2.5\text{--}3.0 \times 10^9$ W

Table 4: Polarity Analysis for PDD/NLDN Events

Month	Num Econt	Num w/ NLDN	% ECONT w/NLDN	# CG	# IC	# AMB	POS CG	NEG CG	AMB CG
APR	6106	939	15.8%	883	49	7	135	307	441
MAY	7664	784	10.2%	755	28	1	86	395	274
JUN	5342	825	15.4%	802	23	0	66	488	248
JUL	19332	2661	13.8%	2601	60	0	94	1215	1292
AUG	24764	3460	4.0%	3393	62	5	136	1998	1259
SEP	13307	645	4.8%	628	16	1	41	179	408

Peak Power	Num Econt	Num w/ NLDN	% ECONT w/NLDN	# CG	# IC	# AMB	POS CG	NEG CG	AMB CG
$\geq 10^{10}$ W	413	150	36.6%	150	0	0	27	44	79
$< 10^{11}$ W									
$\geq 10^{10}$ W	9376	2739	29.2%	2708	27	4	263	1419	1026
$< 10^{11}$ W									
$\geq 10^{10}$ W	37470	5217	13.9%	5046	166	5	242	2740	2064
$< 10^{11}$ W									
$\geq 10^{10}$ W	29194	1208	4.1%	1158	45	5	26	379	753

that is absent in the peak power distribution for global PDD events. Also, in August, there is a slight peak in the East Continental US events at $\sim 2.0 \times 10^9$ W that is absent in the global data. Generally, the East Continental US events represent the global population, but some regional bias appears to exist in the data.

The monthly distributions for PDD/NLDN events presented in Figures 8 (a)–(f) can be compared to the East Continental US distributions to see if the power characteristics of the PDD/NLDN events (i.e. flashes seen by the PDD which had associated ground flashes) differ from the power characteristics of the background population of PDD events. What can be seen from the comparison of the two populations is that PDD/NLDN events tend toward higher power ranges than the total events seen by the PDD over the same area.

Are “bright” PDD events associated with +CG events? This question can be broken down into two questions. First, are “bright” PDD events associated primarily with CG events? When the total number of events are considered for the entire six-month time period, $\sim 36\%$ of the “bright” PDD events were associated with NLDN CG events, but if one looks month to month, $15\text{--}60\%$ of the bright events are associated with NLDN CG events. In the East Continental US data, approximately $5\text{--}15\%$ of the PDD events are associated with NLDN CG events. Therefore, the bright PDD events are more likely associated with CG events than the underlying PDD event population. Second, are the associated CG events primarily positive or negative? When one considers only the events for which polarity can be determined, the “bright” events trend more toward the positive (38% +CG) than the total population of PDD/NLDN events ($\sim 12\%$ +CG). “Bright” PDD/NLDN events are also more likely to be positive than the PDD/NLDN events in the other three peak optical power ranges investigated here. Furthermore, when one considers that positive CG events have been shown to comprise less than 10% of all CG events over the U.S. (Orville [1994]), the PDD/NLDN data indicate that bright PDD events with an associated CG also have a greater tendency to be positive than the underlying climatology.

This does *not* mean that all bright PDD events are caused by positive CG strokes. However, one can not discount that possibility that positive CG strokes may more frequently cause the lightning flashes associated with them to be more optically powerful when viewed from above. One last caveat to consider is that this data set covers a warm-season period. Though the overall number of lightning events is much smaller for winter

storms than for summer storms. +CG flashes are thought to account for a greater percentage of the total lightning (*Orville [1994]*). Whether bright PDD/NLDN pairs for winter storms would show an even stronger relationship to flashes that include +CG strokes remains to be investigated.

The second major question being investigated with the PDD/NLDN analysis is whether the peak optical power of a PDD event, in general and not just for "bright:" events, can be related to flash type. When one considers the percentage of each power range "bin" of East Continental US events which had NLDN correlations, a clear pattern emerges. For greater values of peak optical power, a greater percentage of PDD events are associated with NLDN events. This trend is visible for all months in the April–September 1998 period, though the actual percentages vary. When the six months of data are taken as a whole, roughly 30% of all PDD events with peak powers $> 10^{10}$ W (those events in power ranges 1 and 2) are associated with NLDN events, while only about 9% of PDD events with peak powers $< 10^{10}$ W (those events in power ranges 3 and 4) are associated with NLDN events. From this, high-power PDD events are more likely than low-power PDD events to be associated with CGs.

Again, it can not be stated that all high power PDD events are associated with CG and all low power PDD events are associated with IC events, but on a seasonal and regional basis, there is evidence that the likelihood that a PDD lightning event is associated with a CG can be determined based on peak optical power of the event. To quantify this relationship to the point where it could be perhaps used operationally, the effects of seasonality need to be investigated. Also, the land/ocean bias in the data needs to be removed. Because the relaxed criteria NLDN data include ground-flashes that are over the ocean, it is possible that the ratio of IC to CG events over the oceans may be causing the percentages of PDD events that are associated with NLDN events to appear low. Also, it should be noted that the NLDN detection efficiency over the ocean is greatly reduced, while the PDD's ability to detect lightning over the ocean is no different than its ability to detect lightning over land. Because the NLDN is underreporting the number of CGs over the ocean, this almost certainly has introduced a great deal of error in the current results.

CHAPTER 6

COMPARISON BETWEEN PDD AND LMA DETECTED EVENTS

In this chapter, data from the New Mexico Tech Lightning Mapping Array (LMA) are used to provide ground truth for the PDD. Data from these two instruments are used together in order to investigate the following questions. Is there a relationship between the physical dimensions of a lightning flash and whether or not that flash is detected by the PDD? Do the PDD and the National Lightning Detection network see different parts of the lightning flash process? How does what each system sees relate to what the other sees?

In this chapter, a case study from June 25, 2000 is presented and used to investigate the questions stated above. Section 6a describes the Severe Storm Electrification and Precipitation Study (STEPS) 2000 LMA, gives an overview of the June 25 storm, and an overview of the nature of the LMA, PDD, and NLDN data that are available for this case. Section 6b describes how the data were used, and Section 6c discusses the results.

6a. COINCIDENT DATA ON 25 JUNE 2000, DURING STEPS

On June 25, 2000 the FORTE satellite passed over a storm that was also in view of the LMA during the STEPS 2000 experiment. The storm was within the field of view of

the satellite for approximately 2 minutes and 45 seconds (from 07:52:00 UT to 07:54:45 UT).

For STEPS 2000, a total of 13 lightning mapping stations were deployed over a four county area in northwest Kansas and eastern Colorado. The network was in operation from mid-May to mid-August, 2000. Figure 9 shows the locations of the mapping stations and the radars used during STEPS. The lightning mapping array covered an area about 80 km in diameter. Each of the stations was linked back into an operations center next to the National Weather Service Office in Goodland, KS (which is located on the lower right on the map. Data was transmitted over wireless links at a throughput rate of 4 Mbits/Second (*Krehbiel et al. [2000b]*).

Figure 10 shows the Central Plains Composite of Level 1 NEXRAD radar data for 08:00:00 UT on June 25, 2000. There is a large area of storm activity in the area of the Texas and Oklahoma panhandles, but this area is outside of the STEPS LMA detection range. The storm to be investigated here is the storm that is almost due North of Goodland (GLD). Figure 11 shows a summary of LMA activity over a ten minute period beginning at 07:50:00 UT. The large box shows a plan-view. The small green boxes are the location of the LMA stations. The greatest density of LMA points is shown in red. The activity for this storm occurred about 120 km from the center of the LMA array. The data available for this case are a coarse-resolution analysis of LMA locations that has a 500 μ s time-resolution (as opposed to the fine-resolution data which provides 100 μ s resolution).

Errors in the LMA event locations for LMA events occurring outside the STEPS network can be approximated as follows (*Ron Thomas, personal communication, [2001]*):

$$\text{error in altitude} = 0.5 (r / 100)^2 (10 / h)$$

$$\text{error in range} = 0.5 (r / 100)^2$$

$$\text{error in azimuth} = 0.5 (r / 100)$$

where "r" is the distance from the center of the LMA array (km) and "h" is the altitude of the source (km). For the June 25, 2000 storm the altitude error on a source at 10 km height is 0.7 km, the range error is 0.7 km, and the azimuth error is 0.6 km. The error in most

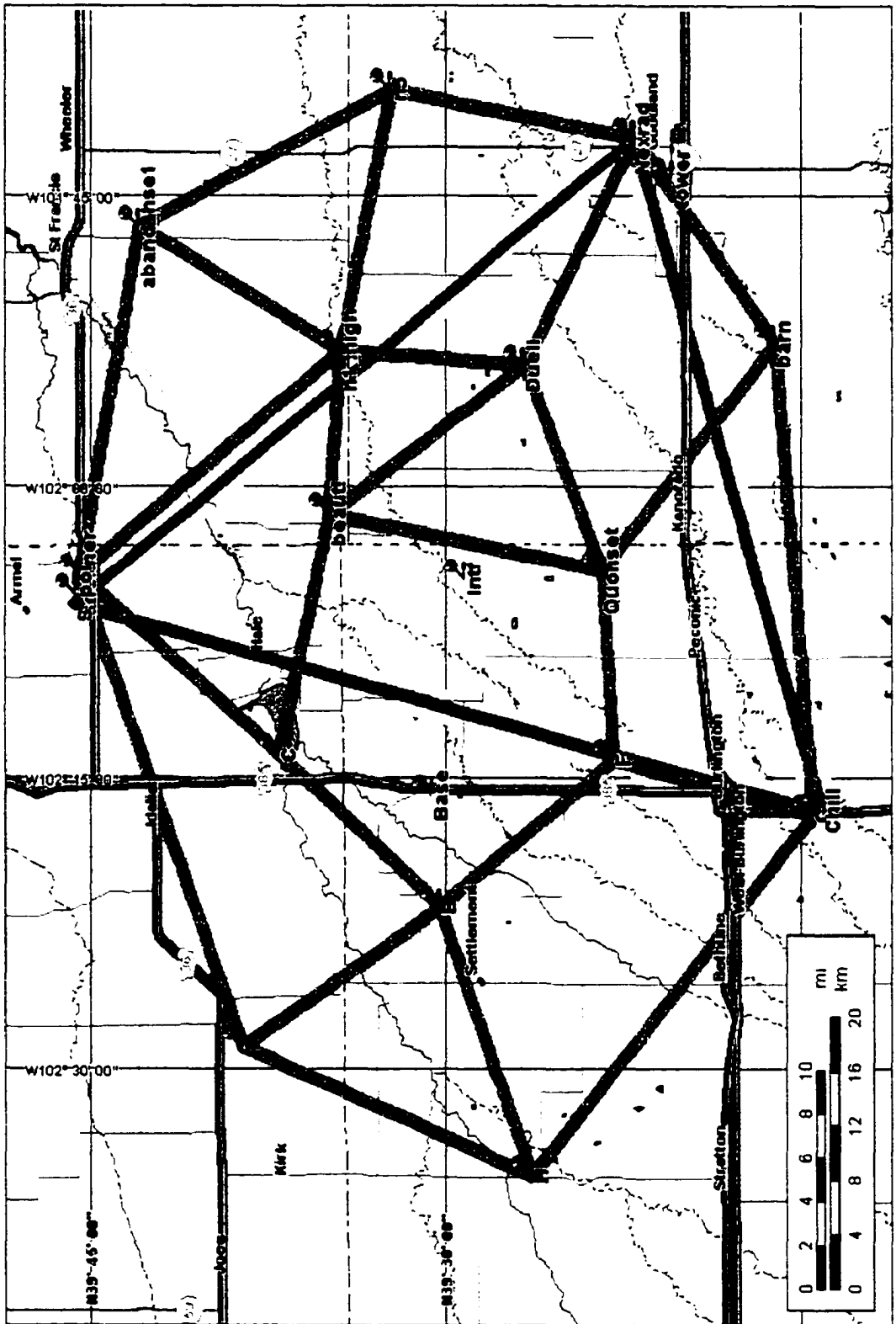
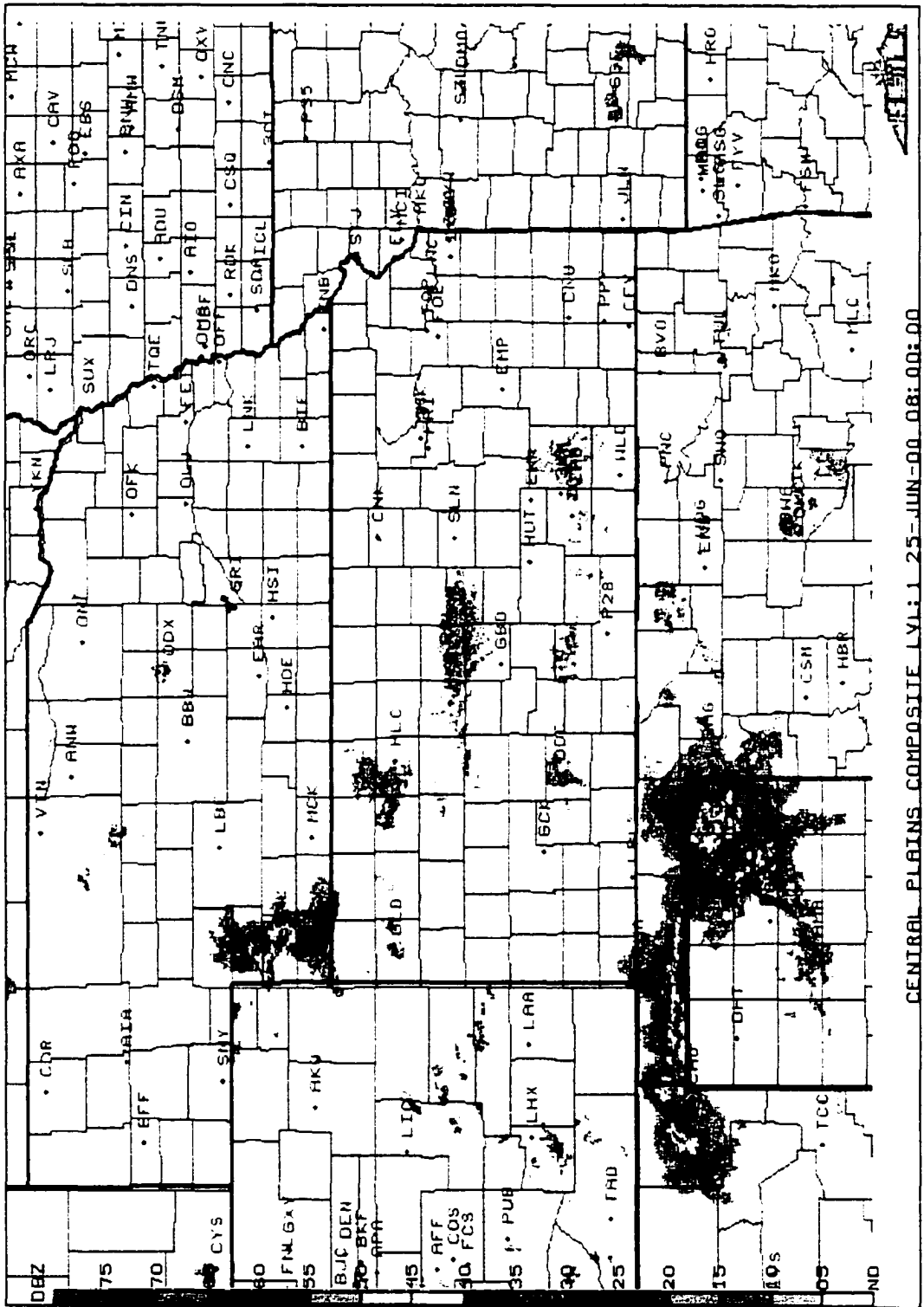


Figure 9: Location of STEPS 2000 LMA stations (Krehbiel et al. [2000])
 LMA stations are connected by the thick red lines.



CENTRAL PLAINS COMPOSITE LVL1 25-JUN-00 08:00:00

Figure 10: Central Plains Lvl-1 Radar Composite June 25, 2000 0800 UT
 Storm of interest is in southwest Nebraska.

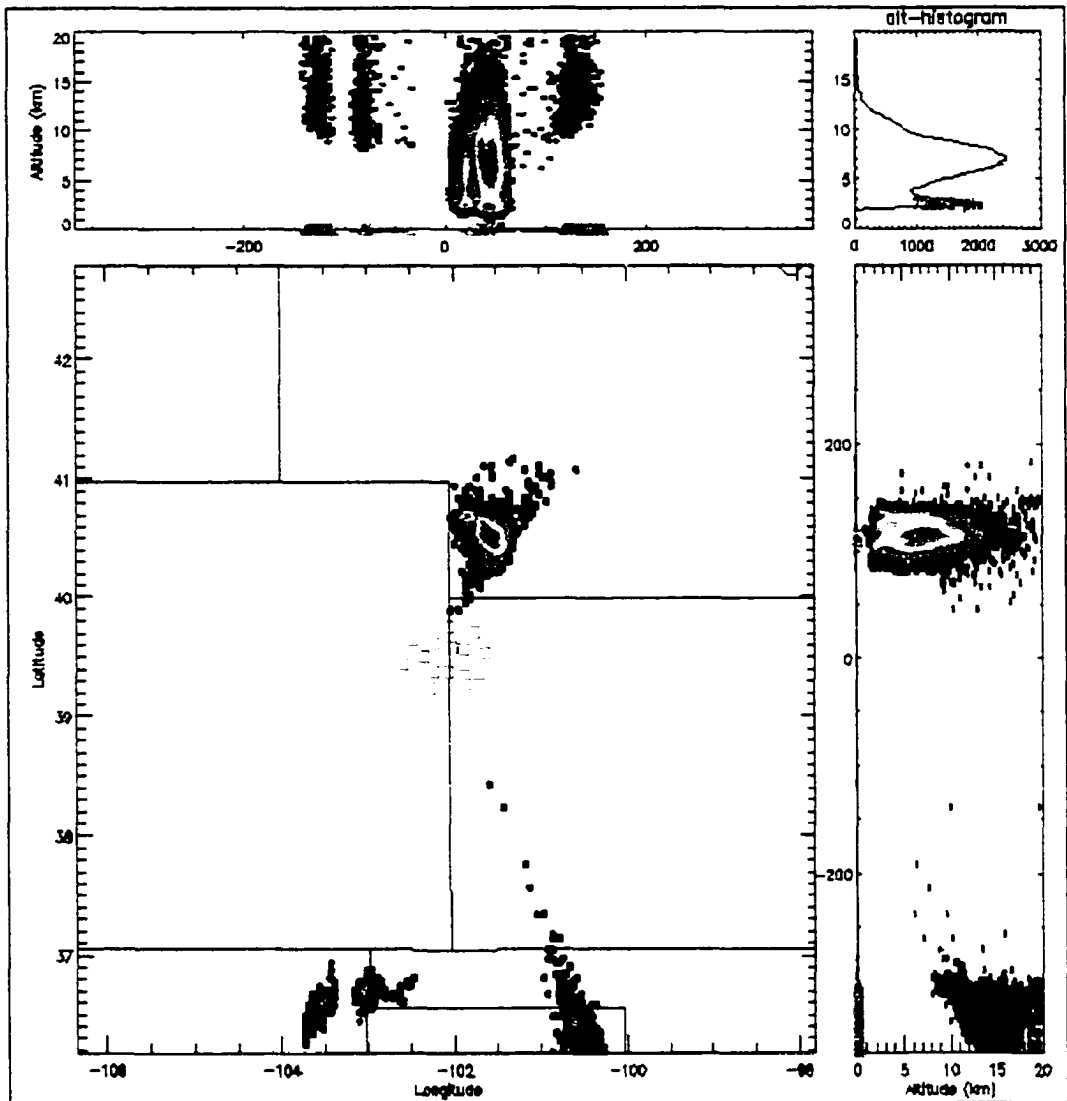


Figure 11:
Summary of LMA activity 07:50-08:00 UT on June 25, 2000

Upper left panel shows east-west distance from LMA array center (km) vs altitude of LMA activity (km). Green "X" along x-axis represents the east-west distance (km) of positive polarity NLDN event from center of LMA array. Upper right panel shows altitude histogram of LMA activity. Lower left panel shows a plan view of LMA activity. Units are Lat/Lon. Small green squares are the locations of LMA stations. Lower right panel shows north-south distance (km) from the center of LMA array vs. altitude of LMA activity. Red areas indicate the greatest density of LMA points. dark purple indicates the least density of LMA points.

LMA locations is due to errors in measuring the exact time of the arrival of a VHF impulse at each ground station. Less than 1% of LMA locations have an error with standard deviations about 10 times as great. This error is due to incorrect correlation of arrival times (that is, when not all stations used to locate an event are using the same event in the solution). Thus, there will be a few points in a flash with much greater errors than those caused by errors in measuring the arrival time.

During its 2 minute 45 second pass over the June 25, 2000 storm, the FORTE PDD recorded 63 lightning-triggered events. The estimated peak optical power for these events ranged from $\sim 1.6 \times 10^9$ W to $\sim 2.4 \times 10^{10}$ W. Figure 12 shows the path of the satellite during this pass. The asterisks (*) are the sub-satellite locations of the PDD triggers mentioned above. The small squares are the locations of the LMA stations. At FORTE's closest approach, the distance between the sub-satellite point and the center of the LMA array is approximately 120 km.

Locations of ground strokes during this period from the National Lightning Detection Network are also available. Unlike the NLDN data described in Chapter 5, Section 5b, the NLDN data used here are standard NLDN data. The region of interest is well within the NLDN network, so the detection efficiency is $\sim 90\%$ for first return strokes. The timing of the NLDN data is good to 1 ms.

6b. ANALYSIS METHODS AND RESULTS

Several steps are necessary in order to use the LMA data as ground truth for the FORTE PDD data. First, the LMA data must be examined, and individual flashes must be identified. Second, the PDD events must be matched up in time with the flashes mapped by the LMA. Once the correlations are made, characteristics of the LMA-mapped flashes that were seen by the PDD and those that were not seen by the PDD must be identified and compiled. Then the characteristics can be examined for differences between the population of LMA-mapped flashes that were seen by the PDD and the population of LMA-mapped flashes that were not seen by the PDD.

The LMA flashes were identified by careful visual inspection of the time series of

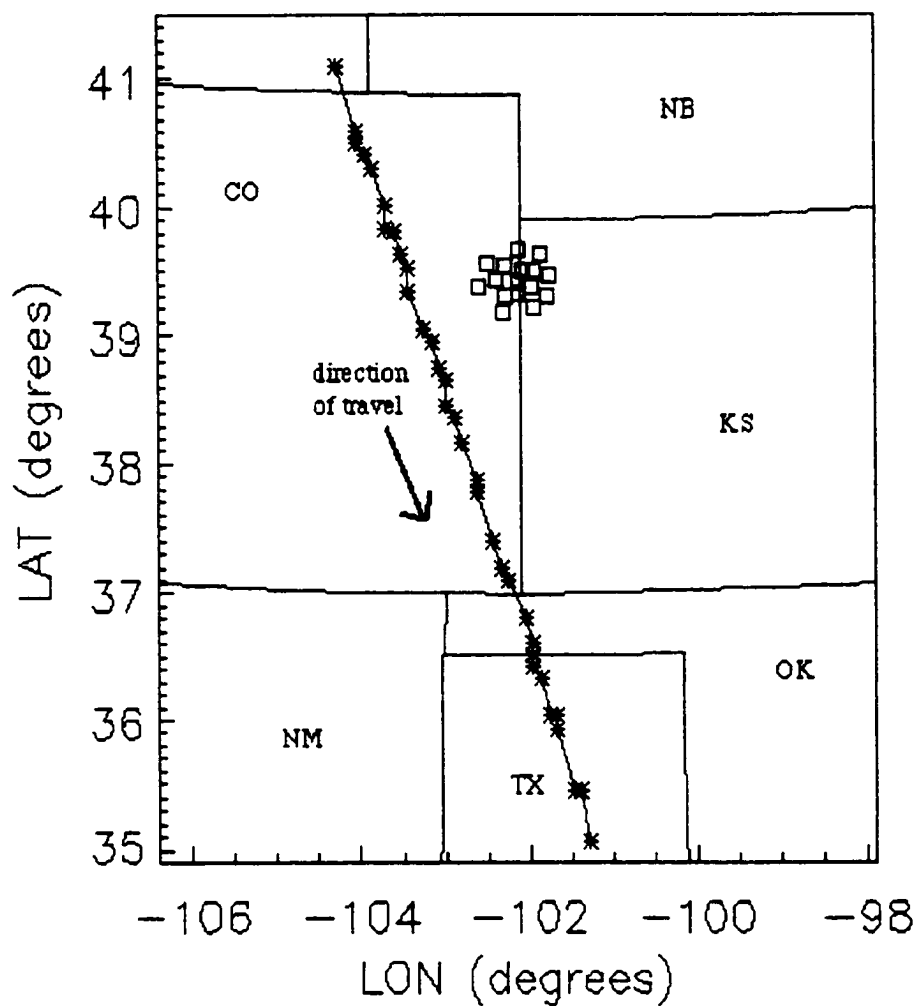


Figure 12: Subsattelite Locations of PDD events during June 25, 2000 pass

Asterisks are the subsattelite locations of PDD events during the June 25, 2000 pass. Small squares are the locations of the STEPS LMA stations.

VHF source locations. For each 15 second period during the PDD pass overhead, a plot of LMA altitude vs. time of the LMA point was examined. Groupings of LMA points which were closely spaced in time, with a time-difference of less than 0.2 s between the last LMA point in one group and the first LMA point in the next group, were identified. Spatial and temporal animations of each time grouping were examined in detail. A grouping of points was identified as a single "flash" if:

- The progression of LMA points in space and time was continuous.
- There was not more than a few kilometers of spatial separation between where the LMA points were occurring
- And/or the LMA activity occurring late in the time-grouping seemed to follow a similar spatial path to LMA activity which occurred at the start of the grouping.

In this manner, ~190 separate LMA flashes were identified during the PDD pass, ranging in duration from ~0.2 s to ~1.6 s. Only three of these LMA flashes had an associated ground stroke location from the NLDN, and of these three, two were of positive polarity. Another interesting characteristic of the LMA flashes identified during the PDD pass is that most were "inverted polarity" IC flashes, as described by *Krehbiel et al.* [2000b]. Intracloud discharges identified in LMA data usually occur between negative charge at midlevels in the storm and positive charge in the upper part of the storm. Inverted IC discharges do the opposite: they start in the upper part of the storm and develop downward. Findings described by *Krehbiel et al.* indicate that, for storms with predominantly inverted IC discharges, the electrical polarity of the parent storm is also inverted, with a positive charge layer at midlevels and a negative charge layer in the upper part of the storm.

PDD lightning-triggers were matched with LMA flashes in the following manner. First, a general check was done to count the number of LMA points that occurred within ± 20 ms of the PDD trigger time. These points were then plotted relative to the LMA array, the PDD sub-satellite point, and the PDD field of view to confirm that the events were occurring where the PDD could see them. An example of these plots is presented in Figure

13. Next, the PDD lightning-trigger times were examined against spatial and temporal plots for each LMA flash, and matched up in terms of flash-level correlation. PDD events for which there were no LMA points or only a few LMA points over the Texas or Oklahoma panhandles were attributed to lightning in the storms that were occurring in the Texas and Oklahoma panhandle region, far south of the LMA. These southern storms were within the PDD field of view for almost the entire pass over the LMA array. A check was done to make sure that PDD lightning-triggers that were matched with LMA flashes in the target storm were not time-correlated with any NLDN ground strokes reported from the Southern area of activity. But some uncertainty remains as to whether some of the PDD lightning-triggers which are matched with LMA flash events in the northern storm were really caused by IC lightning events in the southern storms. In the end, 41 PDD events were attributed to being associated with 26 LMA flashes.

The next step was to identify and compile characteristics for each LMA flash, so that the characteristics for flashes that were seen by the PDD and characteristics for the LMA flashes that were not seen by the PDD could be compared. Maximum height of an LMA point within the flash was chosen because studies with the LIS indicate that a spacecraft-based optical instrument might preferentially detect flashes which reach highest in the storm (*Thomas et al. [2000]*). Because a flash with large horizontal extent might illuminate a greater area of the cloud, thereby increasing the possibility of being detected from above by an optical instrument, spatial extent of the LMA flash was also investigated. North-south extent (km) and east-west extent (km) of each LMA flash were chosen as ways to quantify the overall spatial extent of each LMA flash because they could be easily compiled by viewing a "plan-view" map of each flash. Height of maximum activity within the flash and duration of flash were also compiled.

The distribution of maximum height reached by any one LMA point in a flash for the population of LMA flashes seen by the PDD and the population of LMA flash events which were not seen by the PDD is presented in Figure 14. Distributions of North-South extent and East-West extent for the two populations are presented in Figure 15 and Figure 16, respectively. Figure 17 shows the resulting distributions of area of LMA flash events (North-South extent multiplied by East-West extent). Figure 18 shows the distributions for height of maximum LMA activity, and Figure 19 shows the distributions for duration of

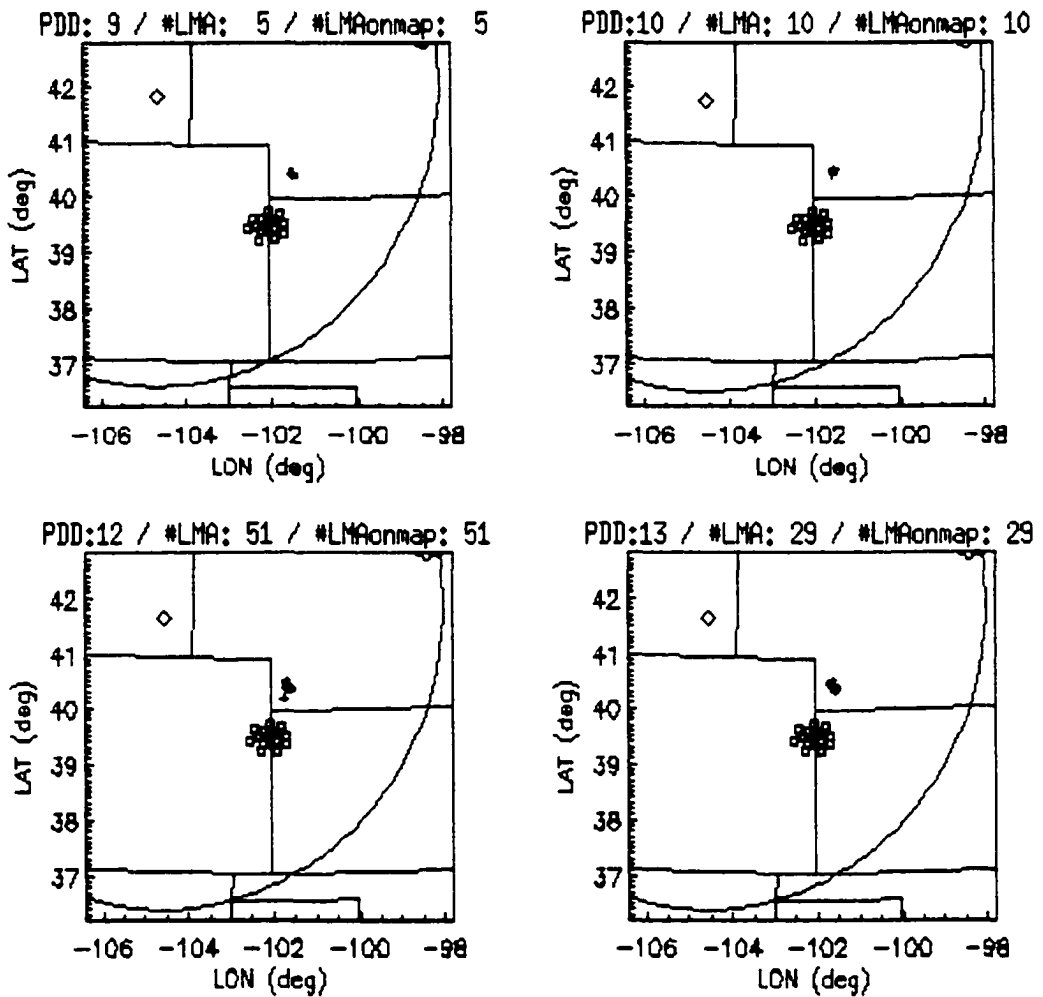


Figure 13: ± 20 ms LMA Plots

These plots were used to confirm that an LMA flash of interest was occurring within the PDD field of view. Caption at the top of each panel gives the pass-relative PDD event index, the number of LMA points found within ± 20 ms of the PDD trigger time, and the number of LMA points on the map. Plus signs are locations of LMA points, diamonds are the subsatellite location of the PDD, small squares are the locations of the LMA stations, and the large circle is the edge of the PDD field of view. Plotted here are PDD events with index 9, 10, 12, and 13.

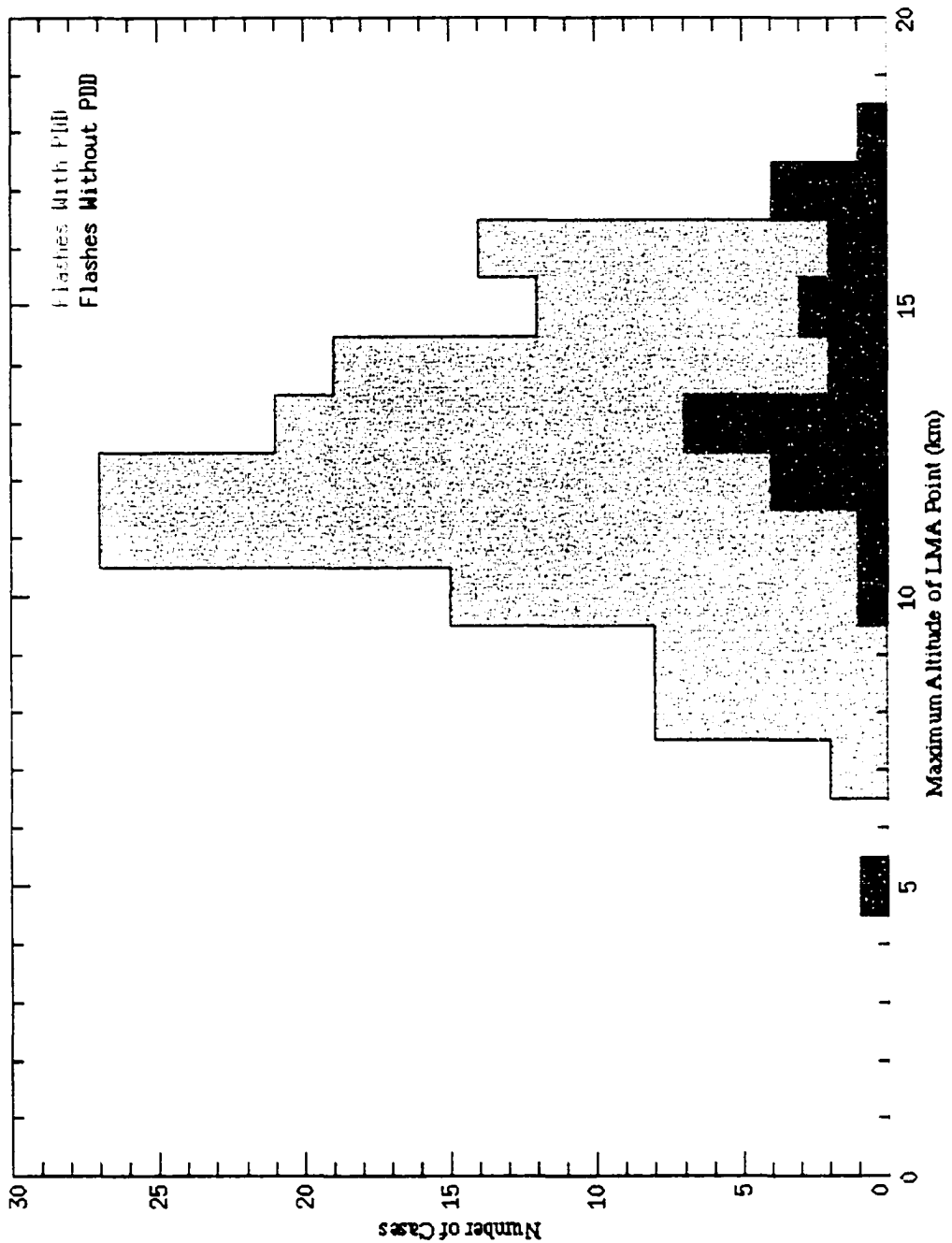


Figure 14: Maximum Altitude of LMA point

Distribution for LMA flashes that were seen by the PDD is in red. Distribution for LMA flashes that were not seen by the PDD is in gray. The means are different (Wilcoxon Rank-Sum p-value = 0.0013). The distributions are similar (Two Sample Kolmogorov-Smirnov p-value = 0.6181)

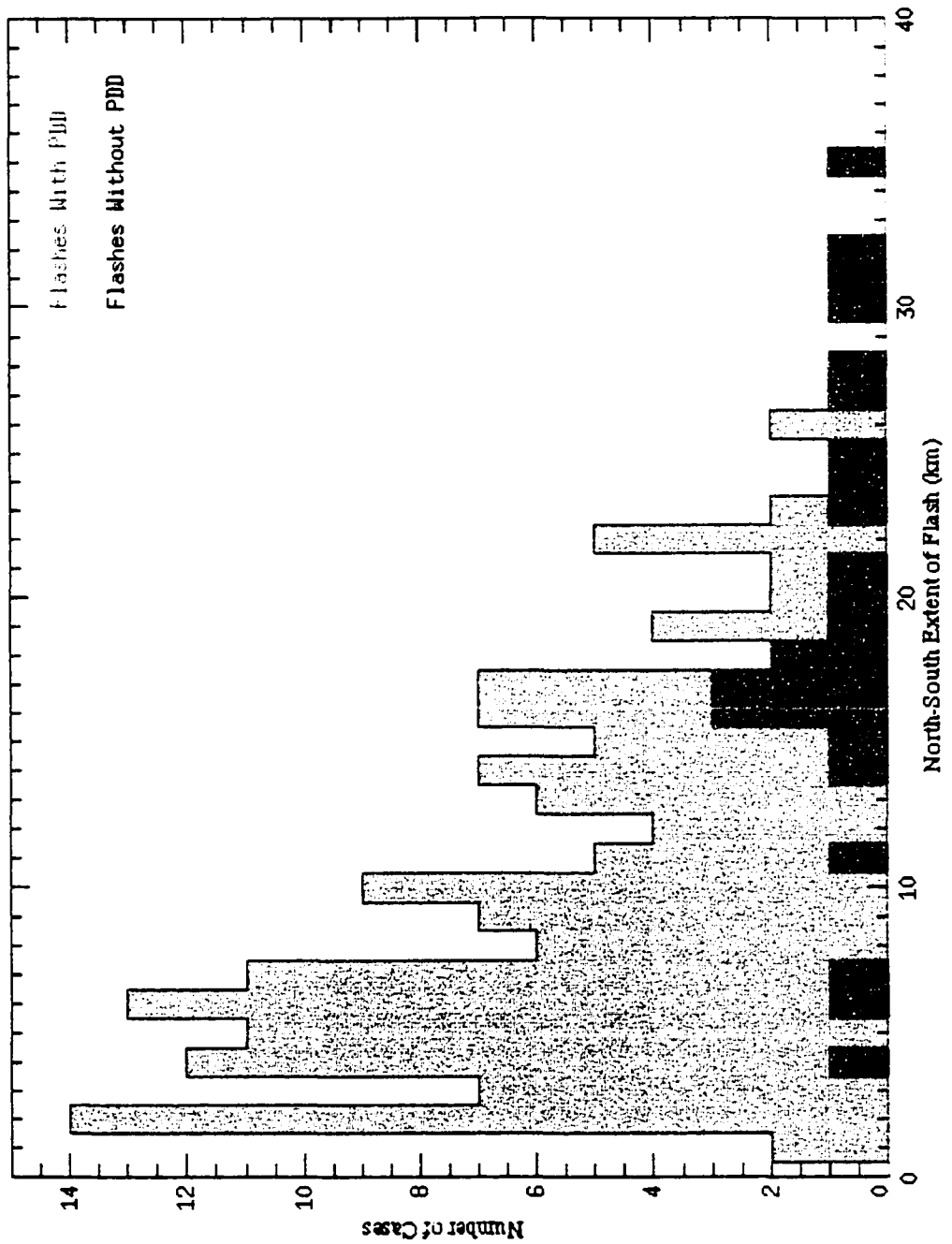


Figure 15: North-South Extent of LMA Flash

Distribution for LMA flashes that were seen by the PDD is in red. Distribution for LMA flashes that were not seen by the PDD is in gray. The means are different (Wilcoxon Rank-Sum p-value < 0.0001). The distributions are similar (Two Sample Kolmogorov-Smirnov p-value = 0.4726).

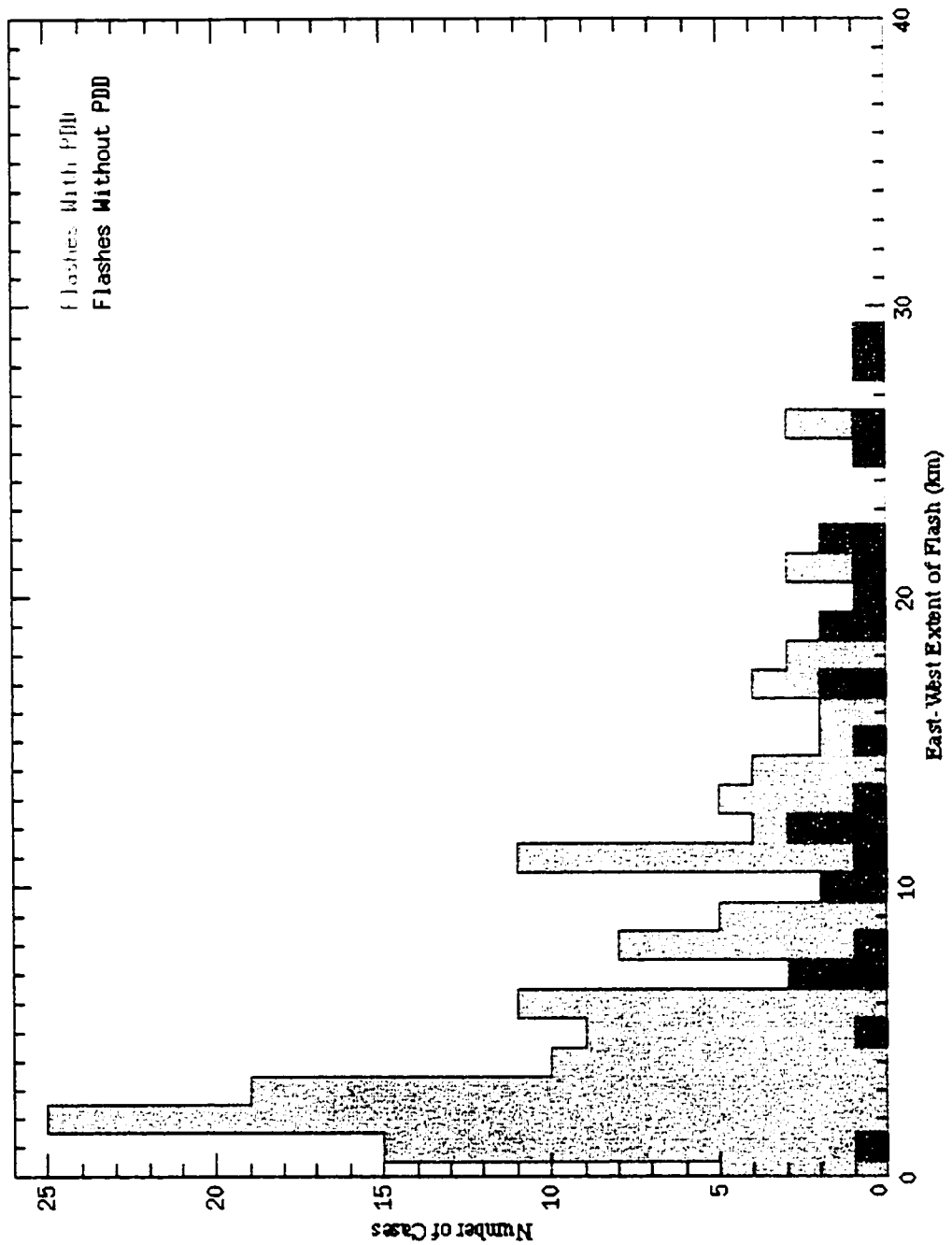


Figure 16: East-West Extent of LMA Flash

Distribution for LMA flashes that were seen by the PDD is in red. Distribution for LMA flashes that were not seen by the PDD is in gray. The means are different (Wilcoxon Rank-Sum p-value < 0.0001). The distributions are similar (Two Sample Kolmogorov-Smirnov p-value = 0.1354).

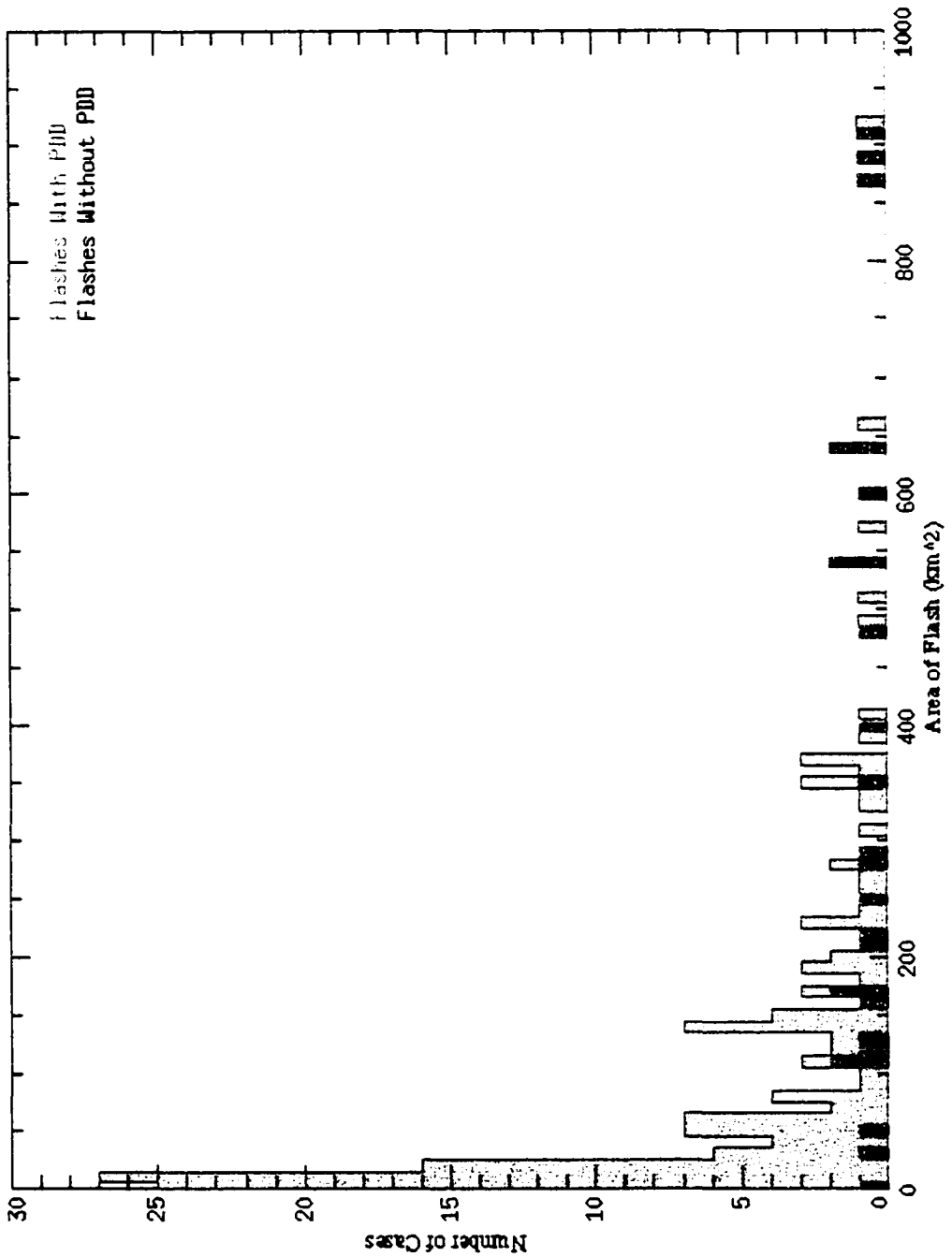


Figure 17: Area of LMA Flash

Distribution for LMA flashes that were seen by the PDD is in red. Distribution for LMA flashes that were not seen by the PDD is in gray. The means are different (Wilcoxon Rank-Sum p-value < 0.0001). The distributions are different (Two Sample Kolmogorov-Smirnov p-value < 0.0001)

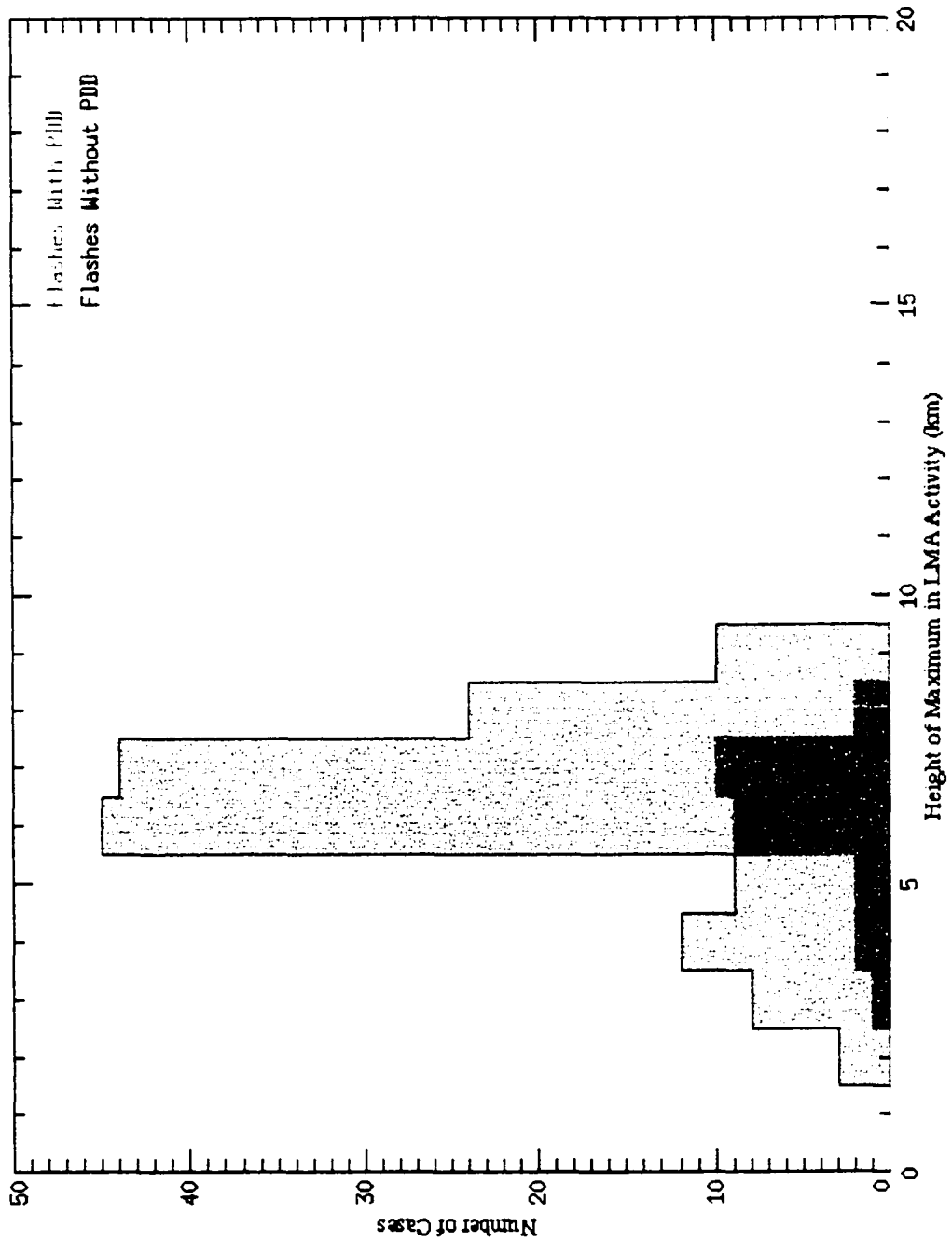


Figure 18: Height of Maximum in LMA Activity

Distribution for LMA flashes that were seen by the PDD is in red. Distribution for LMA flashes that were not seen by the PDD is in gray. The means are similar (Wilcoxon Rank-Sum p-value = 0.6853). The distributions are similar (Two Sample Kolmogorov-Smirnov p-value < 0.4182).

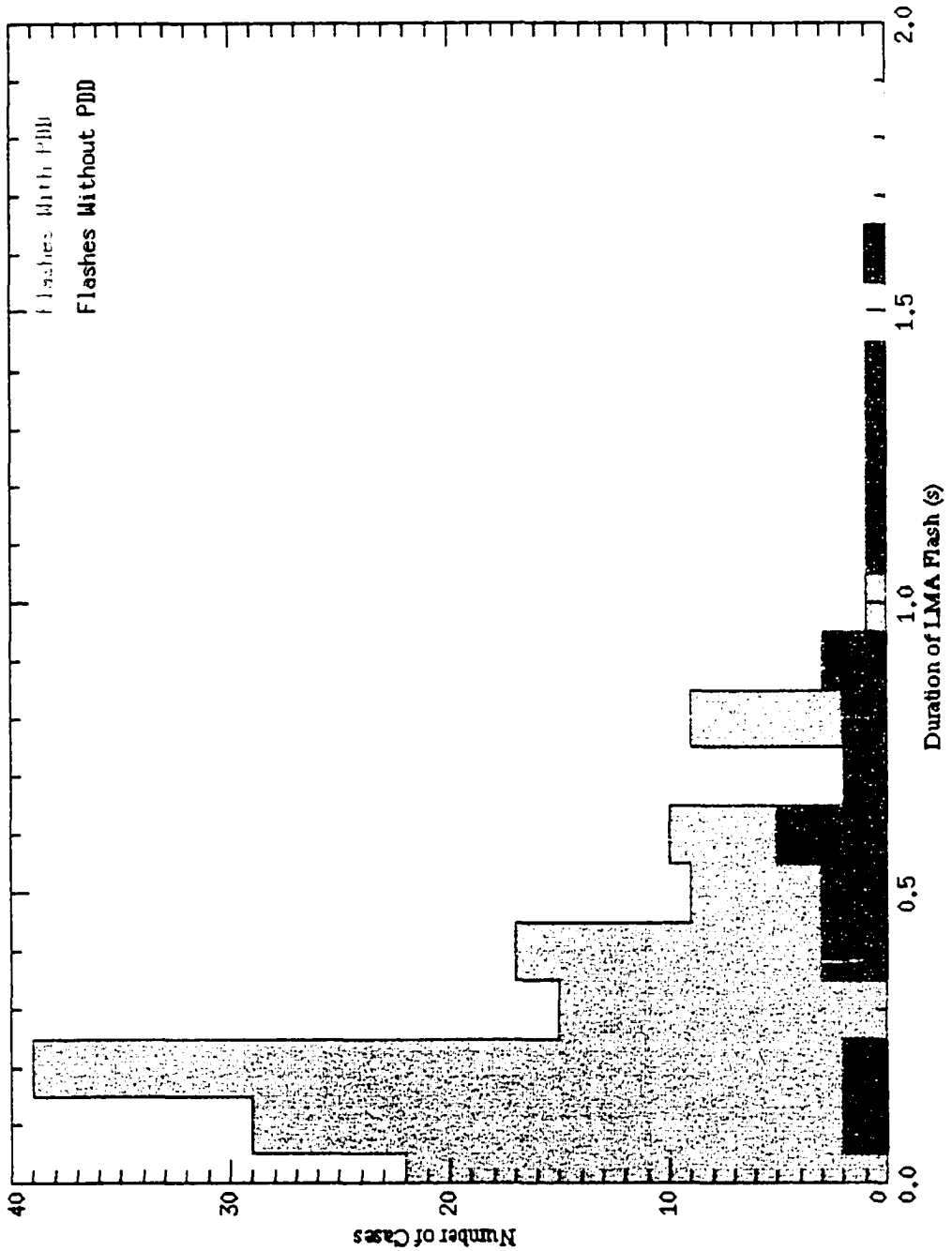


Figure 19: Duration of LMA Flash

Distribution for LMA flashes that were seen by the PDD is in red. Distribution for LMA flashes that were not seen by the PDD is in gray. The means are different (Wilcoxon Rank-Sum p -value < 0.0001). The distributions are similar (Two Sample Kolmogorov-Smirnov p -value = 0.5969)

LMA flashes.

A two-sample Wilcoxon rank-sum test was used to test for a statistical difference in the mean for the population seen by the PDD versus the population that was not seen by the PDD. For the Wilcoxon test, the null hypothesis was that the means of the two populations are the same. The alternate hypothesis was that the mean value of the given flash characteristic for the population that was seen by the PDD is greater than the mean for the population that was not seen by the PDD. The difference in the means was then subtracted from the population seen by the PDD, and a Two-Sample Kolmogorov-Smirnov Goodness-of-Fit test was run to determine if the shapes of the two distributions are different. The resulting P-values are given in Table 5.

The last step in the analysis was to examine the 26 LMA flashes which were seen by the PDD, in relationship to when the PDD was triggered, to see if these 26 flashes share any common characteristics in terms of rate of activity or height of activity before, during, and after each PDD lightning-trigger. For the 41 PDD lightning-triggers which were matched with LMA flashes, the rate of activity as measured by the LMA was investigated by comparing a time-of-flight corrected PDD time to the time of each LMA point within ± 20 ms. The number of LMA points was counted in a 5 ms window before, during and after the PDD trigger time. Because of the $500 \mu\text{s}$ resolution of the LMA data used in this study, the maximum number of LMA points which could occur in a 5 ms time-window is 10. The results of these counts are shown in Table 6.

Finally, the relationship between PDD trigger-times and the activity of the lightning event with height were investigated. In order to do this, the PDD trigger-times were again corrected for time-of-flight, but this time they were corrected to an average LMA point location within the flash. These corrected trigger times were then plotted along with a time-vs-altitude plot for each LMA flash event. If an LMA flash also had an associated NLDN, the time of the NLDN event was also included in the plot. This displays the relationship among observations by the three different observing systems. Figure 20 (a)–(g) shows the PDD/LMA/NLDN plots for all 26 LMA flash events which had time-correlated PDD events. The diamonds represent the time of a PDD event. The red plus signs (+) show the altitude of LMA points at time t (from the start of the flash). An “X” on the x-axis shows the time of a positive NLDN event. A triangle on the x-axis shows the time of a

Table 5: Results of Statistical Analysis of LMA Flash Characteristics for Flashes With PDD vs. Flashes without PDD

5(a) Results of Wilcoxon Rank-Sum Test

Flash Characteristic	p-value	Interpretation
Maximum Altitude	0.0013	Mean for Events with PDD > Mean for Events w/o PDD
North-South Extent	< 0.0001	Mean for Events with PDD > Mean for Events w/o PDD
East-West Extent	< 0.0001	Mean for Events with PDD > Mean for Events w/o PDD
Area of flash	< 0.0001	Mean for Events with PDD > Mean for Events w/o PDD
Altitude of LMA Maximum	0.6853	Cannot reject the null hypothesis that the Mean for events w/ PDD = that for events w/o PDD
Duration of flash	< 0.0001	Mean for Events with PDD > Mean for Events w/o PDD

5(b) Results of Kolmogorov-Smirnov Goodness-of-fit Test

Flash Characteristic	p-value	Interpretation
Maximum Altitude	0.6181	Cannot say that the distributions are different for events w/ PDD and w/o PDD
North-South Extent	0.4726	Cannot say that the distributions are different for events w/ PDD and w/o PDD
East-West Extent	0.1354	Cannot say that the distributions are different for events w/ PDD and w/o PDD
Area of flash	< 0.0001	Distribution for events w/ PDD is different than that for events w/ PDD
Altitude of LMA Maximum	0.4182	Cannot say that the distributions are different for events w/ PDD and w/o PDD
Duration of flash	0.5969	Cannot say that the distributions are different for events w/ PDD and w/o PDD

Table 6: Rate of LMA point occurrence for 5ms window Before, During and After PDD trigger-time:

PDD Index	LMA Count Before Trigger	LMA Count During Trigger	LMA Count After Trigger
0	4	5	1
1	2	5	8
3	5	4	7
4	7	4	4
6	0	3	0
7	4	5	6
8	0	2	0
9	0	3	1
10	1	0	0
12	7	8	7
13	5	3	4
14	0	0	1
15	7	10	3
16	4	4	4
19	4	4	1
21	6	7	5
22	6	8	4
25	2	5	8
26	10	9	7
27	7	6	5
28	6	7	5
29	1	5	0
30	1	4	6
31	8	2	0
32	0	3	6
34	1	6	5
35	5	5	4
41	7	7	3
42	4	8	8
43	7	7	6
44	6	3	3
46	6	7	7
48	7	3	1
49	1	4	1
51	1	6	0
53	5	1	0
54	6	6	5
55	4	0	0
57	0	3	5
58	1	1	1
60	7	6	10

*Maximum possible LMA count is 10.

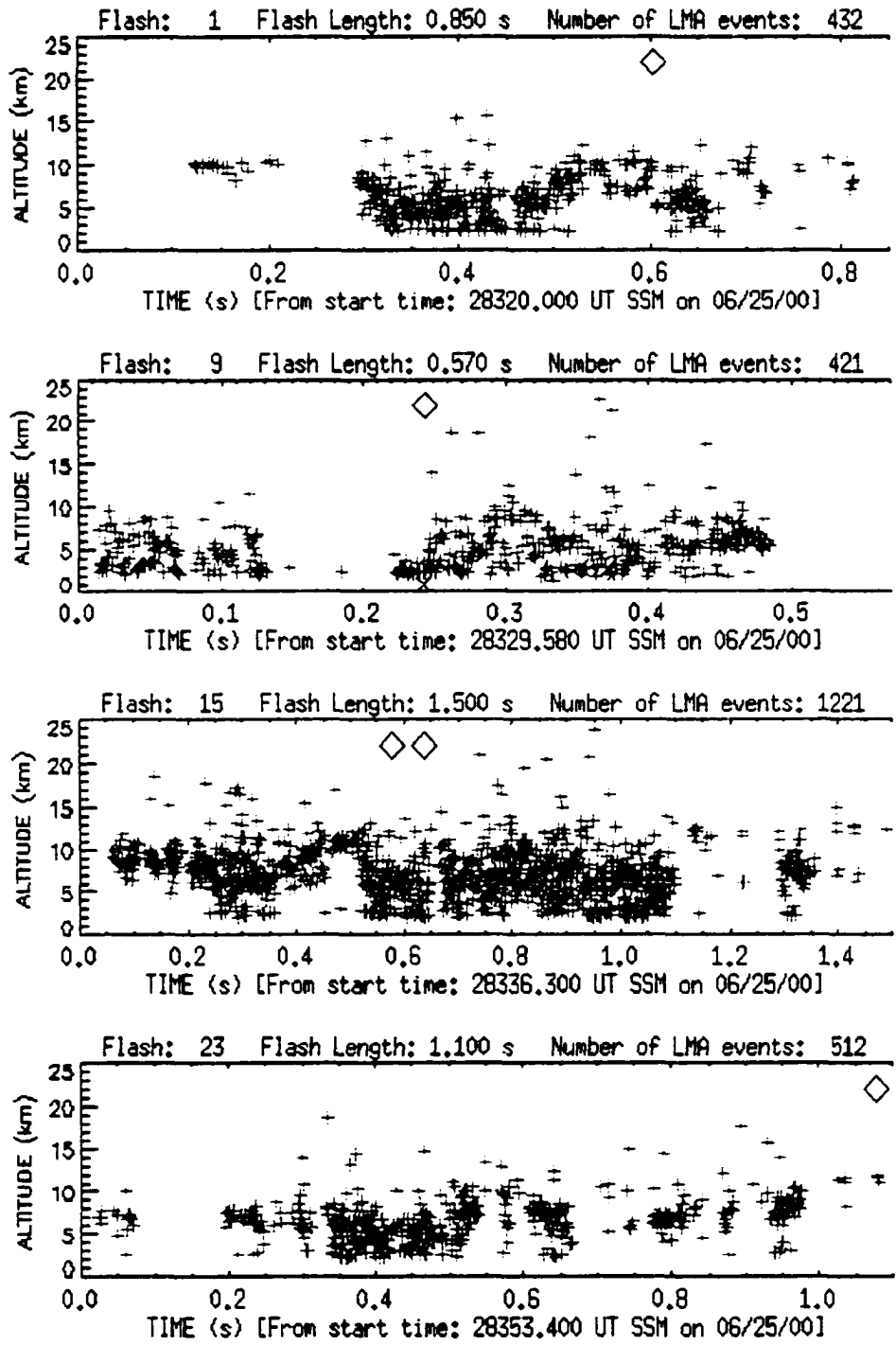


Figure 20 (a): LMA altitude vs. time plots with PDD and NLDN
 Red plus signs (+) show the altitude (km) of LMA point at time t (s) from start of flash. Flash = LMA flash number. Black diamonds show PDD trigger time. "X" on x-axis shows time of positive NLDN event. triangle on x-axis shows time of negative NLDN event. SSM = Seconds Since Midnight, Universal Time.

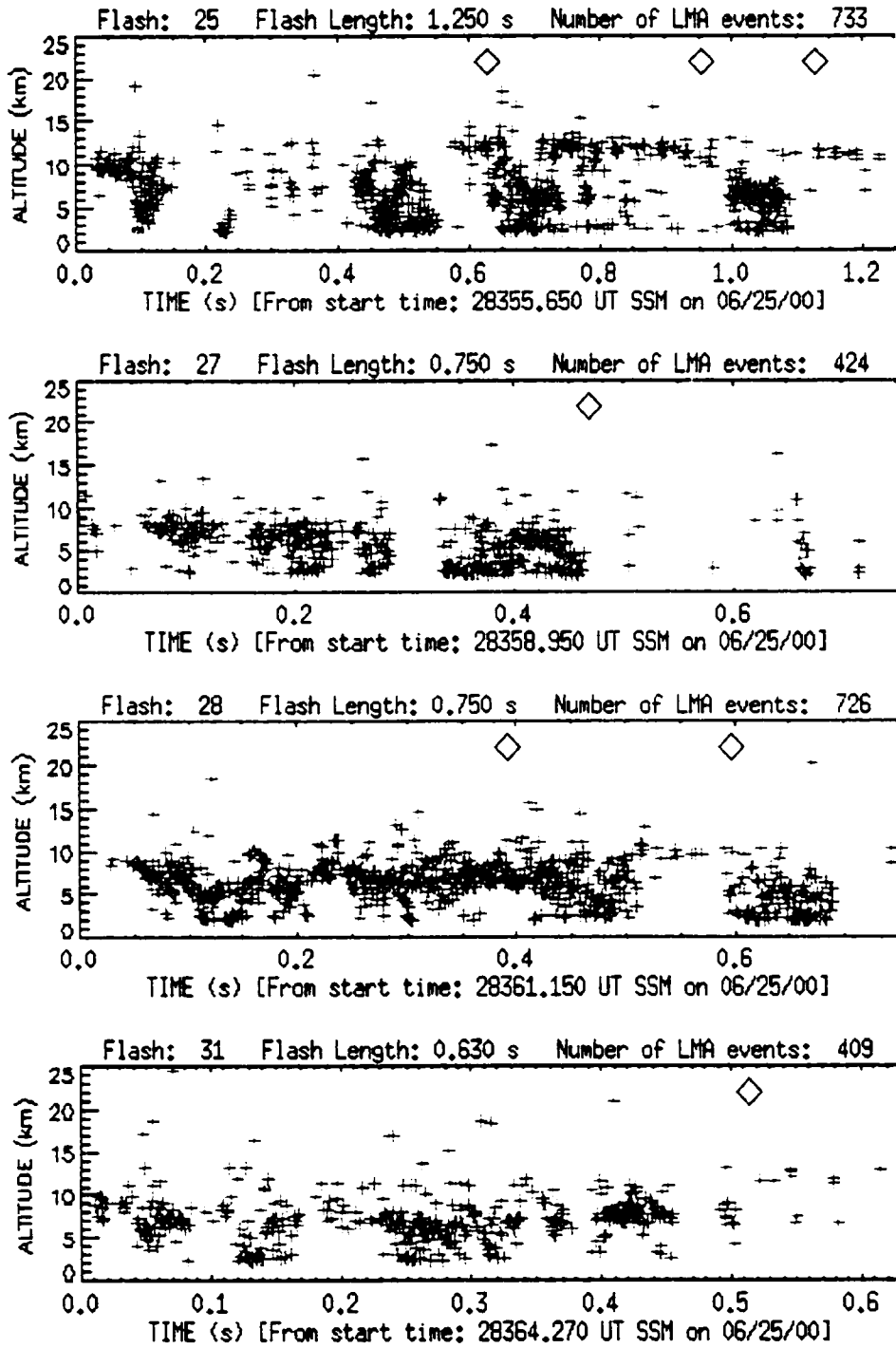


Figure 20 (b): LMA altitude vs. time plots with PDD and NLDN
 Red plus signs (+) show the altitude (km) of LMA point at time t (s) from start of flash. Flash = LMA flash number. Black diamonds show PDD trigger time. "X" on x-axis shows time of positive NLDN event, triangle on x-axis shows time of negative NLDN event. SSM = Seconds Since Midnight, Universal Time.

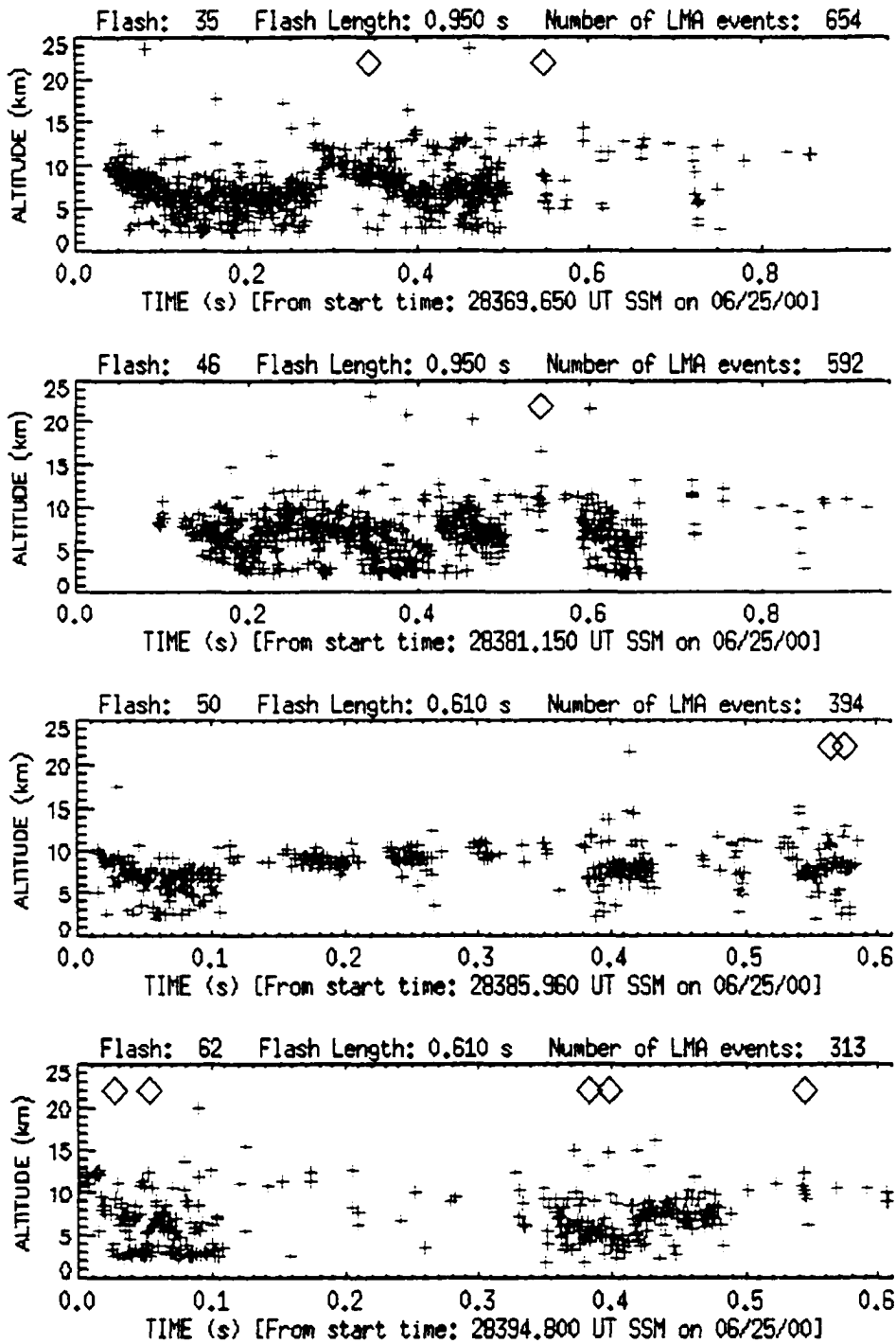


Figure 20 (c): LMA altitude vs. time plots with PDD and NLDN
 Red plus signs (+) show the altitude (km) of LMA point at time t (s) from start of flash. Flash = LMA flash number. Black diamonds show PDD trigger time. "X" on x-axis shows time of positive NLDN event. triangle on x-axis shows time of negative NLDN event. SSM = Seconds Since Midnight, Universal Time.

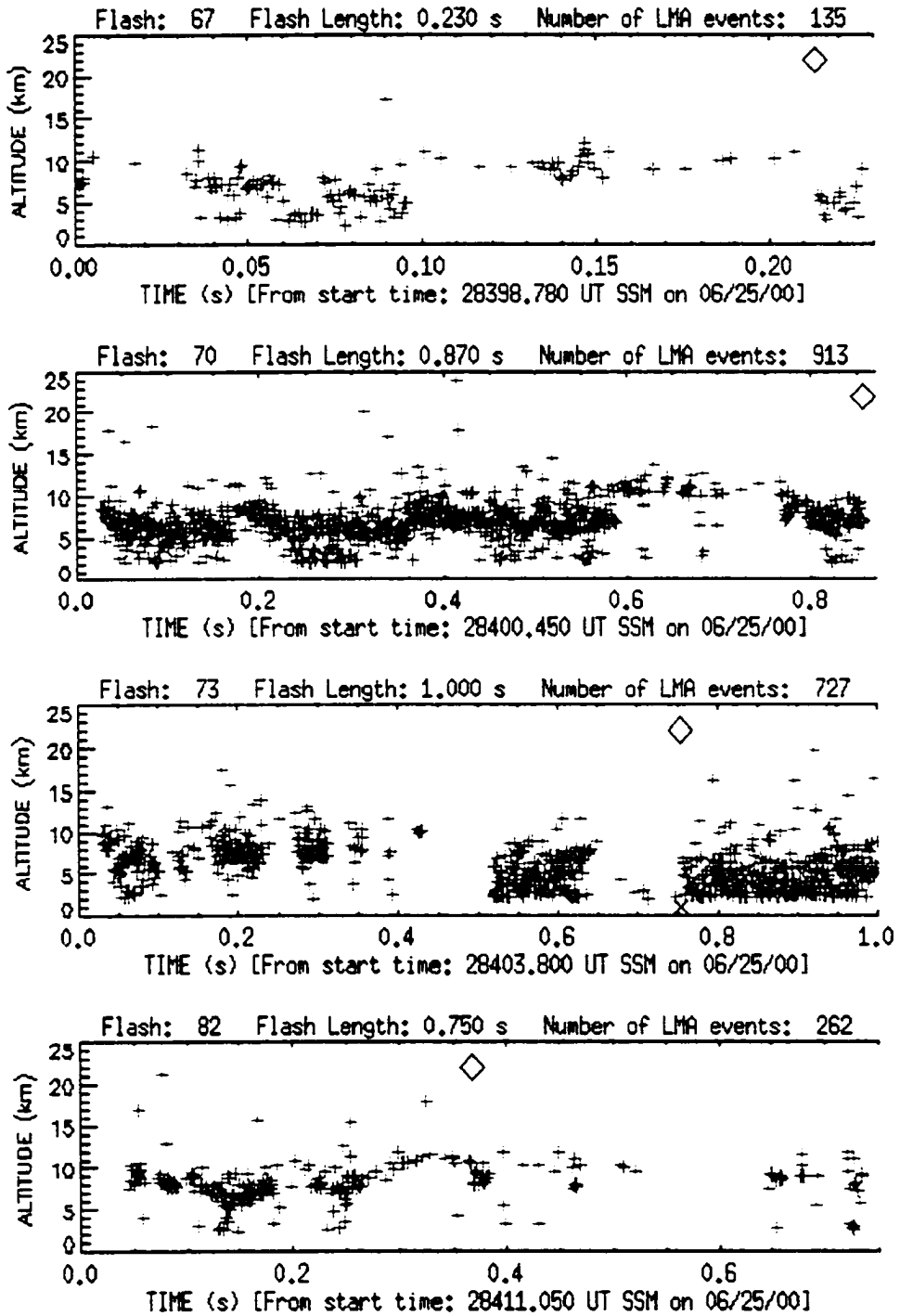


Figure 20 (d): LMA altitude vs. time plots with PDD and NLDN
 Red plus signs (+) show the altitude (km) of LMA point at time t (s) from start of flash. Flash = LMA flash number. Black diamonds show PDD trigger time. "X" on x-axis shows time of positive NLDN event. triangle on x-axis shows time of negative NLDN event. SSM = Seconds Since Midnight, Universal Time.

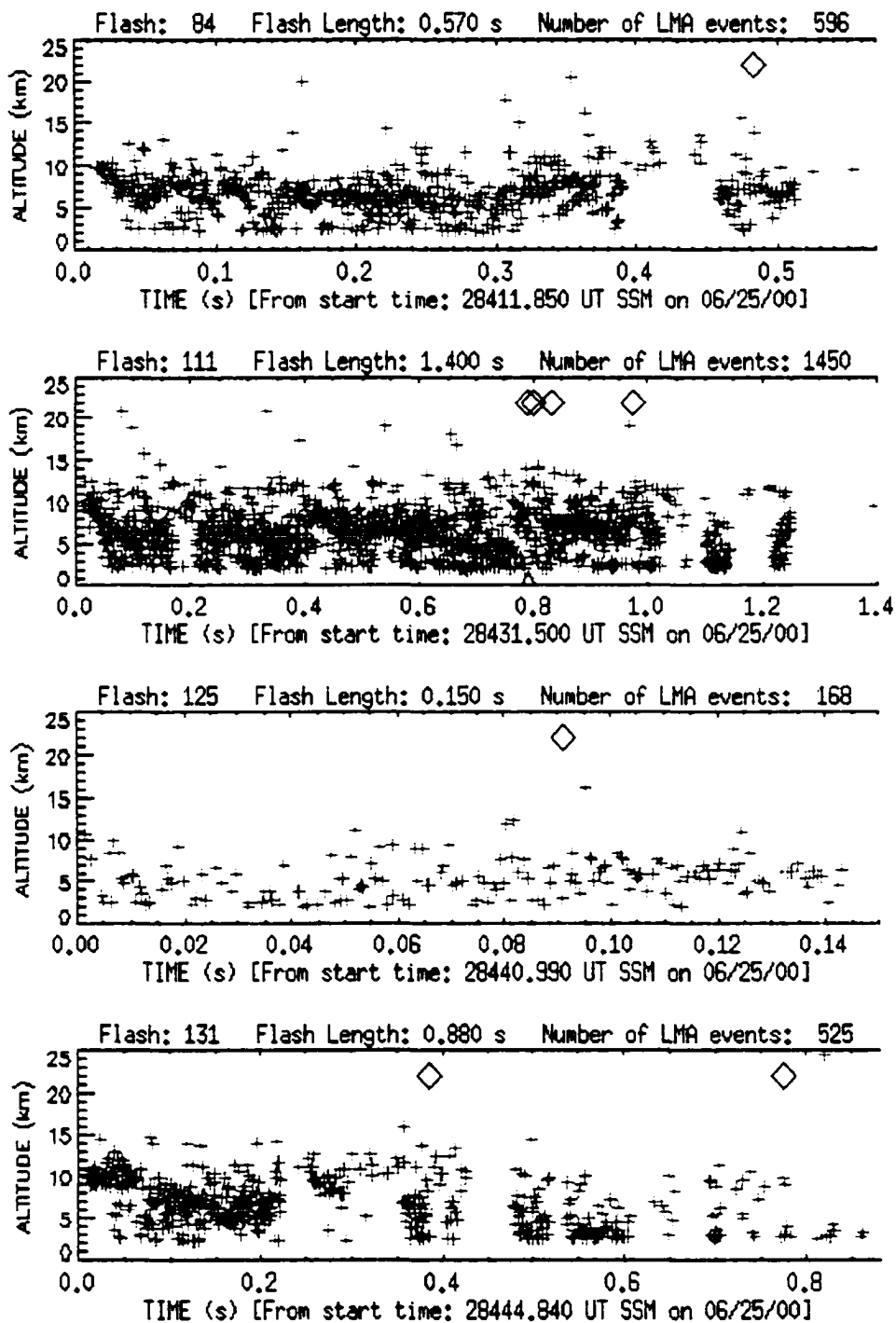


Figure 20 (e): LMA altitude vs. time plots with PDD and NLDN
 Red plus signs (+) show the altitude (km) of LMA point at time t (s) from start of flash. Flash = LMA flash number. Black diamonds show PDD trigger time. "X" on x-axis shows time of positive NLDN event, triangle on x-axis shows time of negative NLDN event. SSM = Seconds Since Midnight, Universal Time.

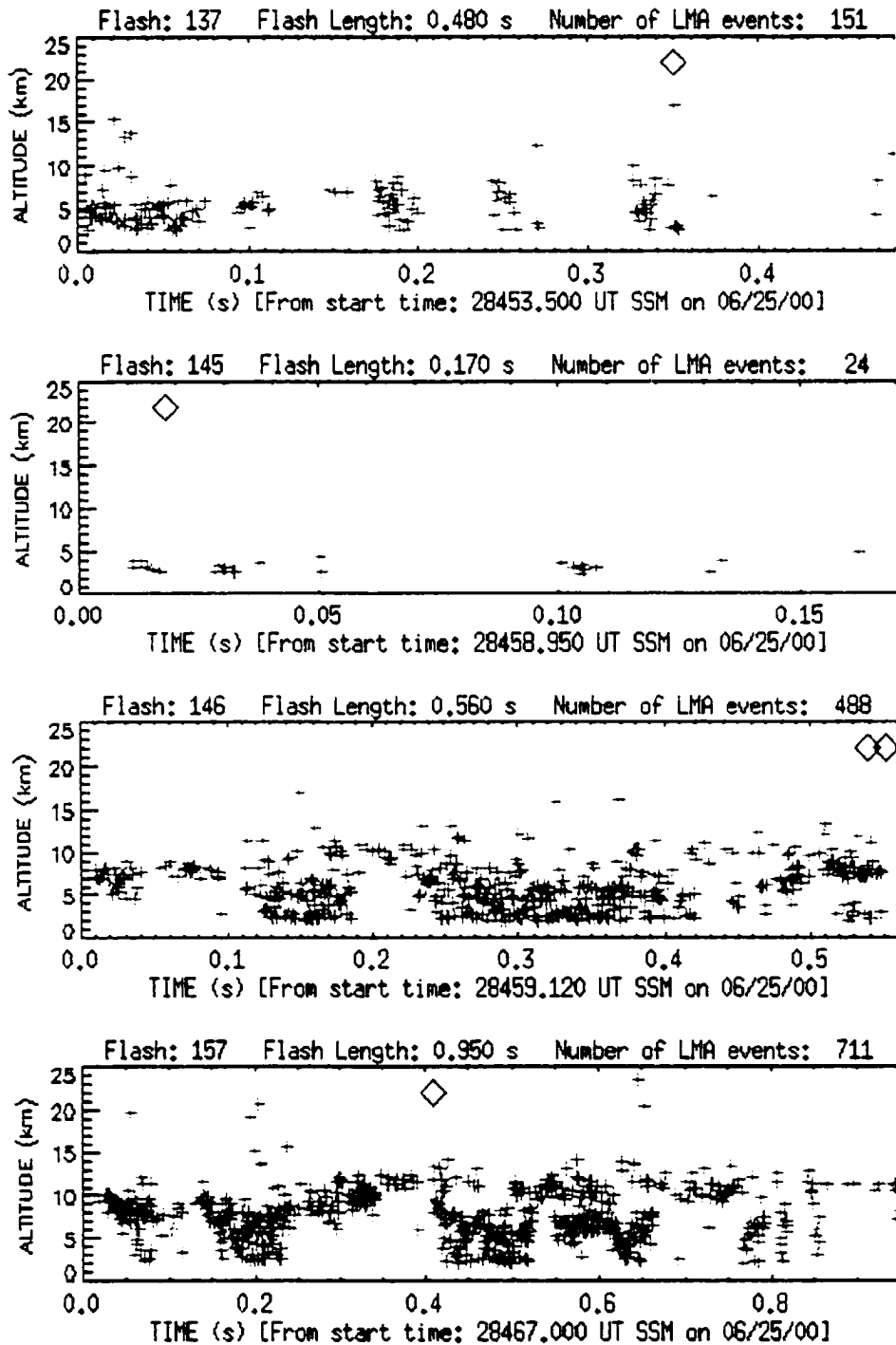


Figure 20 (f): LMA altitude vs. time plots with PDD and NLDN
 Red plus signs (+) show the altitude (km) of LMA point at time t (s) from start of flash. Flash = LMA flash number. Black diamonds show PDD trigger time. "X" on x-axis shows time of positive NLDN event, triangle on x-axis shows time of negative NLDN event. SSM = Seconds Since Midnight, Universal Time.

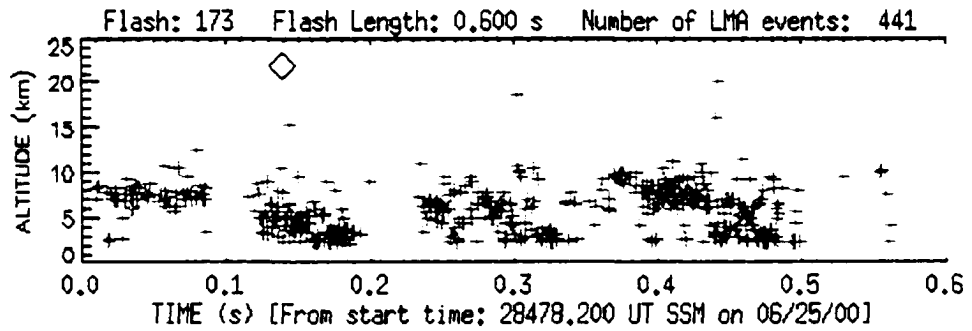
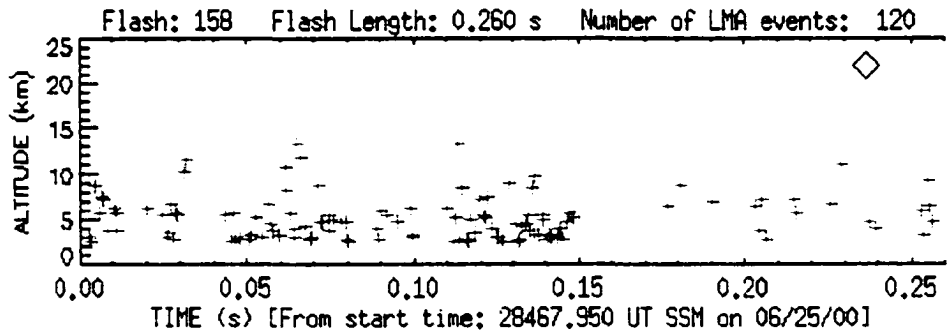


Figure 20 (g): LMA altitude vs. time plots with PDD and NLDN
 Red plus signs (+) show the altitude (km) of LMA point at time t (s) from start of flash. Flash = LMA flash number. Black diamonds show PDD trigger time. "X" on x-axis shows time of positive NLDN event, triangle on x-axis shows time of negative NLDN event. SSM = Seconds Since Midnight, Universal Time.

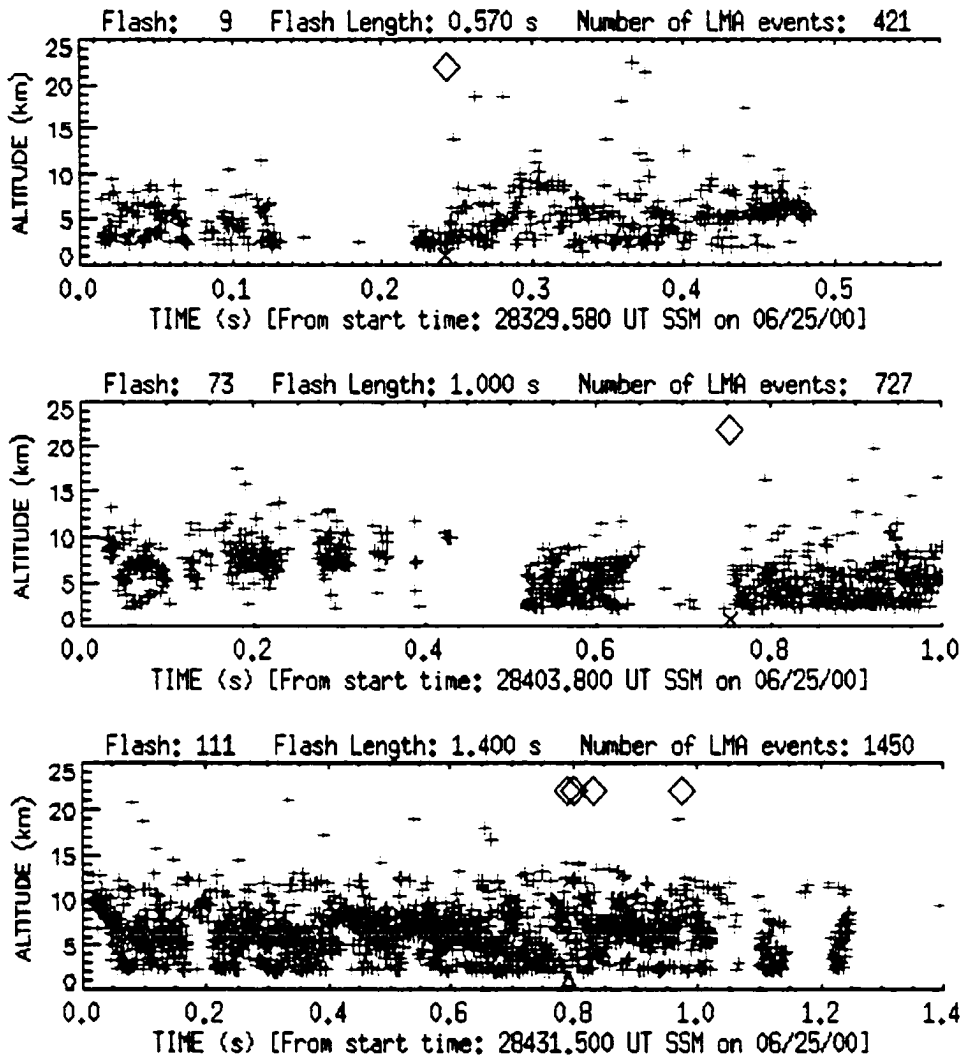


Figure 21: LMA altitude vs. time plots for PDD/LMA/NLDN Events
 As for Figure 20, but for the three LMA flashes where there were both PDD and NLDN coincidences. Red plus signs (+) show the altitude (km) of LMA point at time t (s) from start of flash. Flash = LMA flash number. Black diamonds show PDD trigger time. "X" on x-axis shows time of positive NLDN event, triangle on x-axis shows time of negative NLDN event. SSM = Seconds Since Midnight, Universal Time.

negative NLDN event. Figure 21 shows the PDD/LMA/NLDN plots for the three events that had an NLDN ground flash.

6c. DISCUSSION

The first question being investigated by an examination of the PDD/LMA case on June 25, 2000 is whether there may be a relationship between detection by the PDD and the physical characteristics of the flash. In the analyses performed above, flashes that were detected by the PDD tended to reach higher in the storm and tended to have a greater horizontal extent than flashes that were not seen by the PDD. Flashes that were detected by the satellite also tended to have a longer duration than flashes that were not detected. One speculation as to why this might be the case is that for flashes with longer duration and/or flashes with a larger horizontal extent, there is a greater chance that some portion of the lightning channel will satisfy the conditions (whatever those might be) that produce an optical signal greater than the PDD detection threshold when seen from above. For area of the flash, the difference in the two populations is not quite as strong as for the individual measurements of north-south or east-west extent. This reflects the fact that the flashes usually did not spread out equally in all directions. Flashes with large north-south extents tended to have smaller east-west extents and vice versa. In fact, flashes with the greatest extent in either dimension tended to be long, narrow channels, which often traveled diagonally across the north-south, east-west rectangle used to try and quantify the spatial extent in this simple analysis.

There was no difference in the distributions for height of maximum LMA activity for flashes that were seen by the PDD versus flashes that were not seen. In retrospect, this makes perfect sense. What this characteristic actually measures is the height of the main positive charge center in the storm. This value should be the same for all flashes.

It is also clear that the simple relationship where flashes that extend above 7 km in the storm are subsequently detected by the satellite above (found by *Thomas et al.* [2000]), does not hold in this case. For this storm, nearly all of the flashes extended above 7 km, and most were inverted flashes which began at 9-10 km altitude and then developed

downward. The majority of these flashes were not seen by the PDD. This could be the result of a myriad of individual factors, or a combination thereof. The Lightning Imaging Sensor (LIS) used in the Thomas et al. study is a CCD camera array. LIS pixels activate according to the integrated light reaching that pixel over a 2 ms period, whereas the PDD triggers based on a point sample taken every 15 μ s. It makes sense that the two very different types of optical sensors might not detect all optical signals equally. Also, it could be that the actual height to which the activity is extending in the June 25 storm is poorly sampled. If the polarity of the storm in the June 25 case is indeed inverted, this indicates that there would be a region of positive charge at the midlevels and a region of negative charge in the upper part of the storm. The LMA does not sample positive leaders moving through regions of negative charge very well, so even if the flashes are extending higher in the cloud for all of the PDD/LMA events, it's possible that the LMA data is not resolving that activity, especially with coarse time-resolution LMA data.

The second main question being investigated in this chapter is how what each instrument sees may or may not relate to what the other instruments see. There is no clear relationship between the LMA activity and detection by the PDD. Table 6 shows that the rates of LMA activity before detection by a PDD vary across the board from the minimum value of zero points to the maximum value of 10 points in the time period considered. The same can be said for the rates during a PDD trigger and after a PDD trigger. Likewise, Figure 21 shows that there is no clear relationship between the height of LMA activity and detection by the PDD. PDD triggers sometimes occurred when there was considerable activity at 10 km altitude and above. But sometimes PDD triggers seemed to occur when the LMA activity was occurring at low altitudes, and sometimes PDD triggers seemed to occur when there was almost no LMA activity. This suggests that perhaps the processes which produce the VHF radiation mapped by the LMA are not the same as the processes which produce the optical signals which are detected by the PDD. Or perhaps there is something about inverted-polarity flashes that produces a weaker optical signal when viewed from above the storm, as compared to normal-polarity IC flashes. One interesting feature that can be seen from Figure 21 is that, in the absence of a connection to ground, most PDD lightning triggers occurred part way through or toward the end of the LMA flash. The same behavior was seen in the LIS data (Thomas et al. [2000]), where it was

found that the activity in normal-polarity IC flashes often produced extensive, impulsive illumination in the cloud part-way through or late in the discharge.

Figure 22 can be used to explore whether the PDD and the NLDN see the same processes within a lightning flash. One clear pattern that emerges is that each of the three NLDN events that occurred during the FORTE pass is followed very closely in time by a PDD lightning event. This would seem to support the findings of *Suszcynsky et al.* [2000], that the PDD often sees light from the same “process” as the connection to ground, though it does not see the ground-connection point itself. Rather, when a connection to ground occurs, the PDD sees the return stroke process once it propagates up into the cloud. Just what it is about certain ground connections makes them more visible from above, when little or no high-altitude LMA activity is recorded, remains to be explored.

CHAPTER 7

SUMMARY, CONCLUSIONS, AND FUTURE WORK

Lightning and storm electrification have been studied from many different points of view: from the ground, from aircraft, from rockets, from balloons, from satellites, and even from the space shuttle. In addition to looking at the discharge from different angles, different types of instruments may observe altogether different aspects of the lightning discharge and/or the electrical environment in and around the parent storm. One challenge becomes to understand how data from the myriad of different instruments and points of view relate to each other, and how data from each individual instrument and particular point of view relate to the actual physical processes which lead to and take place within a lightning discharge. The study presented in this dissertation addresses one piece of this complex puzzle. Namely, how do the optical data received at a satellite relate to the physical characteristics of the lightning flash which produced the optical emissions?

Because satellites have the advantage of a relatively global point of view, they often have the capability to collect lightning data in remote areas where other observation systems are impractical, or to collect long time-series of data that show how lightning is distributed over the Earth. It has been proposed that satellite lightning data can be used as an indication of deep convection, and therefore can be useful in model initiations, convective parameterization, and global climate studies. It has also been proposed that optical detection is perhaps the best way to study lightning from space. Optical lightning signals

detected from instruments aboard spacecraft-borne platforms have even been used as an indicator of convective processes and atmospheric composition on other planets, most notably on Jupiter. For satellite-based optical data to be most useful, and for their use to be most meaningful, we need a good understanding of what optical lightning data actually tell us about the physical situation.

To address this problem, this study used two different ground-based platforms to provide ground-truth or “cloud-truth” for optical lightning data collected by the FORTE Photodiode detector (PDD). Data from the National Lightning Detection Network (NLDN) was used to investigate the relationship between estimated peak-optical power of lightning events detected by the PDD and flash type and polarity. A case study using data from the New Mexico Tech Lightning Mapping Array (LMA) was used to investigate the relationship between flash characteristics and whether a flash was detected by the satellite, and the case was also used to investigate whether the PDD, LMA, and NLDN are sampling the same or different “parts” of the lightning discharge.

In Chapter 5 it was found that there is a relationship between positive cloud-to-ground flashes and PDD events with peak optical power at the source $\geq 10^{11}$ W (called “bright” events in this study and called “superbolts” by Turman (1977)). There seemed to be a definite signal that bright PDD events are more likely to be associated with ground flashes than PDD events with weaker peak optical power, and cloud-to-ground strokes that were associated with bright PDD events had a greater tendency to be positive than the background population of PDD events or than the general climatology of the area would suggest. This does not mean, however, that all +CG events will produce a “bright” PDD event if the satellite is overhead. In general, when peak power of a PDD source-event was related to flash type, it was found that events with peak powers $> 10^{10}$ W were much more likely to be associated with ground flashes and events with peak power $< 10^{10}$ W were much more likely to be associated with intracloud flashes. More work needs to be done before this possible relationships between peak optical power of a PDD event and flash-type can be verified. First, the detection bias of the NLDN needs to be removed, by considering only cases over the network, where detection efficiency is high. Second, the influence of continental vs. oceanic lightning on the relationship between PDD detection,

peak power and flash type, needs to be explored. Third, regionality and seasonality needs to be more closely considered. Data from winter storms needs to be looked at in terms of the relationship between bright events and positive cloud-to-ground flashes, since +CGs are thought to be relatively more frequent in winter storms. Lastly, the two data sets for 1998 and 1999 need to be considered together, to add to the total number of cases being considered in the study.

In Chapter 6, the main finding is that flashes that are detected by the PDD tend to reach a greater maximum altitude, tend to have greater horizontal extent, and tend to have longer a longer duration than flashes that are not detected by the PDD. Most likely it is some combination of flash characteristics, storm characteristics, and viewing angle which makes a flash detectable by an instrument such as the PDD. One speculation as to why flashes that are detected by the PDD tend to be longer in duration, larger in extent and reach higher in the storm is that for these "bigger" flashes, the probability of the lightning channel reaching high enough in the cloud to be detected is increased. The relationship between height of the LMA sources and PDD detection was not as strong as expected, but this could be due to the fact that the LMA is sampling inverted-polarity flashes in this case. For inverted polarity flashes, the LMA does not sample whatever aspect of the flash is common to all or most PDD detections.

Though the PDD and the LMA appear to see different processes within the lightning flashes of this case, it seems that the PDD and the NLDN are sampling the same physical piece or "leg" of the total lightning flash event. The PDD sample just appears slightly after the NLDN event, when the return stroke process has moved up into the cloud. Obviously, because this is just one case and the sample size of the events is small, no underlying conclusions can be made about whether the relationships seen in this storm would hold for all other storms, or even most other storms. More cases are needed, sampling all sorts of different types of storm systems, before any larger conclusions can be drawn. Future work includes obtaining an high-time resolution analysis of the June 25 case and repeating the analysis, checking the remainder of the STEPS LMA data to see if any more cases are to be found there, checking with other VHF mapping array systems which have been operated around the US starting in 2000 to see if any other storms can be found, and perhaps flying another instrument similar to the FORTE PDD, once the FORTE mission

runs its course. Also, the relationship between processes which produce VHF radiation and processes which produce the optical radiation in a flash need to be considered. And a measure of the amount of cloud between the lightning channel and the PDD above and how this might affect the peak optical source power needs to be investigated.

And what of the interpretation of lightning data at Jupiter? If it is likely that "superbolts" are often caused by CG flashes, and if Jovian lightning is indeed similar to terrestrial superbolts, what might be the analogous process on Jupiter, where there is no solid surface? Also, the results of this study underscore that one must be careful when comparing more than one type of instrument, even when comparing the results from different optical instruments (such as a Photodiode Detector and a CCD Imager). Because "Superbolts" are not physical phenomena but instead are a category of bright observations from a photodiode detector, one must be careful about assigning physical meaning to such events for the purposes of comparison to Jovian lightning data. Also, the relationship between a lightning discharge and the optical signal seen from an orbiting platform might not be as simple as light from a point source, or even a line source, being scattered through a cloud. If models of relatively simple lightning sources, coupled with the very small amount of optical lightning data that has been collected at Jupiter begin to produce anomalous results, before theories of where Jovian lightning is occurring and how it is occurring are completely changed, perhaps some of the more complex relationships between lightning discharges and the optical signals they produce should be considered. Also, in order for statements of comparative planetology (such as the statement that Jovian lightning is similar to terrestrial superbolts) to have any meaning, we must first understand what is going on in the terrestrial case.

GLOSSARY OF ACRONYMS

CCD — Charge Coupled Device

CG — Cloud-to-Ground lightning flash

DF — Direction Finding location technique

DMSP — Defense Meteorological Satellite Program

FORTE — Fast on-Orbit Recording of Transient Events satellite

GPS — Global Positioning System

IC — Intracloud lightning flash

IMPACT sensor — combined MDF and TOA sensor for locating lightning

LDAR — Lightning Detection and Ranging (NASA)

LIS — Lightning Imaging Sensor (NASA) aboard TRMM satellite

LLS — Lightning Location System aboard FORTE satellite

LMA — Lightning Mapping Array

LRD — Lightning and Radio emission Detector aboard Galileo atmospheric probe

MDF — Magnetic Direction Finding technique for locating lightning

NEXRAD — NEXt generation weather RADar

NLDN — National Lightning Detection Network

OLS — Optical Lightning System on FORTE Satellite (comprised of PDD and LMA)

OSO — Orbiting Solar Observatory

OTD — Optical Transient Detector (NASA)

PBE — PiggyBack Experiment sensor aboard DMSP satellite

PDD — Photodiode Detector aboard FORTE

RF — Radio Frequency

SSI — Solid State Imager aboard Galileo orbiter

STEPS — Severe Thunderstorm Electrification and Precipitation Experiment

TOA — Time of Arrival location technique

TRMM — Tropical Rainfall Measurement Mission

VHF — Very High Frequency

REFERENCES

- Arietio, J., I. Herrero, A. Ezcurra. "Lightning Characteristics in the 1992-1996 Period in the Basque Country Area: Lightning-Precipitation Relationships". *Proceedings of the 11th International Conference on Atmospheric Electricity*, NASA/CP-1999-209261, p.392-395.
- Argo, P., A. R. Jacobson, S. O. Knox (1999) "Geolocation of recurrent-emission lightning storms using the FORTE satellite". *J. Geophys. Res.*, in press.
- Baker, M. B. et al. (1999). "Relationships between lightning activity and various thundercloud parameters: satellite and modelling studies". *Atmospheric Research*, Vol. 51, No. 3, p. 221-236.
- Beasley, W. H. (1995). "Lightning Research: 1991-1994". *Reviews of Geophysics*, Supplement, p. 833-843.
- Blyth, A., H. Christian, J. Latham (1999). "Determination of Thunderstorm Anvil Ice Contents and Other Cloud Properties from Satellite Observations of Lightning". *Proceedings from the 11th International Conference on Atmospheric Electricity*, NASA/CP-1999-209261, p. 363.
- Boccippio, D. J., W. J. Koshak, H. J. Christian, S. J. Goodman (1998) "Land-Ocean Differences in LIS and OTD Tropical Lightning Observations". *Proceedings from the 11th International Conference on Atmospheric Electricity*, NASA/CP-1999-209261, p. 734-737.
- Boeck, W. L., D. Mach, S. J. Goodman, H. J. Christian (1999). "Optical observations of lightning in Northern India, Himalayan mountain countries and Tibet." *Proceedings of the 11th International Conference on Atmospheric Electricity*, NASA/CP-1999-209261, p.420-421.
- Bondiou-Clergerie, A., P. Blanchet, C. They, A. Delannoy, J.Y. Lojou, A. Soulage, P. Richard, F. Roux, S. Chauzy (1999). "<<Orages>>: A project for space-borne detection of lightning flashes using interferometry in the VHF-UHF band". *Proceedings of the 11th International Conference on Atmospheric Electricity*, NASA/CP-1999-209261, p.184-187.
- Borucki, W.J., A. Bar-Nun, F. L. Scarf, A. F. Cook II, G.E. Hunt (1982). "Lightning Activity on Jupiter". *Icarus*, 52, p. 492-502.
- Borucki, W. J. and M. A. Williams. (1986). "Lightning in the Jovian Water Cloud". *J. Geophys. Res.*, vol 91, No. D9, p. 9893-9903.
- Borucki, W. J. and J. A. Magalhaes (1992). "Analysis of Voyager 2 Images of Jovian Lightning". *Icarus*, 96, p. 1-14.
- Buechler, D. E., S. J. Goodman, E. W. McCaul, K. Knupp (1999). "The 1997-98 El Nino Event and Related Lightning Variations in the Southeastern United States". *Proceedings of the 11th International Conference on Atmospheric Electricity*, NASA/CP-1999-209261, p.519-521.

- Chang, D. E., C. A. Morales, J. A. Weinman, W. S. Olson (1999). "Combined microwave and sferics measurements as a continuous proxy for latent heating in mesoscale model predictions". *Proceedings of the 11th International Conference on Atmospheric Electricity*, NASA/CP-1999-209261, p.372-375.
- Changnon, S. A. (1993). "Relationships between Thunderstorms and Cloud-to-Ground lightning in the United States". *Journal of Applied Meteorology*, 32, No.1, p.88-105.
- Christian, H. J., J. Latham (1998). "Satellite Measurements of Global Lightning". *Q. J. R. Meteorol. Soc.* 124, pp. 1771-1773.
- Christian, H. J. (1999). "Optical Detection of Lightning from Space". *Proceedings of the 11th International Conference on Atmospheric Electricity*, NASA/CP-1999-209261, p.715-718.
- Christian, H. J., R. J. Blakeslee, D. J. Boccippio, W. J. Boeck, D. E. Buechler, K. T. Driscoll, S. J. Goodman, J. M. Hall, W. J. Koshak, D. M. Mach, M. F. Stewart (1999a). "Global frequency and distribution of lightning as observed by the Optical Transient Detector (OTD)". *Proceedings of the 11th International Conference on Atmospheric Electricity*, NASA/CP-1999-209261, p.726-729.
- Christian, H. J., R. J. Blakeslee, S. J. Goodman, D. A. Mach, M. F. Stewart, D. E. Buechler, W. J. Koshak, J. M. Hall, W. L. Boeck, K. T. Driscoll, D. J. Boccippio (1999b). "The Lightning Imaging Sensor". NASA/CP-1999-209261: *Proceedings of the 11th International Conference on Atmospheric Electricity*, p.746-749.
- Cook, A. F., T. C. Duxbury, and E. G. Hunt. (1979). "First Results on Jovian Lightning". *Nature*, 280, p. 794.
- Cummins, K. L., M. J. Murphy, E. A. Bardo, W. L. Hiscox, R. B. Pyle, A. E. Pifer (1998). "A Combined TOA/MDF Technology Upgrade of the U.S. National Lightning Detection Network" *J. Geophys. Res.*, vol 103, no. D8, p. 9035-9044.
- Cummins, K. L., R. B. Pyle, G. Fournier (1999). "An integrated North American lightning detection network". *Proceedings of the 11th International Conference on Atmospheric Electricity*, NASA/CP-1999-209261, p.218-221.
- Del Genio, A. and K.B. McGrattan (1990). "Moist Convection and the Vertical Structure and Water Abundance of Jupiter's Atmosphere". *Icarus*, vol 84, p. 29-53.
- Driscoll, K. (1999). "A comparison between lightning activity and passive microwave measurements." *Proceedings of the 11th International Conference on Atmospheric Electricity*, NASA/CP-1999-209261, p.523-526.
- Edgar, B. C., L. M. Friesen, B. N. Turman, W. H. Beasley, M. A. Uman, Y. T. Lin, C. F. Jacobs, P. G. Beck (1979). "Satellite Optical sensing of lightning activity over the eastern United States and gulf regions". Space Sciences Laboratory Report No. SSL-79(4639)-i.

- Edgar B. C. and B. N. Turman (1980). "Optical Pulse Characteristics of lightning as observed from space". Unpublished.
- Filiaggi, Michael Thomas. (1997) "Cloud to Ground Lightning Relative to Storm Cell Evolution in the Southern Plains". Masters Thesis, University of Oklahoma School of Meteorology.
- Gierasch, P.J., A. P. Ingersoll, D. Banfield, S. P. Ewald, P. Helfenstein, A. Simon-Miller, A. Vasavada, H. H. Breneman, D. A. Senske, and the Galileo Imaging Team (2000). "Observation of moist Convection in Jupiter's Atmosphere". *Nature*, 403, p. 628-629.
- Gurnett, D.A., R. R. Shaw, R. R. Anderson, and W. S. Kurth (1979). "Whistlers Observed by Voyager 1: Detection of lightning on Jupiter". *Geophys. Res. Lett.*, Vol. 6, No. 6, p. 511-514.
- Hansell, S. A., W.K. Wells, and D. M. Hunten (1995). "Optical Detection of Lightning on Venus". *Icarus*, Vol. 117, p. 345-351.
- Hobara, Y., O. A. Molchanov, and M. Hayakawa (1995). "Propagation Characteristics of Whistler Waves in the Jovian Ionosphere and Magnetosphere". *J. Geophys. Res.*, Vol. 100, No. A12, p. 23523-23531.
- Hobara, Y., S. Kanamaru, M. Hayakawa, and D. Gurnett (1997). "On estimating the amplitude of Jovian whistlers observed by Voyager 1 and implications concerning lightning". *J. Geophys. Res.*, Vol. 102, No. A4, p. 7115-7125.
- Ingersoll, A.P., A. R. Vasavada, A. H. Bouchez, B. Little, and the Galileo Imaging Team (1998). "Imaging Jupiter's Atmosphere: Lightning Aurora. New White Oval". *EOS Transactions*, American Geophysical Union 1998 Fall Meeting, Vol. 79, No. 45, p. F529.
- Ingersoll, A.P., P. J. Gierasch, D. Banfield, A. R. Vasavada, and the Galileo Imaging Team (2000). "Moist Convection as an Energy Source for the large-scale motions in Jupiter's Atmosphere". *Nature*, vol. 403, p. 630-631.
- Jacobson, A. R., K. L. Cummins, M. Carter, P. Klingner, D. Russel-Dupre, and S. Knox (1999). "FORTE observations of lightning radio-frequency signatures: Prompt coincidence with strokes detected by the National Lightning Detection Network." Rep. *LA-UR-99-870*. Los Alamos National Laboratory, Los Alamos NM.
- Kawasaki, Z. and S. Yoshihashi (1999). "TRMM/LIS observations of lightning activity". *Proceedings of the 11th International Conference on Atmospheric Electricity*, NASA/CP-1999-209261, p.176-179.
- Kirkland, M.W. (1999). "An examination of superbolt-class lightning events observed by the FORTE satellite." Rep. *LA-UR-99-1685*, Los Alamos National Laboratory, Los Alamos, NM.
- Kirkland, M.W., D.M. Suszcynsky, R. Franze, S.O. Knox, J.L.L. Guillen, J.L. Green, and R.E. Spaulding (1998). "Observations of terrestrial lightning at optical wavelengths by the photodiode detector on the Forte Satellite". Rep. *LA-UR-98-4098*, Los Alamos National Laboratory, Los Alamos, NM.

- Kirkland, M.W., D.M. Suszcynsky, J.L.L. Guillen, and J.L. Green (2001). "Optical observations of terrestrial lightning by the FORTE photodiode detector." *J. Geophys. Res., Atmospheres*, in press.
- Klumov, B. (1999). "Impact of Lightning Discharge on Stratospheric Ozone". *Proceedings of the 11th International Conference on Atmospheric Electricity*, NASA/CP-1999-209261, p.660-663.
- Krehbiel, P.R., R. J. Thomas, W. Rison, T. Hamlin, J. Harlin, and M. Davis (1999). "Three Dimensional Lightning Mapping Observations During MEAPRS in Central Oklahoma". *Proceedings of the 11th International Conference on Atmospheric Electricity*, NASA/CP-1999-209261, p. 376-379.
- Krehbiel, P.R., R.J. Thomas, W. Rison, T. Hamlin, J. Harlin, and M. Davis. (2000a) "GPS-based Mapping System Reveals Lightning Inside Storms." *EOS, Transactions, American Geophysical Union*, Vol. 81, No. 3, January 18, 2000. p. 21
- Krehbiel, P.R., W. Rison, R. Thomas, T. Hamlin, J. Harlin, M. Stanley, M. Jones, J. Lombardo, and D. Shown. (2000b). "Lightning Mapping Observations During STEPS 2000" http://lightning.nmt.edu/nmt_lms/steps_2000/index.html
- Kurth, W.S., B. D. Strayer, D. A. Gurnett, and F. L. Scarf (1985). "A Summary of Whistlers Observed by Voyager 1 at Jupiter". *Icarus*, Vol. 61, p. 497-507.
- Huffines, G.R. and R.E. Orville (1999). "Lightning Ground Flash Density and Thunderstorm Duration in the Continental United States". *Journal of Applied Meteorology*, Vol. 38, No. 7, p.1013-1019
- Hobara, Y. O.A. Molchanov, M. Hayakawa, and K. Ohta (1995). "Propagation characteristics of whistler waves in the Jovian ionosphere and magnetosphere". *J. Geophys. Res.*, Vol. 100, No. A12, p. 23532-23531.
- Hobara, Y., S. Kanamaru, M. Hayakawa, and D.A. Gurnett (1997). "On estimating the amplitude of Jovian whistlers observed by Voyager 1 and implications concerning lightning". *J. Geophys. Res.*, Vol. 102, No. A4, p.7115-7125.
- Lanzerotti, L.J. et al. (1996). "Radio Frequency Signals in Jupiter's Atmosphere". *Science*, Vol. 272, p. 858-860.
- Levin, Z., W. J. Borucki, and O. B. Toon (1983). "Lightning Generation in Planetary Atmospheres". *Icarus*, Vol. 56, p. 80-115.
- Light, T.E., D.M. Suszcynsky, M.W. Kirkland, A.R. Jacobson. (2001) "Simulations of optical waveforms as seen through clouds by satellites." *J. Geophys. Res.*, Vol. 106, No. D15, p. 17,103-17,114.
- Light, T.E., D.M. Suszcynsky, A.R. Jacobson (2001b). "Optical Emissions from Lightning, Observed with the FORTE Satellite." *J. Geophys. Res.* In press.
- Little, B., C. D. Anger, A. P. Ingersoll, A. R. Vasavada, D. A. Senske, H. H. Breneman.

- W. J. Borucki, and the Galileo SSI Team (1999). "Galileo Images of Lightning on Jupiter". *Icarus*, Vol. 142, p. 306-323.
- Lopez, R.E., R.L. Holle (1996). "Fluctuations of Lightning Casualties in the United States: 1959-1990". *Journal of Climate*, Vol. 9, No.3, p.608-615.
- Lopez, R.E., R.L. Holle (1997). "Changes in the Number of Lightning Deaths in the United States during the Twentieth Century." *Journal of Climate*, Vol. 11, p. 2070-2077.
- Lopez, R.E., R. L. Holle, and A. I. Watson (1997). "Spatial and Temporal Distribution of Lightning over Arizona from a Power Utility Perspective". *Journal of Applied Meteorology*, Vol. 36, No. 6, p. 825-831.
- Lopez, R.E., R.L. Holle (1998). "Changes in the number of Lightning Deaths in the United States during the Twentieth Century". *Journal of Climate*, Vol. 11, No.8, p.2070-2077.
- Mazur, V., E. Williams, R. Boldi, L. Maier, D.E. Proctor. (1997). "Initial comparison of lightning mapping with operational Time-Of-Arrival and Interferometric Systems." *J. Geophys. Res.*, Vol. 102, No. D10, p. 11071-11085.
- Macgorman, D.R. and W.D. Rust. (1998). "The Electrical Nature of Storms". Oxford University Press, Inc., 198 Madison Avenue, New York, NY, 10016. 422 pages.
- Orville, R. E. (1994). "Cloud-to-Ground lightning flash characteristics in the contiguous United States 1989-91". *J. Geophys. Res.*, Vol. 99, p.10833-10841.
- Petersen, W.A., L. D. Carey, and S. A. Rutledge (1999). "Polarimetric Radar Observations and cloud modeling studies of low lightning producing convection in the Fort Collins flash flood". *Proceedings of the 11th International Conference on Atmospheric Electricity*, NASA/CP-1999-209261, p.480-481.
- Price, C., and D. Rind (1994a). "The impact of a 2X CO₂ Climate on Lightning-Caused Fires". *Journal of Climate*, Vol. 7, No. 10, p.1484-1494.
- Price, C., and D. Rind (1994b). "Possible Implications of Global Climate Change on Global lightning distributions and frequencies". *J. Geophys. Res.*, Vol. 99, No. D5, p. 10823.
- Reeve, N., and R. Toumi (1999). "Lightning activity as an indicator of climate change". *Quarterly Journal of the Royal Meteorological Society*, Vol. 125, No. 555, p.893-903.
- Reuter G., and S. Kozak (1999). "Lightning in Supercell Storms". *Proceedings of the 11th International Conference on Atmospheric Electricity*, NASA/CP-1999-209261, p. 476-479.
- Rinnert, L.J. et al. (1979). "Electromagnetic Noise and Radio Wave Propagation Below 100 kHz in the Jovian Atmosphere 1. The Equatorial Region". *J. Geophys. Res.*, Vol. 84, No. A9, p. 5191-5198.

- Rinnert, K. (1985). "Lightning on other Planets". *J. Geophys. Res.*, Vol. 90, p. 6225-6237.
- Rison, W., R.J. Thomas, P.R. Krehbiel, T. Hamlin, J. Harlin. (1999). "A GPS-based Three-Dimensional Lightning Mapping System: Initial Observations in Central New Mexico" *Geophysical Research Letters*, Vol. 26, No. 23, p. 3573-3576.
- Rhodes, C. T., M. Kirkland, D. M. Suszcynsky, A. R. Jacobson, P. E. Argo, S. O. Knox, R. C. Franz, J. L. L. Guillen, J. L. Green, R. E. Spalding (1998). "Optical and RF Emissions from Superbolt-class Lightning Events as observed by the FORTE Satellite". *EOS Transactions*, American Geophysical Union, 1998 Fall Meeting, Vol 79, No. 45, p. F128.
- Roohr, P. B. and T. H. Vonder Haar (1994). "A Comparative Analysis of the Temporal Variability of Lightning observations and GOES imagery". *Journal of Applied Meteorology*. Vol. 33, p 1271-1290.
- Rorig, M.L., and S. A. Ferguson (1999). "Characteristics of Lightning and Wildland Fire Ignition in the Pacific Northwest". *Journal of Applied Meteorology*, Vol. 38, No. 11, p. 1565-1575.
- Sanger, N.T., R. Zhang, R. E. Orville, X. Tie, W. Randel, and E. R. Williams (1999). "Enhanced NO_x by Lightning in the Upper Troposphere and Lower Stratosphere Inferred from the Global NO₂ Measurements of the Upper Atmosphere Research Satellite (UARS)." *Proceedings of the 11th International Conference on Atmospheric Electricity*, NASA/CP-1999-209261, p.652-653.
- Schroeder, V., and M. Baker (1999). "Inferring Selected Cloud Properties from Satellite Lightning Data". *Proceedings from the 11th International Conference on Atmospheric Electricity*, NASA/CP-1999-209261, p. 276-279.
- Shao, X.M. and P.R. Krehbiel. (1996). "The spatial and temporal development of lightning". *J. Geophys. Res.*, Vol. 101, No. D21, p. 26641-26668.
- Sinha, A., and Toumi R. (1997). "Tropospheric Ozone, lightning, and climate change". *J. Geophys. Res.*, 102, No.D9, p.10.
- Soula, S., G. Molinie, S. Defoy, S. Chauzy, N. Simond. "Some Aspects of Correlation Between Lightning Activity and Rainfall in Thunderstorms". *Proceedings of the 11th International Conference on Atmospheric Electricity*, NASA/CP-1999-209261, p. 384-387.
- Suszcynsky, D.M., M. W. Kirkland, P. Argo, R. Franz, A. Jacobson, S. Knox, J. Guillen, J. Green, and R. Spalding (1999). "Thunderstorm and Lightning Studies using the FORTE Optical Lightning System (FORTE/OLS)". *Proceedings from the 11th International Conference on Atmospheric Electricity*, NASA/CP-1999-209261, p.672-675.
- Suszcynsky, D. M., M. W. Kirkland, A. R. Jacobson, R. C. Franz, S. O. Knox, J. L. L. Guillen, and J. L. Green (2000). "FORTE observations of simultaneous VHF and optical emissions from lightning: Basic Phenomenology". *J. Geophys. Res.*, Vol. 105, No. D2, p. 2191-2201.

- Suszcynsky, D. M. and T. E. Light (2000). "Coordinated Observations of Optical Lightning from Space using the FORTE Photodiode Detector and the CDD Imager". Rep. LA-UR-00-3041, Los Alamos National Laboratory, Los Alamos NM.
- Suszcynsky, D. M., T. E. Light, S. Davis, J. L. Green, J. L. L. Guillen, and W. Myre. (2001). "Coordinated observations of optical lightning from space using the FPORET photodiode detector and CCD imager." *J. Geophys. Res.*, Vol. 106, No. D16, p. 17897-17906.
- Tapia, A., J. A. Smith and M. Dixon (1998). "Estimation of Convective Rainfall from lightning observations" *Journal of Appl. Meteor.*, Vol. 37, p.1497-1509.
- Thomas, R.J. et al. (1999). "Comparison of ground-based 3-dimensional lightning mapping observations with Satellite-based LIS observations in Oklahoma". *Proceedings from the 11th International Conference on Atmospheric Electricity*, NASA/CP-1999-209261, p.172.
- Thomas, R.J. , P. R. Krehbiel, W. Rison, T. hamlin, D. J. Boccippio, S. J. Goodman, and H. J. Christian (2000). "Comparison of ground-based 3-dimensional lightning mapping observations with Satellite-based LIS observations in Oklahoma". *Geophys. Res. Lett.*, Vol. 27, No.12, p. 1703-1706.
- Thomason, L.W. and E.P. Krider. (1982) "The Effects of Clouds on the Light Produced by Lightning." *Journal of the Atmospheric Sciences*, Vol. 39, No. 9. p. 2051-2065.
- Tierney, H. E., A. R. Jacobson, W. H. Beasley, and P. A. Argo (2000). "Determination of source thunderstorms for VHF emissions observed by the FORTE satellite" Unpublished.
- Toumi, R., and J. D. Haigh (1996). "A Tropospheric ozone-lightning climate feedback". *Geophys. Res. Lett.*, Vol. 23, No. 9, p. 1037-1040.
- Turman, B.N. (1977). "Detection of Lightning Superbolts". *J. Geophys.Res.*, Vol. 82, No. 18, p. 2566-2568.
- Turman, B.N. (1978). "Analysis of lightning data from the DMSP Satellite". *J. Geophys. Res.*, 83, No. C10, p. 5019-5024.
- Turman, B.N. (1979). "Lightning Detection from Space". *American Scientist*, Vol. 67, p. 321-329.
- Turman, B. N., and B. C. Edgar (1982). "Global Lightning Distributions at Dawn and Dusk". *J. Geophys. Res.*, Vol. 87, No. C2, p 1191-1206.
- TRMM Web Site - NASA (2000). <http://trmm.gsfc.nasa.gov/>
- Watson et al. (1995) "Lightning from Two National Detection Networks Related to vertically Intergrated Liquid and Echo Top Information from WSR-88D Radar". *Weather and Forecasting*, Vol 10, p. 592-605.

- Williams, E., K. Rothkin, D. Stevenson, and D. Boccippio (1999). "Global Lightning Variations caused by changes in flash rate and by changes in number of thunderstorms" *Proceedings of the 11th International Conference on Atmospheric Electricity*, NASA/CP-1999-209261, p. 750-753.
- Yair, Y., Z. Levin, and S. Tzivion (1995). "Microphysical Processes and Dynamics of a Jovian Thundercloud". *Icarus*, Vol. 114, p. 278-299.
- Yair, Y., Z. Levin, and S. Tzivion (1995). "Lightning Generation in a Jovian Thundercloud: Results from an Axisymmetric Numerical Cloud Model". *Icarus*, Vol. 115, p. 421-434.
- Yair, Y., Z. Levin, and S. Tzivion (1998). "Model Interpretation of Jovian Lightning Activity and the Galileo Probe Results". *J. Geophys. Res.*, Vol. 103, No. D12, p. 14157-14166.
- Zajac, B. A., S. A. Rutledge, and L. A. Carey (1999). "Characteristics of Cloud-to-Ground Lightning in the Contiguous U.S. from 1995-1997". *Proceedings of the 11th International Conference on Atmospheric Electricity*, NASA/CP-1999-209261, p. 750-753.
- Zuelsdorf, R.S., A. R. Jacobson, M. Kirkland, R. J. Strangeway, C. T. Russell (1999) "Detection Rates of Lightning Generated Radio emissions by FORTE" *Proceedings of the 11th International Conference on Atmospheric Electricity*, NASA/CP-1999-209261, p.676-679.